UNIVERSITY OF CALIFORNIA
RIVERSIDE

The Roles of Parasitic Nematode Effectors on Host Immunity and Lipid Signaling

A Dissertation submitted in partial satisfaction
of the requirements for the degree of

Doctor of Philosophy

in

Environmental Toxicology

by

Sophia C. Parks

December 2021

Dissertation Committee:
Dr. Adler Dillman
Dr. Naoki Yamanaka
Dr. Isgouhi Kaloshian

The Dissertation of Sophia C. Parks is approved:

_____

_____

_____

Committee Chairperson

University of California, Riverside

ACKNOWLEDGMENTS

Great success is achieved with determination, perseverance, and support. There are many people who have contributed to furthering my academic career and personal development over the years. First, I would like to thank my advisor and number one supporter, **Dr. Adler Dillman** for believing in me and my abilities as well as bringing excitement and inspiration to the science we do. I couldn't have chosen a better PI to guide me through doctorate research and I cannot fully explain how much of a perfect fit it was for me to be in your lab. You are an amazing leader, teacher, and scientist. Thank you for giving me to the space to mature as a scientist while building my confidence and independence. I am amazed by the lab environment you have created and the mentoring I received. Thank you for treating me as a colleague and showing me the ins and outs of being a PI and researcher. Thank you for being my biggest cheerleader and always speaking so highly of me, it really made all the difference. I hope to continue our relationship as I matriculate through my academic career and you deserve all that you wish for.

To my parents, **Andrea and Tony Parks** thank you for supporting me throughout my entire life and setting me up to achieve anything I set my mind to. Thank you for always providing for me and giving me everything I ever wanted and needed. I look up to both of you and I am blessed to have you as parents. You both valued my education over almost everything else and gave me the time and space to excel to the highest level. I love you dearly and I am so proud to be your daughter. I share this accomplishment with you.

I could not have made it through grad school without the support of my closest friends. To my girls **Aalekyah Reddam, Miranda Aiken, Tori McGruer**. Girl's nights were the sweetest, camping trips were the best way to unwind, and having you around campus helped me through everything in more ways than you know. It was so special to meet all of you year one and to have gone through it all together. I will cherish these times forever. To my mentor and friend **Marissa Giroux**, thank you for your continuous support and guidance and all of our outdoor trips. I appreciate our friendship and how you understand my truest self. To **Adam Ruppert**, thank you for being my best friend and climbing partner through all my years at UCR, I don't know what I would have done without your friendship. I love you always. To my boyfriend **Trevor Berry**, thank you for loving all of me and reminding me that everything is going to be okay. With you by my side I feel like I can live through anything, I love you with all my heart.

To the Dillman Lab thank you for putting up with my overactive senses and supporting my endeavors. **Dr. Harpal Dhillon, Dr. Dihong Lu, Jake Shurkman, Ogadinma Okakpu, Aklima Khanam Lima,** thank you for providing support, wisdom, and making lab fun! I could not have asked for a better lab dynamic; you all are so special to me and I know you will achieve great things in life. Thank you to those who went before me and provided guidance and wisdom, **Dr. Tiffany Baiocchi** and **Dr. Dennis Chang**. I learned a lot from you and the foundation you set in lab was key to my success. To my lab mate **Kyle Anesko**, thank you for standing up for me and always being there when I need you. I am lucky to have you in my life. To all my undergrads that have worked with me, **Damien Juncaj, Shyon Nasrolahi, Jasmin Bedi, Josh Malilay, Stephanie Martinez-**

Beltran, Isaiah Claudio. I owe you all so much gratitude, without each of you I could not have completed as much work as I did, thank you for stepping up a serving me and the lab. We were a great team and I wish you the best in your future endeavors. To the undergrad who's done the most work with me and has been with me the longest, **Susan Nguyen**, thank you for being my right hand, I appreciate all the time you put in. You are going to be a great doctor and I am amazed by your intellect. I am honored to have mentored all of you. To my colleague and sister at heart **Valentina Alonso**, thank you for all the laughs at UCR and beyond, I know you are developing into a great scientist at UCLA and I can't wait to see what you do next. I am here whenever you need me.

I would also like to thank **Rebecca Brown** and **Dr. Ernest Martinez** from the **MARC U STAR program**. Thank you for believing in me and mentoring me through difficult times, it made all the difference. From my dissertation committee that has helped guide my career I would like to thank **Dr. Naoki Yamanaka** for helping with my project development and teaching me what I needed to know about flies. I appreciate your kind and chill vibes always. Thank you **Dr. Isgouhi Kaloshian** for speaking highly of me, always being in my corner, and supporting my career development. I am grateful for you always thinking of me when it came to special opportunities surrounding media and fellowships, you helped build my confidence more than you know.

I'd like to acknowledge some things and places that were key to my success. I will be wrapping up after almost nine years at UCR and I am thankful for such a beautiful campus and home. Thank you to my car Poopsie, the 2013 Nissan Juke that got me safely to school and back as I commuted up to two hours a day all four years of undergrad and

four years of grad school. Thank you to Goodwin's organic market for providing healthy meals and a great hangout spot. Thank you to the mountains, deserts, and beaches of southern California that I deeply connected with during this time and for keeping me sane through all the work, my forever home.

Finally, I'd like to thank and praise **God** for paving the way for me to achieve my childhood dream of becoming a doctor. The path was riddled with challenges but by your grace, strength, and light I was able to stay the course. At times I felt that you would lay a brick down right in front of my feet so that I could continue to make strides. Your will be done.

DEDICATION

I'd like to dedicate my dissertation work to my mentor Dr. Adler Dillman. You were the exact mentor that I needed, and I would not be where I am today without your guidance, support, and motivation.

I would also like to dedicate this work to my parents Andrea and Tony Parks. Thank you for inspiring me to achieve my goals and for spending so much time teaching me that knowledge is key. Thank you for your unwavering love and support. You exude strength and determination and have taught me to always keep my head up. I love you.

ABSTRACT OF THE DISSERTATION

The Roles of Parasitic Nematode Effectors on Host Immunity and Lipid Signaling

by

Sophia C. Parks

Doctor of Philosophy, Graduate Program in Environmental Toxicology
University of California, Riverside, December 2021
Dr. Adler Dillman, Chairperson

Parasitic nematodes cause significant morbidity and mortality to humans. Much of their ability to successfully infect their hosts is due to the variety of excreted/ secreted proteins (ESPs) they release into host tissues, and their ability to evade or suppress host immunity, yet little is known about the mechanisms behind these interactions. This work identifies and characterizes two ESPs that display immunomodulatory activity in the model host *Drosophila melanogaster*. The fatty acid- and retinol- binding (FAR) proteins and the secreted phospholipase A_2 ($sPLA_2$) enzyme from the entomopathogenic nematode *Steinernema carpocapsae* likely elicit their detrimental effects by preventing essential immune lipid signaling in the fly. The FAR proteins bind to fatty acids and retinol and alter the *in vivo* availability of lipids in the fly hemolymph. They also function to suppress phenoloxidase activity and antimicrobial peptide production, both of which are essential in the fly's ability to resist bacterial infections. In contrast, the $sPLA_2$ enzyme cleaves lipids directly from the membrane and shows specific immunomodulatory effects on toll signaling and phagocytosis. Overall analysis of fly hemolymph post infection revealed several lipids that are depleted and are also able to rescue to course of infection.

This work identifies lipids and prostaglandins that significantly improve the outcome of infection, furthering our understanding of the role of lipids and eicosanoids in *Drosophila* immunity.

II. TABLE OF CONTENTS

III. LIST OF FIGURES

CHAPTER 1

CHAPTER 2

CHAPTER 3

CHAPTER 4

IV. LIST OF SUPPLEMENTAL FIGURES

CHAPTER 2

CHAPTER 3

CHAPTER 4

Chapter 1

The FAR protein family of parasitic nematodes

Sophia C. Parks, Susan Nguyen, and Adler R. Dillman*

Department of Nematology, University of California, Riverside, California, 92521, USA.

*Correspondence: adlerd@ucr.edu (A.R. Dillman)

A version of this chapter is in review at *PLoS Pathogens* 2021

Abstract

Fatty acid- and retinol- binding proteins belong to a unique family of excreted/secreted proteins found in many nematode species that have been studied over the past three decades. Most of our understanding of these proteins, however, is limited to their *in vitro* binding affinities towards various fatty acids and retinol and has not provided much insight to their *in vivo* functions or mechanisms. Recently, research has shown that FARs elicit an immunomodulatory role in plant and animal model systems, likely by sequestering lipids involved in immune signaling. This alludes to the intricate relationship between parasitic nematodes effectors and their hosts.

Significance

Parasitic nematodes infect millions of people worldwide as well as a wide variety of hosts including other mammals, insects, and plants [1,2]. The soil-transmitted helminth *Ascaris lumbricoides* alone infects ~1 billion people globally, while plant parasitic nematodes infecting crops cause billions of dollars in damage every year [3]. During infection, nematodes release a concoction of excreted/secreted proteins (ESPs) into surrounding host tissues which can interfere with host signaling mechanisms and homeostasis, allowing for a more successful infection [4]. Many of these ESPs have not been studied in detail and are essential for our understanding of host-helminth interactions as well as the outcome of infection. One unique protein family in this mixture is the family of fatty acid- and retinol-binding (FAR) proteins. FARs are small alpha-helix rich proteins, around 20 kDa [5]. Numerous papers studying their *in vitro* binding characteristics reveal that FARs' ability to sequester fatty acid and retinol molecules, specifically those

important to immune signaling, can potentially play a crucial role in affecting the host immune system. Despite the wealth of information about FARs' binding properties, little is known about how FARs interact with host immunity [6-18].

History

FAR proteins were first described in *Onchocerca volvulus*, *Ascaris suum* and *Brugia malayi* [12,19,20]. Initially, they attracted attention for their ability to bind retinoids and therefore their potential role in parasitic growth, differentiation, and reproduction [20]. In *O. volvulus* infections retinol concentration was shown to be much greater in the nematode than in the surrounding host tissue, and since there is no visual role of vitamin A in the nematode, it was hypothesized that it is used for other important functions such as growth and reproduction [20]. Retinoic acid is localized to developing embryos and is required for normal growth and development [21]. Further studies revealed that FAR proteins can bind fatty acids in addition to retinol [19]. The initial significance of this fatty acid binding role was first thought to be to sequester and distribute dietary lipids to the nematode, and most of FARs' potential functions were analyzed in the context of the nematode's own biological functions [19]. Later, FARs' presence in ESPs and its binding properties to host lipids raised interest in its potential role in parasitism through immunomodulation and in vaccine development [6,7,12,13,19,22,23].

Unique structures and properties

Parasitic nematode ES contains many proteins and antigens that have the potential to alter host immune functions, as well as other essential mechanisms. The proteins most important to immunity include lipid binding proteins such as nematode polyprotein

antigens (NPAs), nematode fatty acid-binding proteins (nemFABPs), and nematode fatty acid- and retinol-binding proteins (FARs). NPAs are small, helix-rich proteins that are initially synthesized as a large polyprotein before being cleaved into functional copies around 15kDa in size [4,10,24]. NPAs bind to fatty acids and retinoids and, when secreted by the nematode, can elicit a strong host immune response [10,24]. NemFABPs on the other hand have both beta barrel and alpha helical regions and share many similarities with vertebrate FABPs which may have essential roles in nutrient acquisition and development [4,24,25]. FARs' structural characteristics are uniquely distinct from other lipid-binding proteins, and there is a high degree of structural conservation between FARs from different species, despite divergence in amino acid sequence (Figure 1.1). While mammalian lipid-binding proteins contain mostly beta barrel secondary structures, FARs are alpha-helix rich with almost no beta structures present [8,9,13,15,26-28]. They are not made as a polyprotein, like NPAs, and possess an alpha helical fold that is conserved among a diverse group of species. For example, *Necator americanus* Na-FAR-1 and *Caenorhabditis elegans* Ce-FAR-7 both share similar alpha helical fold, despite Ce-FAR-7 being phylogenetically distant from parasitic nematode FARs [27]. FAR proteins are relatively small with a size around 20kDa and contain approximately 160-190 amino acids [6,8,9,15,29]. The presence of a casein kinase II phosphorylation site in addition to a hydrophobic leader signal peptide is thought to play a key role in regulation of FARs' secretion into host tissue [6,8,9,13,15,30]. FAR proteins have two separate binding sites, one for retinol or retinoids and one for fatty acids, which are thought to influence each other's affinity upon ligand-binding [30,31]. In fluorescent binding

experiments with the dansylated fluorophores DAUDA and DACA, binding with FAR proteins causes a significant blue shift, more than previously seen in mammalian lipid-binding proteins, thus signifying a ligand's entrance into an apolar binding site [6-8,13,17,32]. Similarly, binding experiments with naturally fluorescent retinol and cis-parinaric acid also show an increase in fluorescence, signifying a ligand's entrance into a hydrophobic site [7,9]. FAR proteins can have a high affinity for other hydrophobic molecules as well as fatty acids of various lengths, though the specific dissociation constant varies between species [6,11,13,33]. Some FAR proteins do not bind cholesterol, though Na-FAR-1 has been found to bind to polar lipids in addition to fatty acids, such as phospholipids and phosphatidylglycerol [11,13,15]. Kd values for ligand binding are typically in the micromolar range [6,7,11,33].

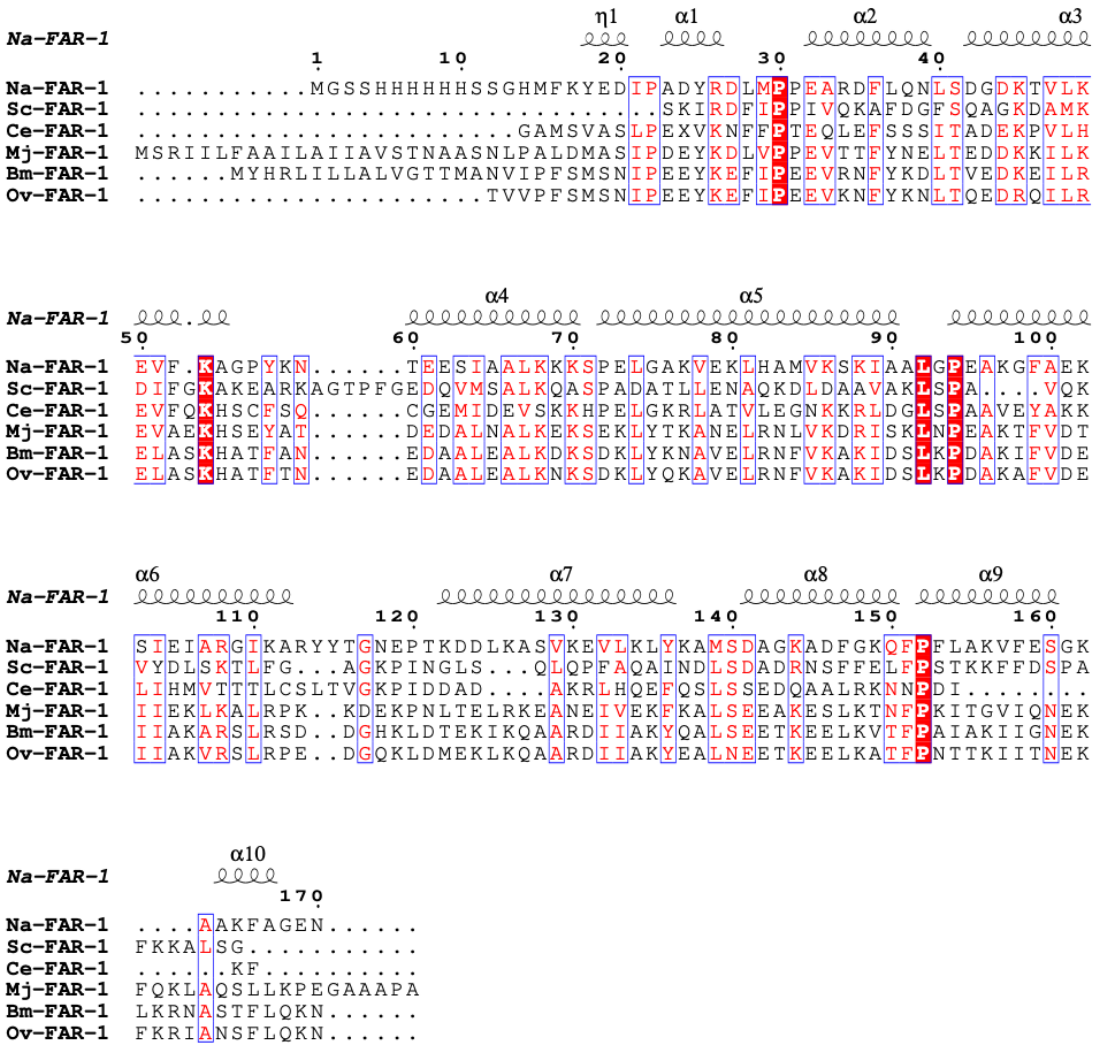

Figure 1.1: Comparison of FAR proteins across free-living and parasitic nematode species. The FAR protein sequences are aligned with clustalW2 with secondary structures shown as an estimation based on the *N. americanus Na*-FAR-1 crystal structure using ESPript. The various secondary structures are labeled α with squiggles for large alpha helices and η with squiggles for 3_{10} helices. Residues that are identical among all groups are highlighted in red and conserved residues are shown in red, both outlined in blue.

The number of FAR proteins in each nematode genome appears to be lineage specific. For example, *Brugia malayi* has 3 FAR proteins, *C. elegans* has 9, and the insect parasitic nematode *Steinernema carpocapsae* has 45 putative FAR proteins [9,14,16,17,33-35]. In

species with multiple FAR proteins, they tend to differ and generally have distinct sequences and ligand binding strengths. For example, both *Heterodera avenae* Ha-FAR-2 and *B. malayi* Bm-FAR-2 have been reported to have weaker binding affinities to retinol and fatty acids compared to Ha-FAR-1 and Bm-FAR-1, respectively [17,33]. Currently, only two FAR protein structures have been confirmed through crystallization, one from *C. elegans,* Ce-FAR-7, and one from *N. americanus*, Na-FAR-1. The Ce-FAR-7 crystal structure reveals nine alpha helix loops with two hydrophobic pockets joined by a surface groove. One of the binding pockets, P1, is predicted to bind fatty acids due to its smaller size, while the other binding pocket, P2, is predicted to bind bulkier retinoids [30]. There are concerns that Ce-FAR-7, derived from a free-living nematode, varies significantly from parasitic FARs for its crystalized structure to be practical in analyzing parasite-derived FAR proteins. Furthermore, Ce-FAR-7 lacks an N-terminal secretion signal, has fewer alpha-helices and more beta structures, and is also significantly shorter at the C-terminus compared to most other FAR proteins [36]. Na-FAR-1, on the other hand, shares more similarities with other parasitic-derived FAR proteins. *N. americanus* belongs to the parasitic nematode subfamily and possesses a classical signal peptide marked for secretion. Compared to Ce-FAR-7, Na-FAR-1 has 11 alpha helices, one internal cavity larger in size, though both share conserved sequences within their respective hydrophobic cavities [15].

The diversity of FARs can be seen through glycosylation patterns, localization within the nematode's body, as well as through sequence identity. For example, *Onchocerca*

volvulus Ov-FAR-1 has three predicted glycosylation sites, *Brugia malayi* Bm-FAR-1 and *Loa loa* Ll-FAR-1have one, while *Brugia pahangi* Bp-FAR-1and *Wuchereria bancrofti* Wb-FAR-1 have none [26]. Differing localization patterns in the nematode's body also contributes to FAR protein diversity. Most FAR proteins in parasitic nematodes can be found in the hypodermis, cuticle surface region, and esophageal glands, which suggests their presence in nematode secretions and potential role in mediating host-parasite interactions [9,14,37]. FARs are also often found in reproductive glands, in larvae, and in higher amounts in females, suggesting a biological importance in development and reproduction in addition to secretion [9,11,38-40]. RNA interference experiments confirmed these two hypotheses. For example, silencing of *Ha-far-1* resulted in a significant reduction in reproduction of *H. avenae*, and analysis of gene expressions showed that Ha-FAR-1 transcript levels during parasitic stages are higher compared to non-parasitic stages [14]. In *Radopholus similis,* a reduction in reproduction and pathogenicity was also observed after *Rs-far-1* knockdown, and *Rs-far-1* expression level is also increased in the more pathogenic nematode population [18]. Similar studies in *Aphelenchoides besseyi, Bursaphelenchus xylophilus,* and *Meloidogyne javanica* further strengthen this understanding of FARs' role in parasitism [9,40,41]. Interestingly, despite sharing similar protein structures and tertiary folds, FARs can have vastly different amino acid sequences (Figure 1.1). As expected, FARs in closely related species have higher sequence homology, such as within the *Meloidogyne* clade with up to 100% sequence identity, while those in more disparate clades can have very lower sequence homology [31,33].

FAR function in plants

Plant-parasitic nematode FARs have been shown to positively affect the nematode infection process. The first plant FAR discovered, Gp-FAR-1 in *Globodera pallida,* is found to bind to precursors of the jasmonic acid signaling pathway and inhibit lipoxygenase activity *in vitro* [6]. Lipoxygenase activity is part of the octadecanoid signalling pathway that eventually leads to the synthesis of jasmonic acid, a signal transducer in systemic plant immunity. By interfering with this pathway, Gp-FAR-1 likely modulates host immunity, contributing to a more successful nematode infection. In *B. xylophilus,* Bx-FAR-1 was shown to participate in the infection process; its expression levels are upregulated in the earlier infection stages of *B. xylophilus,* and RNAi of this FAR resulted in lower infection rates [40]. The expressions of *pr-6* and *lox-5*, genes that are part of the jasmonic acid immune response pathway, are also found to be much higher when Bx-FAR-1 is silenced, thus suggesting that Bx-FAR-1 could interfere with this immune response process upon infection [40]. In *Meloidogyne incognita,* knockdown experiments of *Mi-far-1* also showed that the infection process and parasite reproduction are greatly reduced when Mi-FAR-1 is reduced. Mi-FAR-1 also appears to play a role in nematode defense against bacterial infection, as its reduction results in increased bacterial endospore attachment [42]. In *Pratylenchus penetrans,* suppression of Pp-FAR-1 protein reduced nematode reproduction by up to 70% compared to control lines [29]. In *M. javanica,* the presence of Mj-FAR-1 influences parasitic infection of tomato roots. Transgenic tomato roots that expressed Mj-FAR-1 constitutively, showed a higher susceptibility to nematode infection and allow for faster nematode growth once infected.

This is the strongest evidence suggesting that FARs alter susceptibility to infection in plants. RNA interference experiments showed that nematode maturation slows when *Mj-far-1* is silenced [41]. Furthermore, expression of *Mj-far-1* resulted in suppression of jasmonic acid responsive genes such as *pin2* and *ϒ-thionin*, similar to findings in Bx-FAR-1 research, although LOX gene expression is not significantly affected [41]. These are striking data on phenotypic changes in immunity and resilience to infection in plants. In *R. similis,* comparison between a highly pathogenic population (Rs-C) and a less pathogenic population (Rs-P) showed that *Rs-far-1* expression is 2.5 times higher in the highly pathogenic population. RNA interference assays also indicated that Rs-FAR-1 regulates levels of allene oxide synthase (AOS), a component of the jasmonic acid pathway. In *Arabidopsis thaliana,* compared to control plants, AOS expression is significantly decreased when treated with regular *R. similis,* but is significantly increased when treated with *Rs-far-1*-silenced *R. similis* [18]. Taken together, these findings suggested that FAR proteins assist in parasitic infections by manipulating the host plant jasmonic acid immune signaling pathway and contribute to the nematodes' reproduction in host tissues.

FAR function in animals

Research on the immunomodulatory effects of FARs in animal-parasitic nematodes is much more limited compared to their plant-parasitic counterparts. In *Strongyloides stercoralis,* analysis of differential gene expression showed that in the infective life stage, the gene coding for FAR is among the most highly expressed genes, suggesting that the protein plays a significant role during the infection process [38]. In *Brugia malayi,* both

Bm-FAR-1 and Bm-FAR-2 are found to be targets of strong IgG3 and IgE antibodies in infected individuals, which hint at their potential roles in affecting the host immune response to nematode infection [17]. In *Steinernema carpocapsae,* experiments with FAR-expressing transgenic *Drosophila melanogaster* showed that FAR proteins directly modulate host immunity. Flies expressing or injected with Sc-FARs exhibited a decrease in resistance to bacterial infection, and a significant reduction in other aspects of fly immune responses such as the phenoloxidase cascade and antimicrobial peptide production [43]. Sc-FAR-1 and Sc-FAR-2 bound to fatty acids *in vitro* and altered their availability in circulation *in vivo,* thus suggesting a mechanism for immunomodulation in animals through depletion of lipid signaling molecules necessary for immune response pathways [43].

Conclusion

Parasitic nematode FAR proteins differ from fatty acid-binding proteins in mammals, highlighting the possibility that they may serve as a potential new target for anti-helmenthic treatments [20,44]. For example, ivermectin, one of the main drugs used to treat helminth infections, has been shown to inhibit FARs' activities [44]. FARs elicit a strong antibody response in animal hosts, which mark them as prospective candidates for vaccine therapies against parasitic nematodes [17]. Early vaccination experiments have shown a decrease in worm burden in vaccinated hosts upon infection [11]. Targeted medication to inhibit FAR activity in the host is also another potential therapeutic treatment to pursue, as FARs are unique to nematodes and do not have an equivalent in mammals [45]. Overall, research on FARs shows promising results for their role in

modulating host immunity and more work should be done to mechanistically determine their biological function, binding partners, and other roles *in vivo*.

References

1. Hotez, P.J., et al., *The global burden of disease study 2010: interpretation and implications for the neglected tropical diseases.* PLoS Negl Trop Dis, 2014. **8**(7): p. e2865.

2. Pullan, R.L., et al., *Global numbers of infection and disease burden of soil transmitted helminth infections in 2010.* Parasites & Vectors, 2014.

3. WHO. *Soil-transmitted helminth infections*. 2020 [cited 2020 08/31].

4. Kennedy, M.W., et al., *The unusual lipid-binding proteins of nematodes: NPAs nemFABPs and FARs.* Molecular Biology, Biochemistry and Immunology, 2013. **2**: p. 397-412.

5. Rubin, G.M., et al., *Comparative Genomics of the Eukaryotes.* Science, 2000. **287**.

6. Prior, A., et al., *A surface-associated retinol- and fatty acid-binding protein (Gp-FAR-1) from the potato cyst nematode Globodera pallida: lipid binding activities, structural analysis and expression pattern.* Biochem J, 2001. **356**: p. 387-394.

7. Basavaraju, S., et al., *Ac-FAR-1, a 20 kDa fatty acid- and retinol-binding protein secreted by adult Ancylostoma caninum hookworms: gene transcription pattern, ligand binding properties and structural characterisation.* Mol Biochem Parasitol, 2003. **126**: p. 63-71.

8. Bath, J.L., et al., *Identification of a Secreted Fatty Acid and Retinol-Binding Protein (Hp-FAR-1) from Heligmosomoides polygyrus.* Journal of Nematology, 2009. **41**: p. 228-233.

9. Cheng, X., et al., *Molecular characterization and functions of fatty acid and retinoid binding protein gene (Ab-far-1) in Aphelenchoides besseyi.* PLoS One, 2013. **8**(6): p. e66011.

10. Fairfax, K.C., L.M. Harrison, and M. Cappello, *Molecular cloning and characterization of a nematode polyprotein antigen/allergen from the human and animal hookworm Ancylostoma ceylanicum.* Mol Biochem Parasitol, 2014. **198**(1): p. 37-44.

11. Fairfax, K.C., et al., *Characterisation of a fatty acid and retinol binding protein orthologue from the hookworm Ancylostoma ceylanicum.* Int J Parasitol, 2009. **39**(14): p. 1561-71.

12. Kennedy, M.W., et al., *The ABA-1 Allergen of the Parasitic Nematode Ascaris suum: Fatty Acid and Retinoid Binding Function and Structural Characterization.* Biochemistry, 1995. **34**: p. 6700-6710.

13. Kennedy, M.W., et al., *The Ov20 Protein of the Parasitic Nematode Onchocerca volvulus.* The Journal of Biological Chemistry, 1997. **272**(47): p. 29442-29448.

14. Le, X., et al., *Isolation and characterization of a fatty acid- and retinoid-binding protein from the cereal cyst nematode Heterodera avenae.* Exp Parasitol, 2016. **167**: p. 94-102.

15. Rey-Burusco, M.F., et al., *(1)H, (1)(3)C and (1)(5)N chemical shift assignments of Na-FAR-1, a helix-rich fatty acid and retinol binding protein of the parasitic nematode Necator americanus.* Biomol NMR Assign, 2014. **8**(1): p. 19-21.

16. Wang, D.W., et al., *Identification and function of FAR protein family genes from a transcriptome analysis of Aphelenchoides besseyi.* Bioinformatics, 2018. **34**(17): p. 2936-2943.

17. Zhan, B., et al., *Ligand binding properties of two Brugia malayi fatty acid and retinol (FAR) binding proteins and their vaccine efficacies against challenge infection in gerbils.* PLoS Negl Trop Dis, 2018. **12**(10): p. e0006772.

18. Zhang, C., et al., *Molecular identification and functional characterization of the fatty acid- and retinoid-binding protein gene Rs-far-1 in the burrowing nematode Radopholus similis (Tylenchida: Pratylenchidae).* PLoS One, 2015. **10**(3): p. e0118414.

19. Kennedy, M.W., et al., *The gp15/400 polyprotein antigen of Brugia malayi binds fatty acids and retinoids.* Mol Biochem Parasitol, 1995. **71**: p. 41-50.

20. Sani, B.P., et al., *Novel retinoid-binding proteins from filarial parasites* . Biochem J, 1985. **232**: p. 577-583.

21. Scott, K.M.W.A.L., *Brugia malayi: Retinoic Acid Uptake and Localization.* Experimental Parasitology, 1995. **80**: p. 282-290.

22. BARRETT, J. and N. SAGHIR, *LIPID BINDING PROTEINS IN PARASITIC HELMINTHS.* Research and Reviews in Parasitology, 1999. **59**: p. 107-112.

23. McDermott, L., A. Cooper, and M.W. Kennedy, *Novel classes of fatty acid and retinol binding protein from nematodes.* Molecular and Cellular Biochemistry, 1999. **192**: p. 69-75.

24. Franchini, G.R., et al., *The unusual lipid binding proteins of parasitic helminths and their potential roles in parasitism and as therapeutic targets.* Prostaglandins Leukot Essent Fatty Acids, 2015. **93**: p. 31-6.

25. Ibanez-Shimabukuro, M., et al., *Resonance assignment of As-p18, a fatty acid binding protein secreted by developing larvae of the parasitic nematode Ascaris suum.* Biomol NMR Assign, 2014. **8**(1): p. 33-6.

26. Garofalo, A., et al., *The FAR proteins of filarial nematodes: secretion, glycosylation and lipid binding characteristics.* Mol Biochem Parasitol, 2002. **122**: p. 161-170.

27. Garofalo, A., et al., *The FAR protein family of the nematode Caenorhabditis elegans. Differential lipid binding properties, structural characteristics, and developmental regulation.* J Biol Chem, 2003. **278**(10): p. 8065-74.

28. Barletta, G.P., et al., *Fatty Acid and Retinol-Binding Protein: Unusual Protein Conformational and Cavity Changes Dictated by Ligand Fluctuations.* J Chem Inf Model, 2019. **59**(8): p. 3545-3555.

29. Vieira, P., K. Kamo, and J.D. Eisenback, *Characterization and silencing of the fatty acid- and retinol-binding Pp-far-1 gene in Pratylenchus penetrans.* Plant Pathology, 2017. **66**(7): p. 1214-1224.

30. Jordanova, R., et al., *Fatty acid- and retinoid-binding proteins have distinct binding pockets for the two types of cargo.* J Biol Chem, 2009. **284**(51): p. 35818-26.

31. Iberkleid, I., et al., *Structural characterization and localization analysis of the root-knot nematode Meloidogyne javanica fatty acid and retinol binding protein (Mj-FAR-1).* European Journal of Plant Pathology, 2015. **143**(1): p. 133-149.

32. L, J. and A. E, *The Potential Role of Binding Proteins in Human Parasitic Infections: An In-Depth Look at the Novel Family of Nematode-Specific Fatty Acid and Retinol Binding Proteins*, in *Binding Protein*. 2012.

33. Qiao, F., et al., *Characterization of Three Novel Fatty Acid- and Retinoid-Binding Protein Genes (Ha-far-1, Ha-far-2 and Hf-far-1) from the Cereal Cyst Nematodes Heterodera avenae and H. filipjevi.* PLoS One, 2016. **11**(8): p. e0160003.

34. Kuang, L., et al., *The complexity of the secreted NPA and FAR lipid-binding protein families of Haemonchus contortus revealed by an iterative proteomics-bioinformatics approach.* Mol Biochem Parasitol, 2009. **168**(1): p. 84-94.

35. Dillman, A.R., et al., *Comparative genomics of Steinernema reveals deeply conserved gene regulatory networks.* Genome Biol, 2015. **16**: p. 200.

36. Aymeric, J.L., A. Givaudan, and B. Duvic, *Imd pathway is involved in the interaction of Drosophila melanogaster with the entomopathogenic bacteria, Xenorhabdus nematophila and Photorhabdus luminescens.* Mol Immunol, 2010. **47**(14): p. 2342-8.

37. Duarte, A., et al., *Characterization of the venom allergen—like protein (vap-1) and the fatty acid and retinol binding protein (far-1) genes in Meloidogyne hispanica.* European Journal of Plant Pathology, 2014. **139**(4): p. 825-836.

38. Ramanathan, R., et al., *Microarray-based analysis of differential gene expression between infective and noninfective larvae of Strongyloides stercoralis.* PLoS Negl Trop Dis, 2011. **5**(5): p. e1039.

39. Rey-Burusco, M.F., et al., *Diversity in the structures and ligand-binding sites of nematode fatty acid and retinol-binding proteins revealed by Na-FAR-1 from Necator americanus.* Biochem J, 2015. **471**(3): p. 403-14.

40. Li, Y., et al., *A Bursaphelenchus xylophilus effector, Bx-FAR-1, suppresses plant defense and affects nematode infection of pine trees.* European Journal of Plant Pathology, 2020. **157**(3): p. 637-650.

41. Iberkleid, I., et al., *Fatty acid-and retinol-binding protein, Mj-FAR-1 induces tomato host susceptibility to root-knot nematodes.* PLoS One, 2013. **8**(5): p. e64586.

42. Phani, V., et al., *Meloidogyne incognita Fatty Acid- and Retinol- Binding Protein (Mi-FAR-1) Affects Nematode Infection of Plant Roots and the Attachment of Pasteuria penetrans Endospores.* Front Microbiol, 2017. **8**: p. 2122.

43. Parks SC, Nguyen S, Nasrolahi S, Bhat C, Juncaj D, Lu D, et al. (2021) Parasitic nematode fatty acid- and retinol-binding proteins compromise host immunity by interfering with host lipid signaling pathways. PLoS Pathog **17**(10): e1010027. https://doi.org/10.1371/journal.ppat.1010027

44. Sani, B.P. and A. Vaid, *Specificinteractionofivermectinwithretinol-bindingproteinfrom filarial parasites.* Biochem J, 1988. **249**: p. 929-932.

45. Yuan, D., et al., *Genus-level evolutionary relationships of FAR proteins reflect the diversity of lifestyles of free-living and parasitic nematodes.* BMC Biol, 2021. **19**(1): p. 178.

Chapter 2

Parasitic nematode fatty acid- and retinol-binding proteins compromise host immunity by interfering with host lipid signaling pathways

Sophia C. Parks[1], Susan Nguyen[1], Shyon Nasrolahi[1,6], Chaitra Bhat[1], Damian Juncaj[1], Dihong Lu[1], Raghavendran Ramaswamy[2], Harpal Dhillon[1], Hideji Fujiwara[3], Anna Buchman[4], Omar S. Akbari[4], Naoki Yamanaka[5], Martin J. Boulanger[2], and Adler R. Dillman[1*]

[1]Department of Nematology, University of California, Riverside, California, 92521, USA.

[2]Department of Biochemistry and Microbiology, University of Victoria, BC, Canada V8P 5C2

[3]Division of Endocrinology, Metabolism, and Lipid Research, Washington University School of Medicine, St. Louis, Missouri, 63110, USA.

[4]Division of Biological Sciences, Section of Cell and Developmental Biology, University of California, San Diego, La Jolla, California, 92093, USA.

[5]Department of Entomology, University of California, Riverside, California, 92521, USA.

[6]Present address: Keck School of Medicine, University of Southern California, Los Angeles California, 90033, USA.

* Corresponding: adlerd@ucr.edu

A version of this chapter is published in *PLoS Pathogens* 2021

Graphical Abstract

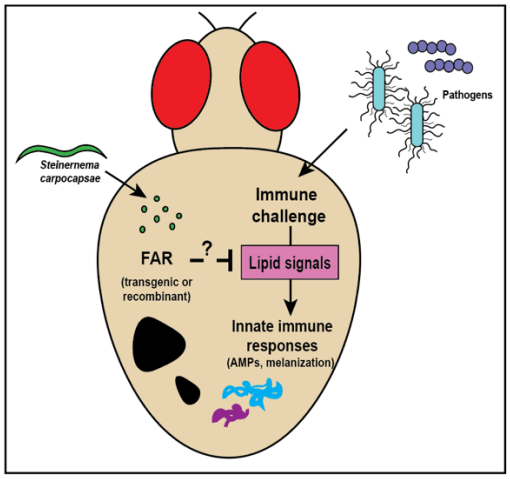

Abstract

Parasitic nematodes cause significant morbidity and mortality globally. Excretory/secretory products (ESPs) such as fatty acid- and retinol- binding proteins (FARs) are hypothesized to suppress host immunity during nematode infection, yet little is known about their interactions with host tissues. Leveraging the insect parasitic nematode, *Steinernema carpocapsae*, we describe here the first *in vivo* study demonstrating that FARs modulate animal immunity, causing an increase in susceptibility to bacterial co-infection. Moreover, we show that FARs dampen key components of the fly immune response including the phenoloxidase cascade and antimicrobial peptide (AMP) production. Our data also reveal that FARs deplete lipid signaling precursors *in vivo* as well as bind to these fatty acids *in vitro,* suggesting that FARs elicit their immunomodulatory effects by altering the availability of lipid signaling molecules necessary for an efficient immune response. Collectively, these data support a

complex role for FARs in immunosuppression in animals and provide detailed mechanistic insight into parasitism in phylum Nematoda.

Author Summary

A central aspect of parasitic nematode success is their ability to modify host biology, including evasion and/or subversion of host immunity. Modulation of host biology and the pathology caused by parasitic nematodes is largely effected through the release of proteins and small molecules. There are hundreds of proteins released by nematodes during an infection and few have been studied in detail. Fatty acid- and retinol-binding proteins (FARs) are a unique protein family, found only in nematodes and some bacteria, and are released during nematode infection. We report that nematode FARs from *S. carpocapsae*, *C. elegans* and *A. ceylanicum* dampen fly immunity decreasing resistance to infection. Mechanistically, this is achieved through modulation of the phenoloxidase cascade and antimicrobial peptide production. Furthermore, FARs alter the availability of lipid immune signaling precursors *in vivo* and show binding specificity *in vitro*.

Introduction

Helminths cause significant morbidity and mortality on a global scale through human disease, sickening of livestock, and a reduction in crop yield [1,2]. Parasitic nematodes are responsible for significant human suffering with a striking 1.5 billion people infected with soil-transmitted helminths alone [3]. Much of the nematodes' success in parasitism is due to their ability to disguise themselves from host immune defenses. Despite the importance of these organisms to human and animal health, little is understood about the molecular mechanisms that underpin these stealth processes. Increasing our

understanding of immune modulation by parasitic nematodes has the significant potential to inform treatment of such infections and lead to therapeutics for immune dysregulation such as autoimmune disorders.

Protein and small-molecule effectors are crucial for parasites to successfully infect plants, invertebrates, and vertebrate hosts [4,5]. Upon infecting their hosts, nematodes release excretory/secretory products (ESPs) into surrounding tissues, which are the primary point of interaction between the parasite and host and are hypothesized to aid in nematode survival and cause damage to the host. A variety of proteins are found in nematode ESPs, some of which are known to cause tissue damage and modulate host immunity. One family of proteins released by parasitic nematodes is the fatty acid- and retinol-binding protein family (FARs). FARs are small (~20 kDa), alpha-helix rich, and may be responsible for sequestering essential lipids required for reproduction and development [6]. FARs were first discovered in the filarial nematode *Onchocerca volvulus*, the causative agent of river blindness. FARs have subsequently been identified in the free-living nematode *Caenorhabditis elegans* as well as several other nematode parasites of animals, plants, and insects [7-9]. In *C. elegans*, FARs are localized in the hypodermis, head and lips which are regularly in contact with the outside environment, as well as the excretory cell connected to the hypodermis [10].

FARs have attracted attention because they were shown to be secreted by parasitic nematodes and are strongly immunogenic in infected hosts [8,11-13]. Moreover, several

studies suggested that FAR proteins modulate plant immunity. The strongest evidence comes from a study on a FAR protein from the plant-parasitic nematode *Meloidogyne javanica*, which, when expressed *in planta*, has been shown to increase the host susceptibility to further infection [14]. FARs are released by infectious-stage parasites, and therefore several studies have suggested the importance of FARs in facilitating parasitism by sequestering host retinol and/or fatty acids interfering with or suppressing immunity [15,16]. Previous research papers on FAR proteins from animal-parasitic nematodes suggest that FARs modulate animal immunity, yet no studies have investigated this experimentally. The functional role of these proteins in animal hosts as well as the mechanism of action behind these functions remains unknown.

One of the challenges to studying these host-parasite interactions is the paucity of studies in model systems to develop testable hypotheses about effector function during infection. Using an insect-parasitic nematode model allows studies to be conducted on large populations and some insect-parasitic nematode species are closely related to vertebrate-parasitic species, leading to insights that may be directly applicable to mammalian diseases [17,18]. Entomopathogenic nematodes (EPNs) are parasites of insects that are related to skin-penetrating nematodes of mammals such as *Strongyloides stercoralis* [19-21]. Using the EPN *Steinernema carpocapsae* as a model parasite and the fruit fly *Drosophila melanogaster* as a model host provides a robust system to characterize potential effectors such as FARs. The fruit fly is a powerful genetic model with a complex innate immune system containing mechanisms conserved in mammals [22]. The

D. melanogaster immune response has been a powerful model for mammalian immunity and is divided into two innate response types; cellular and humoral immunity [23,24]. Furthermore, immune responses are generally activated by two main NF-kB signaling pathways, Toll and Imd, similar to human toll-like receptors (TLR) and tumor necrosis factor (TNF) signaling respectively [25]. The Toll and Imd pathways are activated by different pathogens, depending on properties such as cell wall constituents. The cellular response is carried out by hemocytes and involves processes that surround and kill the invading pathogen including phagocytosis and encapsulation, whereas the humoral response involves the generation of antimicrobial peptides (AMPs) by the fat body, analogous to the mammalian liver and adipose tissues. AMPs are small, cationic and often amphipathic peptides that function as endogenous antimicrobials that "mop up" pathogens left over from the cellular immune defense system by disrupting negatively charged microbial membranes. Systemic production of AMPs is controlled by the two NF-kB pathways, Toll and Imd [24,28]. A combinatorial response by the innate immune system is likely elicited during a nematode infection [26].

In this study, we tested the hypothesis that nematode FAR proteins (Sc-FARs) can dampen the animal immune response (*D. melanogaster*) in the context of various bacterial infections. This work is the first to demonstrate that nematode FARs are detrimental to the outcome of infection and are directly immunomodulatory in an animal system. Significant immune suppression by FARs was observed resulting in decreased host survival to bacterial infections, accompanied by a significant increase in microbe

growth. To understand how Sc-FARs modulate host immunity several readouts of *Drosophila* immunity were assessed including AMP production and phenoloxidase activity. Potential FAR binding partners were assessed using metabolomics and *in vitro* protein-metabolite interactions. In addition to demonstrating the potent immunomodulatory effect of FARs in an animal, these data led us to propose a model for nematode FAR modulation of host immunity.

Results

Genomic analysis of S. carpocapsae revealed an expansion of FAR proteins

Analysis of the genome sequence of the generalist insect-parasitic nematode *S. carpocapsae* revealed an expansion of FARs compared to other nematodes [20]. We evaluated the presence of FARs in a variety of parasitic nematodes and *C. elegans* and found a dynamic range of putative FAR-encoding genes among nematode genomes (Table 1). We found that *S. carpocapsae* had the most with 45 putative FAR proteins, compared to 9 in *C. elegans*, 16 in *S. stercoralis* and 5 in *Ascaris lumbricoides* (Table 1). While FARs are thought to be essential for lipid sequestration, we found no putative FAR-encoding genes in either *Trichinella spiralis* or *Trichiuris muris*, suggesting that either these nematodes have divergent putative FAR genes that were not recognizable by sequence similarity, or that they have evolved a different strategy to acquire lipids from their hosts. Of the 45 putative FARs in *S. carpocapsae*, 5 FARs were found in the ESPs of an *in vitro* infection model [27]. We chose the 2 found in highest abundance, Sc-FAR-1 (L596_023208) and Sc-FAR-2 (L596_016036), for further study.

FAR encoding genes												
Spp.	*Scar*	*Acey*	*Sste*	*Alum*	*Bmal*	*Cele*	*Dmed*	*Hcon*	*Ovol*	*Nbra*	*Tspi*	*Tmur*
# of genes	45	24	16	5	3	9	3	11	3	12	0	0

Table 2.1: Number of putative FAR-encoding genes present in the genomes of various nematode species. Species in order from left to right: *Steinernema carpocapsae* (Scar)*, Ancylostoma ceylanicum* (Acey)*, Strongyloides stercoralis* (Sste)*, Ascaris lumbricoides* (Alum)*, Brugia malayi* (Bmal)*, Caenorhabditis elegans* (Cele)*, Dracunculus medinensis* (Dmed)*, Haemonchus contortus* (Hcon)*, Onchocera volvulus* (Ovol)*, Nippostrongylus brasiliensis* (Nbra)*, Trichinella spiralis* (Tspi)*, Trichiuris muris* (Tmur). *T spiralis* and *T. muris* have no known FAR encoding genes while *S. carpocapsae* shows the greatest expansion of FAR genes in its genome.

Nematode FAR proteins modulate host immunity decreasing resistance to bacterial pathogens

To investigate the immunomodulatory effects of FARs, we used *D. melanogaster* as a model host and the two most abundant ESP-derived *S. carpocapsae* FARs Sc-FAR-1 and Sc-FAR-2, hereafter referred to as FAR-1 and FAR-2, respectively. We tested *D. melanogaster*'s susceptibility to *S. carpocapsae* nematode infection but found that when flies are infected with any number of infective juveniles IJs, they die quickly, and none are able to recover (Figure S2.1). This makes is difficult to observe immune modulation during an *S. carpocapsae* infection in flies. Therefore, to measure immune modulation by FARs in flies, we utilized a bacterial infection and first determined the LD_{30} dose of the Gram-positive, extracellular pathogen, *Streptococcus pneumoniae* in OregonR flies and established the appropriate dose for injection and the baseline outcome of infections at this dose (Figure S2.2). The outcome of infection was assessed using fly survival and microbial growth over time. We found that the LD_{30} (the dose that kills 30% of adult flies in the first 2-7 days post infection) is the optimal dose for injection, since it provides

sufficient sensitivity to detect shifts in the outcome of infection. Recombinant FAR-1 and FAR-2 were co-injected into adult flies, mimicking an EPN infection with delivery of the protein and pathogenic bacteria into the hemocoel. These experiments revealed that a one-time dose of FAR-1 and/or FAR-2 co-injected with the LD_{30} dose of *S. pneumoniae* significantly affects the outcome of bacterial infection in flies. A dose-dependent effect was observed where a high dose (250 ng) decreased host survival while lower doses did not elicit the same effect (Figures 2.1A and 2.1B). We found no additive effects of FAR-1 and FAR-2 after co-injection (Figure S2.3). We measured microbe growth over time for FAR-2 recombinant injections due to its dose-dependent spread of effects on the outcome of survival. A trend in increased microbial load was also observed, where the flies injected with the highest dose of FAR had a greater number of bacterial cells 24-hours post-injection (Figure 2.1C). Heat-denatured recombinant FAR-1 or FAR-2 was co-injected at the highest dose tested (250 ng); no difference was observed when compared to *S. pneumoniae*-only injected flies, confirming that the addition of folded, recombinant FAR in a one-time dose alters the flies' ability to deal with pathogenic infection (Figure S2.4).

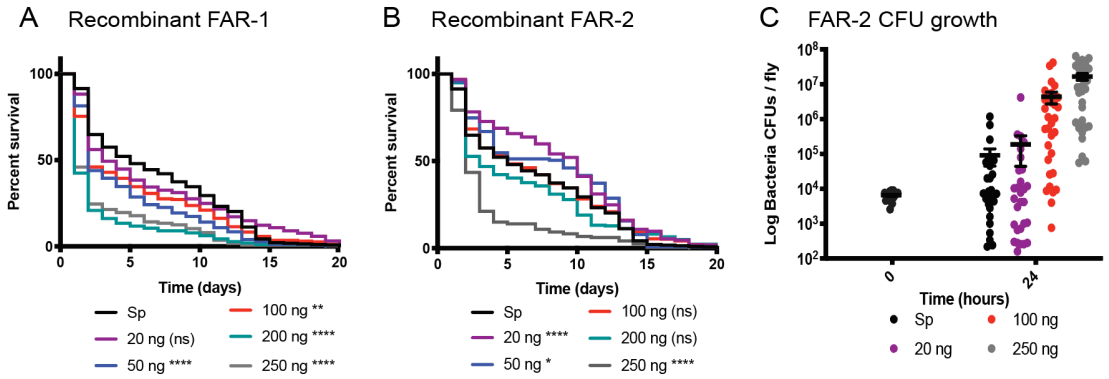

Figure 2.1: Recombinant FARs reduced fly survival in a dose-dependent manner. A&B) 7,000 CFUs of *S. pneumonia* (*Sp*) were co-injected with various nanogram doses of either Sc-FAR-1 or -2. C) CFUs were measured at 24 hours post-injection for panel B which shows a trend of increased bacterial growth with increasing protein doses. All controls for survival curves (black) are *Sp*-injected only, without the addition of FAR proteins. Time 0 CFUs representative of all fly strains. Log-rank test p-value significance indicated by asterisks on Kaplan Meier graphs. CFU graphs show p-value significance of an unpaired t-test (error bars show mean+SEM). Survival curves n≥180, CFU graph n≥24. All raw data available in supplemental materials.

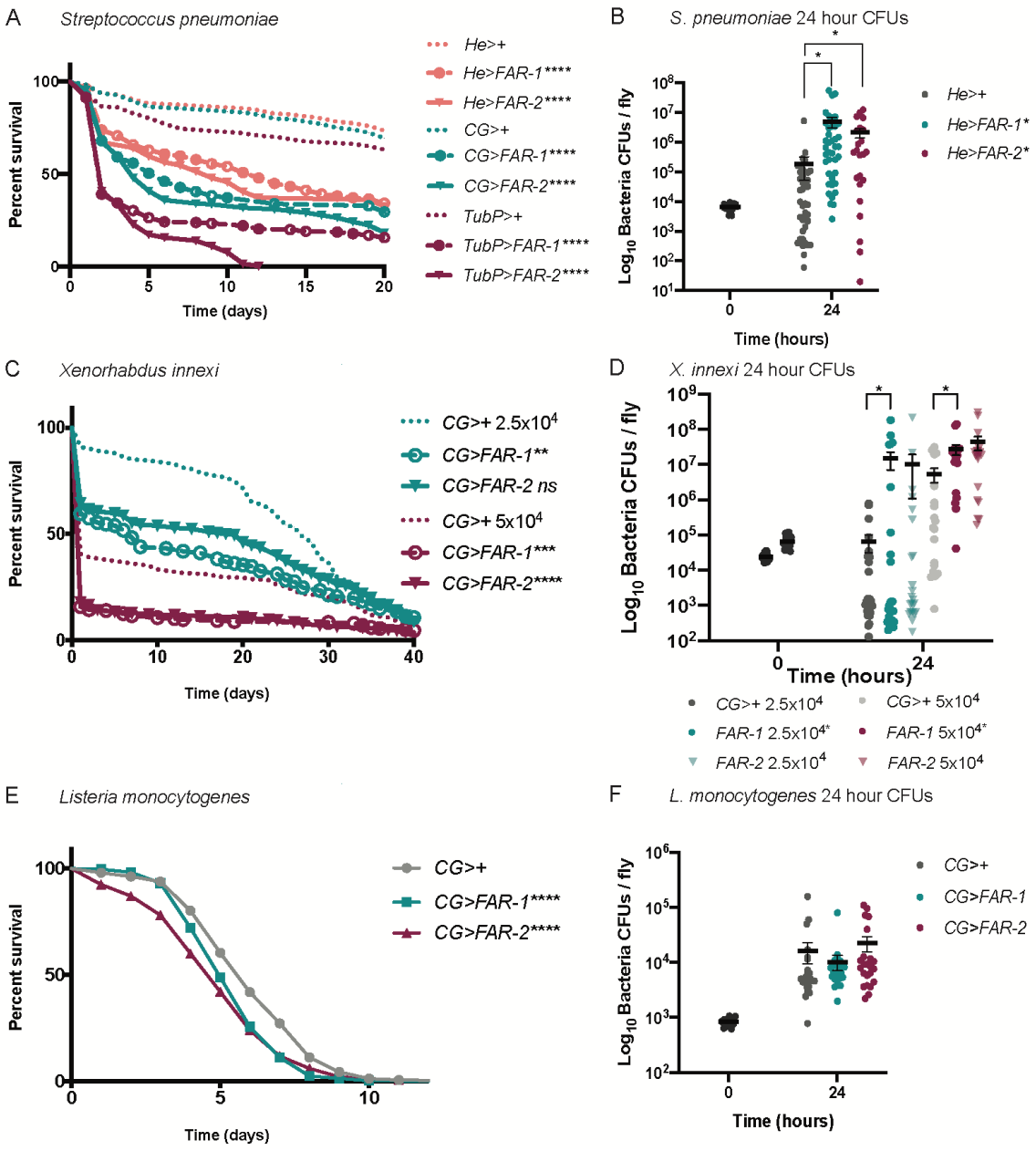
A
Streptococcus pneumoniae
Percent survival
Time (days)
He>+
He>FAR-1****
He>FAR-2****
CG>+
CG>FAR-1****
CG>FAR-2****
TubP>+
TubP>FAR-1****
TubP>FAR-2****
B
S. pneumoniae 24 hour CFUs
Log10 Bacteria CFUs / fly
Time (hours)
He>+
He>FAR-1*
He>FAR-2*
C
Xenorhabdus innexi
Percent survival
Time (days)
CG>+ 2.5x10^4
CG>FAR-1**
CG>FAR-2 ns
CG>+ 5x10^4
CG>FAR-1***
CG>FAR-2****
D
X. innexi 24 hour CFUs
Log10 Bacteria CFUs / fly
Time (hours)
CG>+ 2.5x10^4
CG>+ 5x10^4
FAR-1 2.5x10^4*
FAR-1 5x10^4*
FAR-2 2.5x10^4
FAR-2 5x10^4
E
Listeria monocytogenes
Percent survival
Time (days)
CG>+
CG>FAR-1****
CG>FAR-2****
F
L. monocytogenes 24 hour CFUs
Log10 Bacteria CFUs / fly
Time (hours)
CG>+
CG>FAR-1
CG>FAR-2

Figure 2.2: Transgenic FAR expression significantly decreases fly survival and increases bacterial load 24-hours post-injection. Flies were injected with specified doses of various pathogens. Survival was monitored daily and bacterial load was measured 24 hours post-injection. A&B) Flies FAR-1 & -2 expressed with a tubulin driver (TubP), a fat body, hemocyte and lymph gland specific driver (CG), and a hemocyte only driver (He) were injected with 7,000 CFUs of *Streptococcus pneumoniae*. Survival curves of flies are shown in (A) and bacterial CFUs in the He driver flies at 24-hour post injection in (B). C&D) Flies with FAR-1 & -2 expression with the CG driver were injected with 25,000 and 50,000 CFUs (shown at time 0) of *Xenorhabdus innexi*. Survival curves of flies are shown in (C) and bacterial CFUs in (D). E&F) Flies with FAR-1 & -2 expression with the CG driver were injected with 1,000 CFUs of *Listeria monocytogenes*. Survival curves of flies are shown in (E) and bacterial CFUs in (F). All controls are 86Fa flies crossed with flies containing the specified driver. Time 0 CFUs representative of all fly strains (depicted in black). Statistics shown as log-rank test p-value for survival curves and unpaired t-test for microbe growth with (error bars show mean+SEM). Survival curves n≥180, CFU graph n≥24 over at least 3 experiments. All raw data available in supplemental materials.

In addition to a one-time injection of recombinant of FAR-1 and FAR-2, we also determined the outcome of infection using transgenic flies expressing either FAR-1 or FAR-2. We ectopically expressed these FARs in flies using the Gal4/UAS system and confirmed expression with Western blot (Figures S2.5 and S2.6). We also evaluated the effects of *C. elegans*-derived FAR-8 and a FAR from the human hookworm *A. ceylanicum* (Figure S2.7). Flies expressing nematode FAR proteins in the fat body, hemocytes, and salivary glands in the absence of bacterial infection are healthy and have a normal lifespan (Figure S2.8). An expression-dependent decrease in survival in a bacterial infection model, was observed with strong, ubiquitous expression resulting in the most severe decrease in survival. Expression of FARs only in the hemocytes had the least severe effect on the outcome of infection (Figure 2.2A). The effect observed on survival is specific to FAR-expressing flies since their genetic control did not elicit the same effect (Figure S2.9). In addition, overexpression of mCherry, a protein irrelevant to

the system, does not have any effect on outcome of bacterial infection (Figure S2.10). FAR-expressing flies also displayed a significant increase in microbial load 24 hours post-injection (Figure 2.2B). To determine whether this effect was pathogen-specific, the Gram-negative EPN symbiont *Xenorhabdus innexi*, one of the least virulent bacteria in the genus, was also injected to induce an immune response [28]. Similar to *S. pneumoniae* infection alone, flies expressing FAR-1 had a significant decrease in survival for both doses, whereas FAR-2-expressing flies were only affected when injected with the higher dose (Figure 2.2C). CFUs were also measured post-injection. A significant increase in microbial load was observed in both FAR-1 & 2-expressing flies (Figure 2.2D). The intracellular Gram-positive pathogen *Listeria monocytogenes* was also tested. We found FAR expressing flies to have the same decrease in survival, however there was no significant difference in microbe load 24 hours post-injection (Figures 2.2E and 2.2F). These data demonstrate that FARs significantly affect the outcome of a bacterial infection, in a dose dependent manner, by decreasing survival post infection and dampening the ability of the flies to control the bacterial growth over time. Interestingly, flies expressing *C. elegans* FAR-8 and a FAR from the human hookworm *A. ceylanicum* showed a similar immune deficient phenotype when challenged with an *S. pneumoniae* infection (Figure S2.7). This suggests that the immunomodulatory effects of FARs are conserved across taxa, solidifying the value of this model for understanding the mechanism of FARs in parasitic infection.

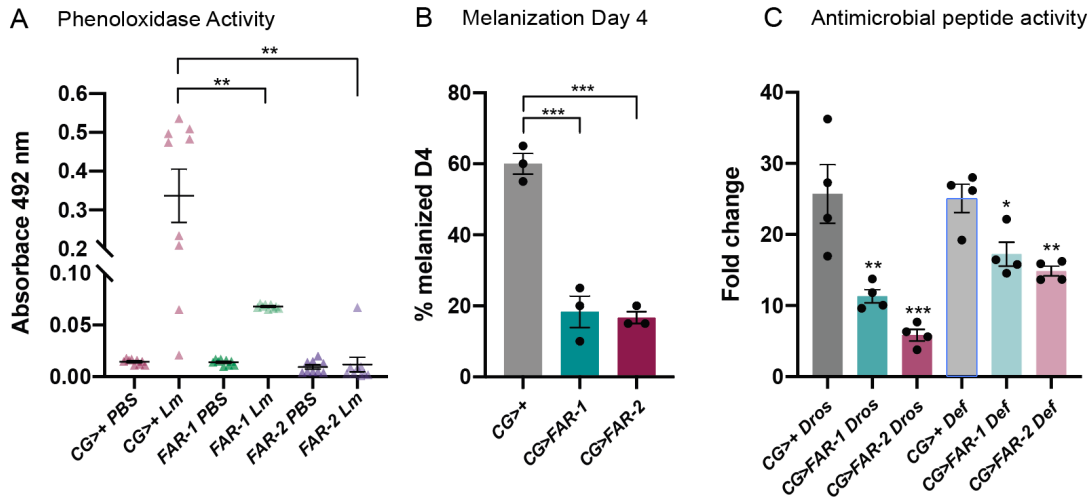

Figure 2.3: Melanization, phenoloxidase and antimicrobial peptide activity were diminished in FAR expressing flies. A) Flies were injected with the LD_{30} of *L. monocytogenes* (1,000 CFUs) and phenoloxidase activity was measured 6 hours post-injection. B) Flies were injected with the LD_{30} of *L. monocytogenes* and disseminated melanization was observed 4 days post-injection. C) 24 hours post-injection with the LD_{30} dose of *S. pneumoniae* the relative increase in the antimicrobial peptides (AMP) *Drosomycin* (Toll) and *Defensin* (Imd) were analyzed. Compared to the CG>+ control, FAR-1 and -2 significantly suppress both AMPs. Four experiments were completed with 15 flies per experimental group. Asterisks indicate statistical significance from one-way ANOVA (A & C) and unpaired t-test (B). All experiments were repeated at least 3 times, error bars show mean+SEM. All raw data available in supplemental materials.

FARs dampen key aspects of immunity in D. melanogaster

D. melanogaster has a sophisticated, evolutionarily conserved, innate immune response that can be categorized into two main branches: a systemic humoral response, and a cellular response mainly carried out by various types of hemocytes (Figure S2.11). To establish the mechanism by which FAR-1 and FAR-2 elicit their immunomodulatory effects, we evaluated several readouts of immunity including phenoloxidase (PO) activity and melanization, which are essential immune defenses during a bacterial infection. Disseminated melanization and PO activity was measured post-injection with *L.*

monocytogenes, which elicits a robust disseminated melanization phenotype 4 days post injection [29]. Flies expressing FAR-1 and FAR-2 showed a significant decrease in survival when injected with ~1,000 CFUs of *L. monocytogenes* (Figure 2.2E). After injection with 1,000 cells of *L. monocytogenes*, FAR-1 and FAR-2 expressing flies were unable to initiate PO activity six hours post-infection (Figure 2.3A). Similarly, disseminated melanization, measured as two or more melanization spots throughout the body, was reduced to only 20%, from 60% in controls, of the population in FAR-expressing flies 4 days post-injection (Figure 2.3B). To further investigate the effect of FARs on innate immunity we assessed their effect on the production of AMPs. We performed RT-qPCR to measure expression levels of two AMP-encoding genes: *Defensin*, mostly regulated by the Imd pathway, and *Drosomycin*, mostly regulated by the Toll pathway [30]. After infection with *S. pneumonia*, both FAR-1 and -2 expressing flies exhibit at least a 14-fold reduction in the AMP response for both *Drosomycin* and *Defensin* (Figure 2.3C). Collectively, these data demonstrate that FARs dampen key aspects of immunity.

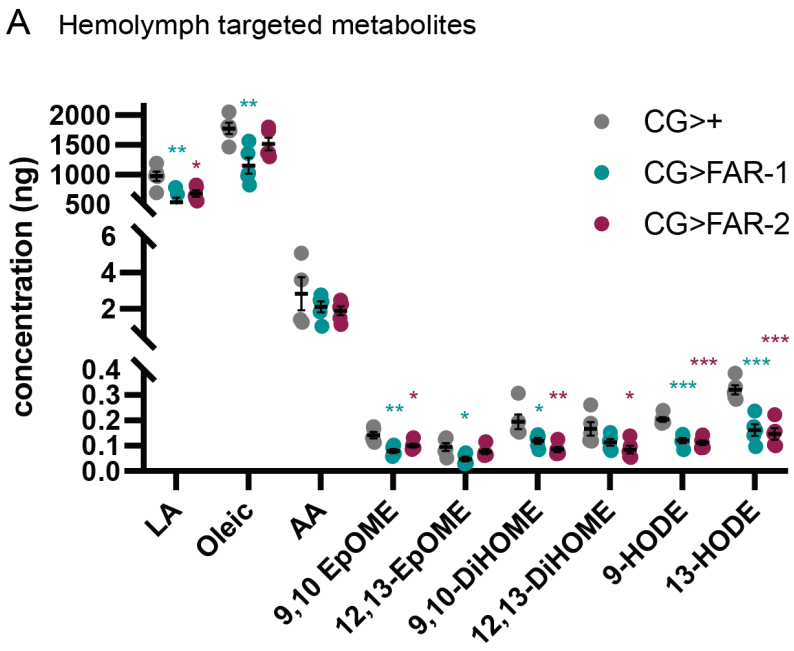

Figure 2.4: Metabolite abundance in FAR expressing and control hemolymph. A) Fly hemolymph samples were analyzed for abundance of various lipids. 9(10)- and 12(13)- EpOME, 9- and 13-HODE and arachidonic acid were depleted in FAR-1 expressing flies. Statistics shown as an unpaired t-test and error bars show mean+SEM. Asterisk color for significance matches sample color. All raw data available in supplemental materials.

FARs alter in vivo fatty acid availability including putative immune signaling molecules

To determine the molecular mechanism underlying the immunomodulatory effects of FAR-1 and FAR-2, we initially screened for potential metabolites available to FAR using an untargeted metabolomics approach. We found many phosphatidylcholines (PC), phosphatidylethanolamines (PE), as well as multiple fatty acids that were less abundant in FAR-expressing flies, suggesting they are somehow depleted by FARs (Figure S2.12). Since many of the molecules that were significantly altered were unclassified, we moved to a targeted metabolomics approach. During an infection, FARs are released into the

host tissue and may remain in circulation to elicit their immunomodulatory effects. Therefore, we proceeded to test differences in lipid metabolite abundance in the hemolymph of the FAR-1- and FAR-2-expressing flies, as well as control flies. Hemolymph was collected from 200 male flies and lipid concentrations between groups were assessed with targeted metabolomics. We found that several fatty acid metabolites including both 9(10)-EpOME and 12(13)-EpOME, which are epoxide derivatives of linoleic acid and leukotoxins in mammals, were significantly lower in FAR-1-expressing flies when compared to the genetic control. Linoleic acid, oleic acid, 9,10-DiHOME, 12,13-DiHOME, 9-HODE, and13-HODE were also significantly reduced in FAR-expressing flies (Figure 2.4).

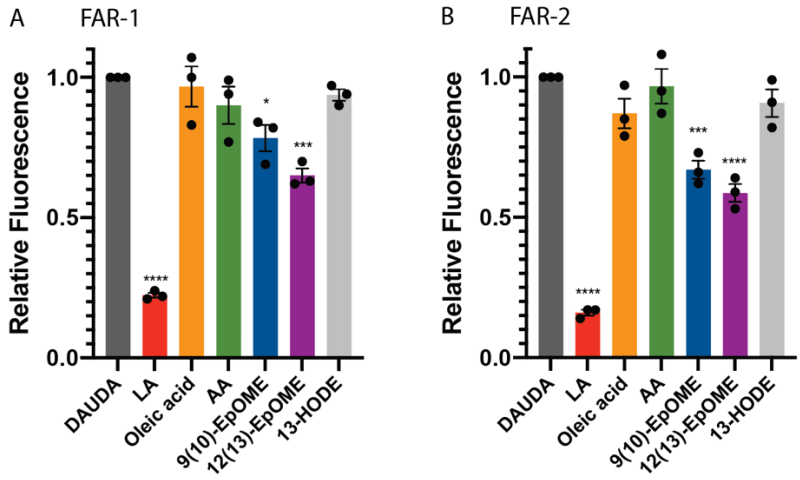

Figure 2.5: In vitro binding of Sc-FARs. A&B) Competitive binding between 10-fold excess linoleic (LA), oleic, arachidonic (AA) acid, and other fatty acids (all 10 µM) and DAUDA (1 µM) was tested in the context of FAR-1 & 2. Linoleic acid displaces DAUDA the most, as seen by the largest reduction in relative fluorescence. Both 9(10)- and 12(13)-EpOME displace DAUDA more easily in the presence of FAR-2, showing tighter binding. Statistics shown as One-way ANOVA and error bars show mean+SEM. All raw data available in supplemental materials.

FARs have measurable differences in binding specificity in vitro

To determine potential binding partners of FARs, we measured the binding affinity to various fatty acids and retinol *in vitro*. Initially, we determined the binding affinity of both Sc FARs to the 11-(Dansylamino) undecanoic acid (DAUDA), and retinol, by calculating the equilibrium dissociation constant (Kd) (Figures S2.10A, B and S2.11AB). We found the Kd to be in the 1-10 μM range (Figures S2.13C, D and S2.14C, D). Using DAUDA as the fluorophore, we tested various fatty acids in 10-fold excess in competition with DAUDA to determine preferred fatty acid binding partners for FARs *in vitro*. When FAR binds to a fatty acid in this assay, DAUDA is displaced from the protein resulting in a reduction in peak fluorescence intensity (Figures S13E, F). Linoleic acid caused the greatest displacement of DAUDA and 9(10)- and 12(13)-EpOME disrupted DAUDA bound to FAR-2 greater than FAR-1 (Figure 2.5). The results indicated that FAR-1 & 2 have measurable differences in binding specificity, suggesting that they may target different lipid signaling molecules during infection.

Discussion

The results of this study provide the first evidence demonstrating that FARs alter the animal immune response. Understanding how parasitic nematodes circumvent host immune responses has significant potential to inform therapeutic intervention strategies. Much of what is known about FAR proteins and their potential interactions with host immunity comes from *in vitro* studies [31-35]. FARs initially attracted attention because they are excreted by parasitic nematodes during an active infection and elicit a host

immune response [8,11-13]. A previous study has shown that FARs increase host susceptibility to nematode infections in plants however after performing *S. carpocapsae* nematode infections, we found that once a fly was infected with even one nematode it was unable to recover from the infection and died quickly [14]. This makes it especially difficult to determine variation in immune responses since the infection is rapidly lethal at any dose. To investigate FAR's effects on immunity we utilized bacterial infections and found that the outcome of infections are significantly worse in flies when FARs are present.

FAR effects on innate immunity

We have investigated the specific aspects of immunity that are affected by FARs, and found modulation of various mechanisms including phenoloxidase activity, a key mechanism to control invading parasites, and antimicrobial peptide production. Upon injury or infection, insects rapidly initiate the melanization cascade leading to deposition of melanin along the wounding site and around invading microbes or pathogens. This serves to block invading pathogens, prevent excess hemolymph loss, and to encapsulate and kill pathogens with reactive oxygen species (ROS) and other toxins. Melanization is independent of the classical immune pathways (Toll & Imd). Rather, it is dependent upon activation of prophenoloxidase (proPO), which is a proenzyme that is cleaved by prophenoloxidase activating enzyme (PPAE) to its active form phenoloxidase (PO). Phenoloxidase is the catalyst for the oxidation of mono- and diphenols to orthoquinones, which form polymers with melanin non-enzymatically, during which ROS is produced [24,36]. Since the family of FAR proteins is highly conserved among many nematode

species it is important to understand whether FARs elicit their immunomodulatory effects in similar ways (Table 1) [36]. Slight differences between the effects of the two Sc-FARs are apparent in flies challenged with *X. innexi*, where FAR-2 expressing flies given a 25,000 CFU dose did not do significantly worse than the control flies, as well as the recombinant studies and AMP production, pointing to a potential mechanistic specificity of FARs. We performed additive recombinant FAR-1 and FAR-2 co-injections and found no difference between a 250 ng dose of FAR-1 or FAR-2 and a 125 ng FAR-1 plus 125 ng FAR-2 combined dose showing that FAR does not have an additive effect. FAR-1 and 2 seem to have similar *in vivo* effects, at least at the level of the outcome of infection, leading us to believe that downstream immune effects are also being affected in similar ways not specific enough to evaluate their differences. We found that even a one-time dose of recombinant FAR has severe adverse effects on the outcomes of a bacterial infection. Flies generally exhibited a decrease in survival in a dose-dependent manner, beginning with a 50 ng dose of FAR-1. During a bacterial infection the host is harmed by two factors: the pathogen and the immune response. In experiments with FAR-2, low doses (20 ng and 50 ng) led to significantly improved survival, which we hypothesize is due to the suppression of immune-induced damage. Although 250 ng is likely greater than physiological concentrations of FAR during EPN infections, it is remarkable that such a phenotype was observed with only a single component of a complex array of venom proteins found in ESPs, where hundreds of proteins usually act in concert to dampen host immunity. Interestingly, FARs not only modulate measurable outputs of immunity but affect the outcome of infection.

Interactions of FARs and host lipid signaling pathways

A key component of understanding how nematodes utilize FARs to dampen host immunity is to understand the mechanism underlying their interactions with immune molecules. We hypothesize that FARs bind to lipids that function as signaling molecules for a diverse range of functions including inflammation, immunity, homeostasis, and reproduction. It has been proposed that most terrestrial insects lack free long-chain polyunsaturated fatty acids (LC-PUFAs) including arachidonic acid (AA), due to its role in oxidative stress [37,38]. Insects have high levels of reactive oxygen species (ROS), such as the superoxide anion (O_2^-), due to their significant production of ATP in the mitochondrial electron transport chain. These ROS can escape the mitochondria and often react with AA and other LC-PUFAs causing lipid peroxidation leading to damaged cell membranes and possible adduct formation to proteins and nucleic acids, giving rise to additional cell damage [37-39]. In mammals, free AA is released when phospholipase A_2 (PLA_2) cleaves phospholipids directly from the membrane. In insects however, PLA_2 has been predicted to yield free linoleic acid (LA) which is then elongated to AA and subsequently converted to downstream lipids such as prostaglandins and leukotrienes that are essential signaling molecules in the immune response (Figure 2.6) [37,40]. Our untargeted metabolomics study revealed that phosphatidylcholine (PC) and phosphatidylethanolamine (PE) were reduced in FAR expressing flies (Figure S2.12). These are essential phospholipids usually incorporated into the cell membrane that give rise to many downstream lipids that could have diverse functions including immune signaling and regulation [41]. We hypothesize that they are depleted by a compensatory

mechanism where more phospholipid is cleaved from the membrane and converted to downstream fatty acids that are likely sequestered and depleted more readily by FARs. Interestingly, our metabolite study of hemolymph shows a low but measurable concentration of AA, with much higher concentrations of C:18 fatty acids including oleic and linoleic acids. These data support the hypothesis that in insects, LA is cleaved directly from the lipid bilayer, providing evidence for the linoleic-to-arachidonic model of C20 biosynthesis in insects. Our data also show that FAR binds tightly to LA and not AA, *in vitro*. We hypothesize that although LA is depleted by FARs, the depletion of downstream lipid products such as 9-HODE and 13-HODE have a more significant effect on immune signaling. In mammals, pro- and anti- inflammatory lipids are produced from identical precursors with the enzymes from each branch competing for substrate [42,43]. Therefore, the regulation of enzyme availability decides the outcome of the immune response. Interestingly, PLA_2 is turned on by the Toll and Imd pathways in *D. melanogaster* and inhibited by the bacterial symbionts of EPNs, *Xenorhabdus* and *Photorhabdus* (Figure 2.6) [28,41,44,45]. It is possible that in *Drosophila* a similar network for substrate and enzyme availability takes place, however the identity of pro- and anti-immune lipid signaling molecules is yet to be determined in this model.

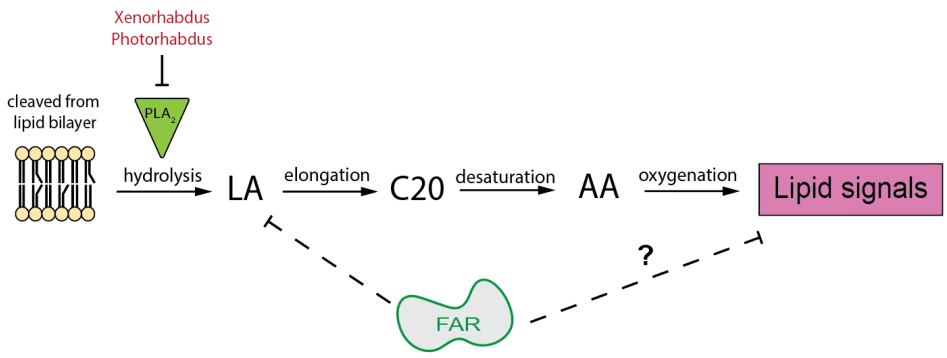

Figure 2.6: Key components of lipid biosynthesis in insects. Our hypothesis is that FAR is sequestering essential fatty acids and/or their upstream lipids to disrupt lipid signaling that is necessary for certain host immune functions. We have shown FARs' ability to bind to L*A in vit*ro which could temporarily disrupt downstream eicosanoid signaling. In insects, phospholipase A2 cleaves linoleic acid (LA) from the lipid bilayer instead of arachidonic acid in mammals. Free LA is then extended via an elongase to a C20 fatty acid. Desaturase oxidizes the C20 to arachidonic acid which can then be oxygenated to yield eicosanoid-like molecules. Eicosanoids are involved in many important functions including gene expression, immune regulation and reproduction. Adapted (Stanley, 2018 #102).

Lipid signals have important roles in mammalian immunity and have been hypothesized to play similar roles in insect immune defenses [46]. We found that *S. carpocapsae* FARs bind to LA and oxidized metabolites of LA *in vitro*, which may suggest their preferred *in vivo* binding partners. Our metabolomics studies showed that FARs deplete linoleic acid, oleic acid, 9(10)- and 12(13)-EpOME, 9,(10)- and 12(13)- DiHOME, and 9- and 13-HODE from the blood of flies. These lipids are known to modulate diverse physiological functions in mammals and have been shown to regulate immunity in insects [47]. 13-HODE has anti-inflammatory functions in mammalian immunity and is often increased under oxidative stress triggered during a disease response, are depleted in the hemolymph of FAR expressing flies [48,49]. During a mammalian immune response, 9(10)- and

12(13)-EpOME are activated by and interact with inflammatory leukocytes or neutrophils [48]. These data support the hypothesis that FARs modulate host immunity by binding to the oxidation products of LA or its upstream precursors to dampen the immune response (Figure 2.6). While little is known about how nematodes use FARs and other ES molecules to interact with host immunity, model systems continue to be invaluable in elucidating functional activity and yielding hypotheses that can be further tested.

In summary, this study shows experimentally that FAR-1 and FAR-2 from *S. carpocapsae* dampen the host immune response and provides evidence that nematodes likely utilize other ESPs in conjunction with FARs to modulate host immunity. These data lead us to hypothesize that FARs act by disrupting lipid signaling necessary for immune responses. Deepening our understanding of how nematode parasites evade or suppress host defenses is key to further our development of treatment options for these infections, and may lead to the development of novel treatments for autoimmune disorders.

Methods

Fly stock/ maintenance

All fly strains were grown on D2 glucose medium from Archon Scientific (Durham, North Carolina) and kept at 25°C with 50% humidity on a 12h light 12h dark cycle.

Nematode Infection assays

Infection of OregonR and transgenic *D. melanogaster* adult flies with the infective juveniles of *S. carpocapsae was* performed using the protocol published by Patrnogic *et al*., 2019. Briefly, 2–4-week-old IJs of *S. carpocapsae* collected from infected waxworms using White traps (White, 1927), were used for the infection. Nematode infections were carried out at two densities, 100 worms/fly and 50 worms/fly. Nematodes were suspended in sterile distilled water (250 µl) and added to vials containing four layers of filter papers (Whatman Grade 1, 20 mm). 250 µl of 1% sucrose was introduced to vials as the source of nutrients for the flies. 250 µl of water plus 250 µl of 1% sucrose was used in uninfected controls. Ten anesthetized flies (five males and females) were added to each vial. The vial flug was pushed down to restrict the movement and increase the probability of infection. Vials were incubated at 25 °C. Infection was set up in 6 vials for each nematode density and each fly type. Flies from 3 vials were dissected 24 h post-infection to quantify the nematode infection. Flies from 3 other vials were transferred on food 24 h post-exposure to IJs and survival was monitored daily for 6 days. Dead flies from each day were dissected to see determine successful nematode infection. On the 6th day, all the flies were dissected to check for nematode infection. Infection experiments were replicated three times.

Plasmid design and assembly

To assemble plasmid OA-1010, the base vector used for generating FAR protein-expressing plasmids, several components were cloned into the piggyBac plasmid

OA959C (Addgene #104968) using Gibson assembly/EA cloning. Plasmid OA959C was digested with AvrII and NotI, and the following components were cloned in with EA cloning: an*attP* sequence amplified from plasmid M{3xP3-RFP attP} with primers 1010.C1 and 1010.C2, a 10xUAS promoter fragment amplified with primers 1010.C3 and 1010.C4 from Addgene plasmid 78897, a p10 3'UTR fragment amplified from Addgene plasmid #100580 with primers 1010.C5 and 1010.C6, and opie2-dsRed marker fragment amplified from Addgene plasmid #100580 using primers 1010.C7 and 1010.C8. The resulting plasmid was then digested with XhoI and PacI, and the coding sequences (CDSs) of various FAR proteins that were codon-optimized for *D. melanogaster* expression and synthesized (GenScript, Piscataway, NJ) were separately cloned in to generate the six final FAR protein-expressing vectors. Specifically, to generate vector OA-1010Av2, the codon optimized CDS of *S. carpocapsae* gene L596_g9608 was amplified with primers 1010.C9 and 1010.C10 from a gene-synthesized plasmid and cloned into the above digested vector using EA cloning. Then, to generate vector OA-1010A, OA-1010Av2 was digested with PacI and a G(4)S linker followed by a 30-amino-acid human influenza hemagglutinin (HA) epitope tag was amplified with primers 1010.C11 and 1010.C12 from the *ninaE*[SBP-His] vector and cloned into the above digested vector using EA cloning. To generate vector OA-1010Bv2, the codon optimized CDS of *S. carpocapsae* gene L596_g25050 were amplified with primers 1010.C13 and 1010.C14 from a gene-synthesized plasmid and cloned into the digested OA-1010 vector using EA cloning. Then, to generate vector OA-1010B, OA-1010Bv2 was digested with PacI and a G(4)S linker followed by a 30-amino-acid human influenza HA epitope tag

was amplified with primers 1010.C15 and 1010.C12 from the *ninaE*[SBP-His] vector and cloned into the above digested vector using EA cloning. To generate vector OA-1010C, a fragment containing the codon optimized CDS of *C. elegans* gene *far-8* followed by a G(4)S linker and a 30-amino-acid human influenza HA epitope tag was amplified with primers 1010.C16 and 1010.C12 from a gene-synthesized plasmid and cloned into the XhoI/PacI-digested OA-1010 vector using EA cloning. To generate vector OA-1010D, a fragment containing the codon optimized CDS of *A. ceylanicum* gene *Ac-far-1* (maker-ANCCEYDFT_Contig87-pred_gff_fgenesh-gene-3.1) followed by a G(4)S linker and a 30-amino-acid human influenza HA epitope tag was amplified with primers 1010.C17 and 1010.C12 from a gene-synthesized plasmid and cloned into the XhoI/PacI-digested OA-1010 vector using EA cloning. All codon optimization was done by GenScript (Piscataway, NJ) using OptimumGene™ algorithms.

Fly transgenesis

Transgenic flies were developed using codon optimized Sc-FAR-1 or Sc-FAR-2 inserted via the PhiC31 site-specific serine integrase method. The transgenic UAS lines were then crossed with several Gal4 drivers from the Bloomington *Drosophila* Stock Center (BDSC), including TubP-Gal4 (#5138; strong, ubiquitous somatic expression), CG-Gal4 (#7011; expressed in the fat body, hemocytes and lymph gland) and He-Gal4 (#8699; expressed in hemocytes). Fly husbandry and crosses were performed under standard conditions at 25°C. Rainbow Transgenics (Camarillo, CA) carried out all of the fly

injections. All constructs were inserted into *attP* line 86Fa (BDSC #24486: y[1] M{vas-int.Dm}ZH-2A w[*]; M{3xP3-RFP.attP'}ZH-86Fa).

Western Blot

A modified version of the abcam general western blot protocol was used. 30 adult HA-tagged transgenic flies were ground up in 200 µL lysis buffer and centrifuged at 20,000g for 20 minutes at 4°C. The supernatant protein concentration was normalized to 1-2 mg/mL. 20 µL anti-HA magnetic beads (Thermo Scientific 88836) were incubated with 150 µL of supernatant protein sample while shaking for 30 minutes. The sample was then removed, and the beads were washed twice with 300 µL of TBST. The beads were then resuspended in 30 µL Tris-Cl pH 8.0 and 10 µL loading buffer. The samples were heated for 10 minutes at 100°C and electrophoresed on the SDS-PAGE gel. The proteins were transferred onto the immobilon P^{SQ} (Millipore) for 1.5 hours at 50 Volts. The membrane was washed with PBS and blocked with 1% BSA for 30 minutes with shaking. The membrane was washed twice with PBST for 10 minutes and then incubated with HA-tag primary anti-rabbit antibody (Abcam ab236623) for 2 hours with shaking. After incubation, the membrane was washed twice again with PBST for 10 minutes. Then anti-rabbit anti-goat antibody (Abcam ab6721) was added and incubated for 2 hours with shaking. Again, the membrane was washed twice with PBST and then developed with Metal enhanced DAB substrate kit (Thermo Scientific 34065).

Bacterial stock maintenance

Streptococcus pneumoniae was grown by shaking in glass vials with 5 mL tryptic soy (TS) broth (Difco TS broth, catalase, streptomycin) at 37°C with 5% CO_2 overnight. The overgrown culture was diluted in catalase (100 µL) and TS to yield a final volume of 20 mL in a flask and incubated shaking until the OD_{600} ~ 0.4 (about 1 hour). The culture was then diluted again to a final volume of 50 mL, with 150 µL catalase, and incubated until the OD_{600} ~ 0.2 - 0.4 (above 0.5 is no longer in log phase). 5% glycerol was added to the final culture and stored then in 1mL aliquots at -80°C. To use the aliquots, one tube was thawed, spun down at 14,000 rpm for 5 minutes, the supernatant was removed, and the pellet was resuspended in the desired amount of PBS (50 - 60 µL yields ~ 100,000 CFUs) and serially diluted to yield the appropriate CFU doses. For quantification of CFUs, *S.p.* was plated on TSA agar plates supplemented with 50 mL/L sheep's blood. *Listeria monocytogenes* (serotype 4b, 19115, (ATCC, VA)) was also grown in batches in brain heart infusion (BHI) medium at 37°C in aerobic condition. Cultures were grown overnight in a flask inoculated with a fresh colony and rediluted under log phase (below OD_{600} ~ 0.2) and grown up to the desired OD_{600} (~0.4). The entire volume was transferred to a 50mL centrifuge tube for vortexing. Before freezing, a 5% glycerol solution was added to the culture and 1mL aliquots were stored at -80°C. To use the aliquots, one tube was thawed, spun down at 14,000 rpm for 5 minutes, the supernatant was removed, and the pellet was resuspended in the desired amount of PBS (90 - 100 µL yields ~ 100,000 CFUs) and serially diluted to yield the appropriate CFU doses. For quantification of CFUs, *L.m.* was plated on BHI plates. *Xenorhabdus innexi* (HGB2121

*att*Tn*7*/Tn*7*-GFP (from pURR25)) was incubated at 27°C shaking in Luria Bertani (LB) broth supplemented with 0.1% sodium pyruvate (sp). Overnight cultures on *X. innexi* were subcultured below log phase (OD_{600}< 0.4) and grown back to log phase (OD_{600} 0.4 - 0.8) and diluted to the desired concentrations before use, as well as streaked on LB+sp plates bi-weekly for storage. LB+sp media was supplemented with 20% glycerol for long term storage of log phase *X. innexi* in -80°C.

Generation of recombinant proteins

The sequence corresponding to *Sc*FARS-1 *and Sc*FARS-2 was obtained from GenBank [50]. The sequences encoding the mature protein was codon-optimized, synthesized by GenScript and cloned into a modified pET28 vector incorporating an N-terminal hexahistidine tag and a TEV cleavage site. *Sc*FARS-1 *and Sc*FARS-2 were produced recombinantly in *E. coli* BL21-CodonPlus cells (Stratagene) grown in autoinduction medium (Invitrogen) from a 1% inoculum. Following four hours of growth at 37°C and 16 hours at 30°C, the cells were harvested, and the pellet resuspended in 20 mM Hepes pH 8.3, 1 M NaCl, 30 mM imidazole. Cells in suspension were lysed using a French press, insoluble material was removed by centrifugation, and the soluble fraction was applied to a HisTRAP FF 5 mL column (GE Healthcare). Bound *Sc*FARs1 and 2 were eluted with an increasing concentration of imidazole, the His tag was subsequently removed by TEV cleavage, and they were further purified by gel filtration chromatography on a Superdex 200 16/60 HiLoad column in HBS (20 mM Hepes pH 7.5, 150 mM NaCl). The purity of was assessed at each stage by SDS-PAGE.

Fly injections, survival and CFUs

For injections and immune assays, 5-7-day-old male flies were anesthetized with CO_2 and injected with various CFU doses yielding a total volume of 50 nL precisely using a MINJ-FLY high-speed pneumatic injector (Tritech Research, CA) and individually pulled calibrated glass needles. Flies were injected into the abdomen close to where the thorax meets and slightly ventral from the dorsal-ventral cuticle axis, easily visible below the haltere. Survival studies were carried out for all the pathogens we tested. After injection of the CFU dose or phosphate buffered saline (PBS) control, flies were placed in vials in groups of 30 with a total of 60 flies per experimental or control group. Flies injected with the human pathogens (*S.p.* and *L.m.)* were kept at 28°C with 50% humidity compared to flies injected with the insect pathogen *X.i.* which was kept at 25°C with 50% humidity. The number of dead flies was counted daily and Kaplan-Meier survival curves were generated with GraphPad Prism software with statistics shown as log-rank analysis (Mantel-Cox). Survival experiments were at least triplicated. CFUs were determined by homogenizing a single infected, or buffer-injected fly in 200 µL of PBS, serially diluted and plated on the appropriate agar plates and incubated overnight. Colonies were counted the next day. At least five flies per condition were homogenized for CFU quantification each time an injection experiment was done to measure time 0 CFUs which are representative of all fly strains. All fly strains were injected at the same time for each experimental replicate. Using GraphPad Prism software, results are shown as scatter plots with statistical significance analyzed using an unpaired t-test.

PO & disseminated melanization

Flies were injected with 1,000 CFUs of *L. monocytogenes* to elicit an immune induced melanization cascade. Phenoloxidase activity was measured as previously described [51,52]. To collect hemolymph, 20-30 flies 4 hours post injection (p.i.) were pricked through the thorax and placed in a pierced 0.5 µL Eppendorf tube and covered with glass beads, then placed inside a 1.5 µL Eppendorf tube containing 30 µL of 1x protease inhibitor cocktail (Fisher, PI78429). Samples were centrifuged at 10,000 rpm for 20 minutes at 4°C. Protein concentrations were measured with Bradford assay (Bio-rad, 5000006) and then diluted in phosphate buffered saline (PBS) to a concentration of 15 µg/uL and a total volume of 100 µL. Using a clear 96-well plate, each well contained 160 µL L-Dopa (3 mg/mL) dissolved in phosphate buffer (37.5% 1 M potassium phosphate, 62.5% 1 M sodium phosphate, pH 6.5), 35 µL of hemolymph sample and 5 µL $CaCl_2$ (20 mM). PO activity was measured by kinetic reads at 29°C at 492 nm every minute for 60 min with 5 seconds of shaking between reads. The OD of a blank control was subtracted from all biological values. Experiments were replicated five times with three technical replicates per experiment. Data were plotted as mean+SEM by taking the peak OD value (timepoint ~ 30 min). Statistics shown as an unpaired t-test was done in GraphPad Prism. For disseminated melanization, flies were observed for melanin deposits in the posterior and anterior abdomen, thorax, head and eyes four days p.i. with *L.m.* An individual was considered to show disseminated melanization if it had two or more deposits of melanin, one often at the wounding site and another either underneath the cuticle or in deeper

tissues as previously described [29]. Data were graphed as percent of the population infected that was melanized by day four p.i. as the mean+SEM. Experiments were replicated three times with 40 individuals per experimental condition per experiment. Statistics shown as unpaired t-test was done in GraphPad Prism.

Antimicrobial peptide gene expression – qPCR

Total RNA was extracted from 15 *S. pneumonia* infected flies per strain 24 hours post-injection using Trizol reagent (Molecular Research Center, Inc; Cincinnati, Ohio) according to the manufacturer instructions. Integrity of RNA was confirmed by observing bands on an agarose gel and concentration was determined by nanodrop. Reverse transcription of RNA using ProtoScript II First Strand cDNA synthesis kit (New England BioLabs, NE, E6560L) following the manufacturer protocol, in a MultiGene OptiMax Thermal Cycler (Labnet international, NJ). The qRT-PCR was done with a CFX Connect Bio-Rad system with Perfecta SYBR green supermix (QuantaBio, MA) and gene specific primers for *Defensin, Drosomycin*, and *Tubulin* (Integrated DNA Technologies, IA). Experiments were carried out with three technical replicates and repeated four times with plots shown as bar graphs with individual points representing each replicate. Statistics shown as One-way ANOVA done in GraphPad Prism.

In vitro binding

The fatty acid- and retinol- binding preferences of Sc-FAR *in vitro* was measured by utilizing the saturated fatty acid fluorescent probe 11-(Dansylamino) undecanoic acid

(DAUDA) (Sigma-Aldrich, USA) and retinol as previously described [9,32]. Fluorescent emission spectra for Sc-FAR bound to DAUDA (1 μM) and retinol (40 μM) were measured at 25°C in a black-walled 96-well plate yielding a total volume of 200 μL with an excitation wavelength of 345 nm and 350 nm respectively. When DAUDA is encompassed by a binding protein a 50nm blue shift is observed with an excitation wavelength of 345nm. The equilibrium dissociation constant (Kd) for Sc-FAR bound to DAUDA or retinol was estimated by adding increasing concentrations of Sc-FAR, in 1 or 2 μM increments, to 1 μM DAUDA in PBS and 40 μM retinol in PBS. The data were normalized to the peak fluorescence intensity of DAUDA or retinol bound to FAR (yielding a value of 1) and corrected for background fluorescence of PBS alone for each concentration. The data were then plotted as relative fluorescence and a nonlinear fit via the one site-specific system was used to find the Kd value in GraphPad Prism. Competition studies were done by measuring the decrease in peak emission of DAUDA in the presence of another fatty acid in 10-fold excess. Oleic, linoleic and arachidonic acid were tested along with 9,(10)- and 12,(13)- EpOME and 13-HODE(Cayman Chemicals, MI). All competition experiments were replicated 3 times with 3 technical replicates per experiment, plotted as bar graphs with mean+SEM and individual points for each replicate, analyzed by an unpaired t-test. All fatty acids and DAUDA were stored in -20°C and freshly diluted before each experiment starting with a working solution of either 10 or 100 μM in 100% ethanol and then subsequently diluted in PBS to achieve the appropriate working solution.

Metabolomics

Whole fly untargeted

Flies were transferred to a 2 mL bead mill tube and weighed, the range was 131 mg to 302 mg. Ice-cold extraction solvent (20:20:30:30 water:IPA:ACN:MeOH) was added, 3.32 µL / 1 mg sample, and samples were homogenized in a liquid nitrogen cooled bead mill, 6, 10 s cycles at 5 m/s. After centrifugation for 15 min at 16,000 x g at 4 C, the supernatant was analyzed by LC-MS. LC-MS metabolomics analysis was performed at the UC Riverside Metabolomics Core Facility as described previously [53]. Briefly, analysis was performed on a Synapt G2-Si quadrupole time-of-flight mass spectrometer (Waters) coupled to an I-class UPLC system (Waters). Separations were carried out on a CSH phenyl-hexyl column (2.1 x 100 mm, 1.7 µM) (Waters). The mobile phases were (A) water with 0.1% formic acid and (B) acetonitrile with 0.1% formic acid. The flow rate was 250 µL/min and the column was held at 40° C. The injection volume was 2 µL in positive ion mode and 4 µL in negative ion mode. The gradient was as follows: 0 min, 1% B; 1 min, 1% B; 8 min, 40% B; 24 min, 100% B; 26.5 min, 100% B; 27 min, 1% B. The MS was operated in positive ion mode (50 to 1200 m/z) with a 100 ms scan time. MS/MS was acquired in data dependent fashion. Source and desolvation temperatures were 150°C and 600°C, respectively. Desolvation gas was set to 1100 L/hr and cone gas to 150 L/hr. All gases were nitrogen except the collision gas, which was argon. Capillary voltage was 1 kV in positive ion mode and 2 kV in negative ion mode. A quality control sample, generated by pooling equal aliquots of each sample, was analyzed every 4-6 injections to monitor system stability and performance. Samples were analyzed in

random order. Leucine enkephalin was infused and used for mass correction. Untargeted data processing (peak picking, alignment, deconvolution, integration, normalization, and spectral matching) was performed in Progenesis Qi software (Nonlinear Dynamics). Data were normalized to total ion abundance. To aid in the identification of features that belong to the same metabolite, features were assigned a cluster ID using RAMClust [54]. An extension of the metabolomics standard initiative guidelines was used to assign annotation level confidence [55,56]. Annotation level 1 indicates a match to an in-house library. Level 2a indicates an MS and MS/MS match to an external database. Level 2b indicates an MS and MS/MS match to the Lipiblast in-silico database [57] or an MS match and diagnostic evidence, such as the dominant presence of an m/z 85 fragment ion for acylcarnitines. Level 3 indicates an MS and partial MS/MS match to an external or in-house database. Several mass spectral metabolite databases were searched against including Metlin, Mass Bank of North America, and an in-house database. Statistical analyses were performed, and figures generated using R.

Hemolymph only (WashU)

Hemolymph from 200 5-7-day old male flies was extracted as previously described in [58]. Briefly, flies were pierced through the thorax with a tungsten needle. Flies were placed in a pierced 0.5 mL Eppendorf tube within a 1.5 mL Eppendorf tube containing 20µL of 10x protease inhibitor cocktail and centrifuged for two rounds of 10 minutes at 10,000 rpm at 4°C with a gentle mixing in between rounds. The supernatant of the collected hemolymph was centrifuged for 10 minutes at 14,000 rpm to remove cells and

debris. The supernatant was flash-frozen in liquid nitrogen and stored at -80°C until prepped for metabolomics experiments.

Each of the pooled drosophila sample was initially homogenized with 260 µL of methanol and 30 µL of water containing 2ng each of deuterated oxidative metabolites (9, 10-EpOME-d_4, 12.13-EpOME-d_4, 9, 10-DiHOME-d_4, 12, 13-DiHOME-d_4, 9-HODE-d_4, and 13-HODE-d_4) as well as deuterated fatty acids (100ng; AA-d_8 and 1000ng; linoleic acid (LA)-d_4) as the internal standards. Fatty acids as well as the internal standards were derivatized from 40 µL of the homogenate with 50 mM DMAPA, 100mM EDC, and 100 mM DMAP. Four- to five-point calibration standards of oxidative metabolites and fatty acids containing their deuterated internal standards were also prepared for the absolute quantification.

The sample analysis for the oxidative metabolites was performed with a Shimadzu 20AD HPLC system coupled to a tandem mass spectrometer (API-6500$^+$Qtrap: Applied Biosystems) operated in MRM positive ion mode. For fatty acid analysis another Shimadzu 20AD HPLC system coupled to the API-4000Qtrap mass spectrometer were used in MRM positive ion mode. All samples were injected in duplicate for data averaging. Data processing was conducted with Analyst 1.6.3 (Applied Biosystems). Metabolomic analysis of fly hemolymph was performed by the Metabolomics Facility of Washington University (St. Louis, MI).

Statistics

All statistics were done with GraphPad Prism 8.4. Statistical significance indicated with asterisks indicating the following p-value cut offs: 0.05-0.033*, 0.033-0.002**, 0.002-0.0002*** and <0.0001****.

Acknowledgements

We thank Joshua Mallilay, Nikhil Prabhakar, and Priscila Robles, for their assistance with experimentation, fly husbandry and maintenance, and Bloomington *Drosophila* Stock Center (NIH P40 OD018537) for providing fly stocks. We thank Jay Kirkwood and the UC Riverside Metabolomics Core Facility, and the Metabolomics Facility at Washington University for their assistance with parts of this study. This research was supported by a USDA National Institute of Food and Agriculture Hatch project (accession #1015192) and R35 GM137934 National Institute of General Medical Sciences to A.R.D. and by a Canadian Institutes of Health Research Grants 148596 to M.J.B. M.J.B. gratefully acknowledges the Canada Research Chair program for salary support. O.S.A and A.B. were supported in part by UCSD startup funds.

Supplemental

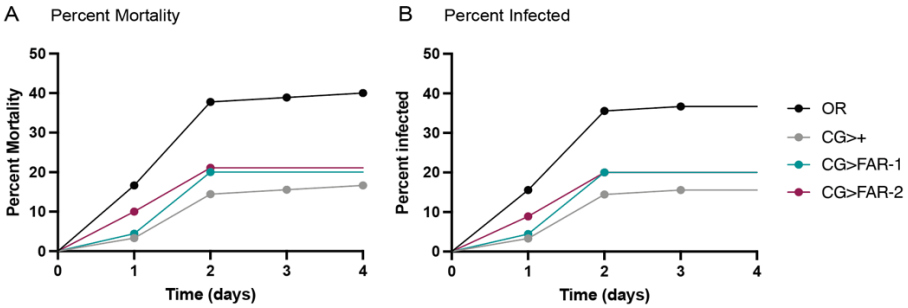

Supplemental figure S2.1: D. melanogaster has little to no survivability to S. carpocapsae infections. Flies were exposed to a dose of 100 IJs/fly, using *S.c.* IJs. The survival rate equals the infection rate. Once a fly is infected with even just one IJ it cannot survive the infection. Percent mortality overlaps with percent infected. As with bacterial infections, various fly strains interact with infections differently. Each line represents at least 90 flies.

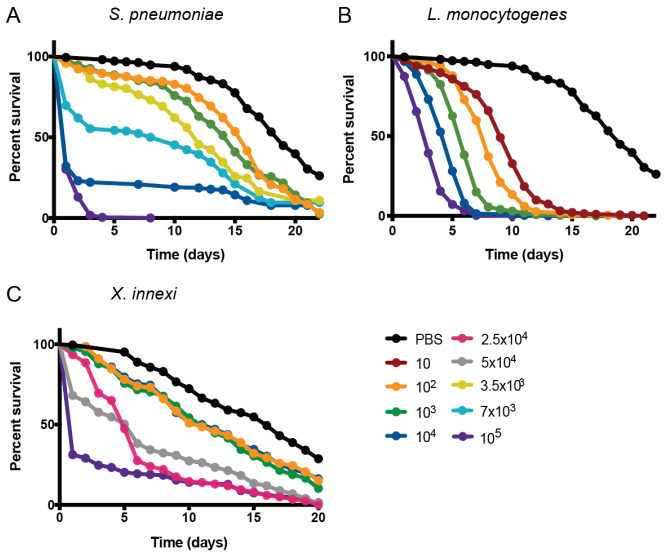

Supplemental Figure S2.2: Dose response of various pathogens in wild-type OregonR flies was used to assess virulence patterns and to identify the LD_{30}, (dose that leads to 30% death of the population within the first 1-5 days depending on the pathogen) an optimal dose to measure variations in immunity. 5-7-day-old male flies were used for all injections with phosphate buffered saline (PBS) shown as the vehicle control. A) 100 to 100,000 CFUs of *Streptococcus pneumoniae* were injected, LD_{30} identified as 7,000 cells. B) 10 to 100,000 cells of *Listeria monocytogenes* were injected, LD_{30} identified as 1,000 cells. C) 100 to 100,000 cells of the insect pathogen *Xenorhabdus innexi* were injected, 25,000 and 50,000 cell doses were chosen for study. All raw data available in supplemental materials.

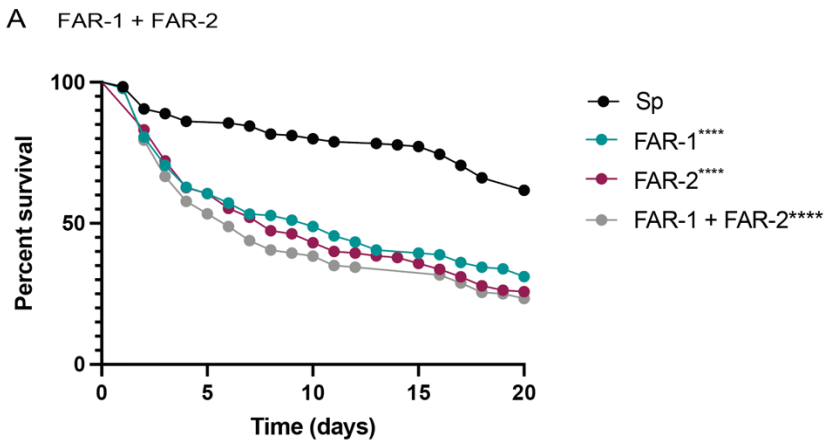

Supplemental Figure S2.3: Additive FAR-1 and FAR-2 test. We performed additive recombinant FAR-1 and FAR-2 injection experiments with the LD_{30} of *S. pneumoniae* and found no difference between a 250 ng dose of FAR-1 or FAR-2 and a 125 ng FAR-1 plus 125 ng FAR-2 combined dose showing that FAR does not have an additive effect. The graph below shows at least 180 flies per line with statistical significance shown as a log-rank test.

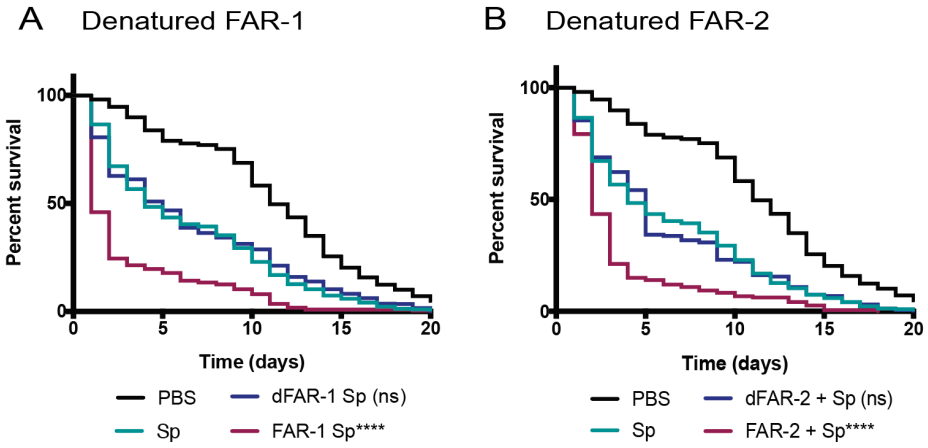

Supplemental Figure S2.4: Recombinant FAR elicits a specific effect on the outcome of a bacterial infection. As a control to validate the effects of recombinant FAR proteins on immunity, denatured *S. carpocasae* FARs were co-injected with 7,000 CFUs of *S. pneumoniae*. A) Denatured Sc-FAR-1 (250ng) co-injected with *S.p.* shows no significant difference from *S.p.*-only injected flies. B) Denatured Sc-FAR-2 (250ng) co-injected with *S.p.* shows no significant difference from *S.p.*-only injected flies. Statistics shown as Log-rank test. All raw data available in supplemental materials. Experiments not found to be significantly different from bacteria-only controls were marked ns.

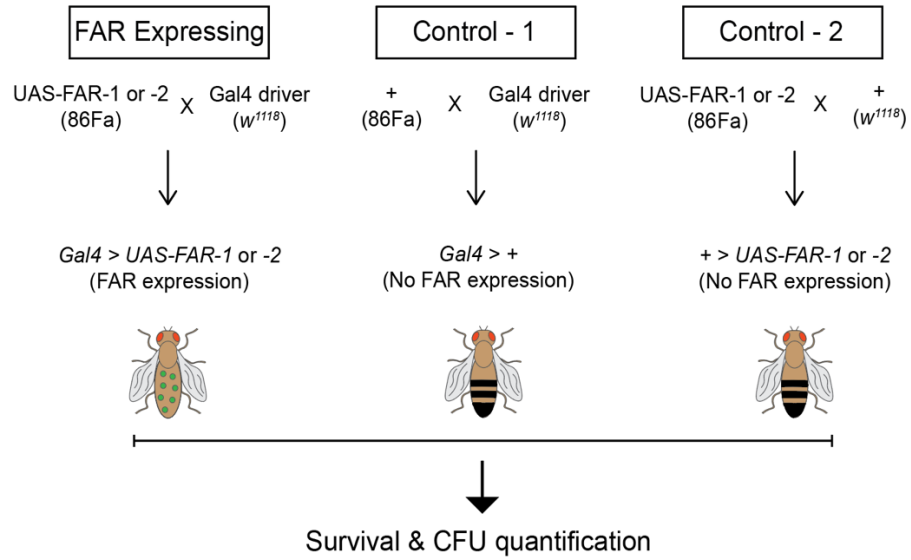

Supplemental Figure S2.5: Overview of the UAS-Gal4 genetic crosses of FAR expressing and control flies. The sequence of FAR-1 or -2 was inserted into the 86Fa fly strain which displays a fluorescent red body and eye color and crossed with various Gal4 promoter strains. As a control, the 86Fa fly was crossed with the Gal4 driver flies as well as the FAR-1 or -2 transgenic flies were crossed with a w^{1118} strain. The male flies yielding the appropriate genotypes were tested for their immunodeficiencies after inducting an immune response with a bacterial injection into the abdomen.

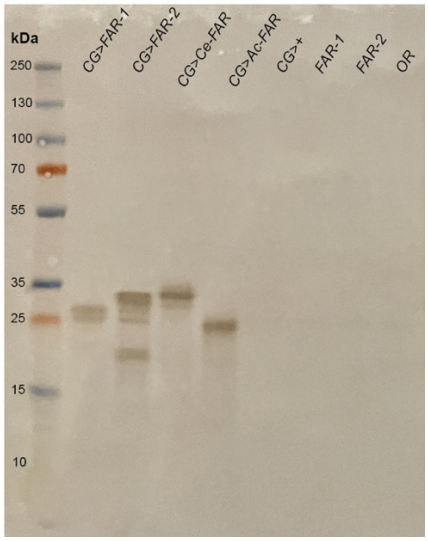

Supplemental Figure S2.6: Western blot shows in vivo production of FAR proteins. FAR is expressed when driven with the Gal4 driver in the first 4 wells (rows 1-4). Control flies not expressed with UAS-Gal4 expression system do not show the presence of FAR proteins (rows 5-8).

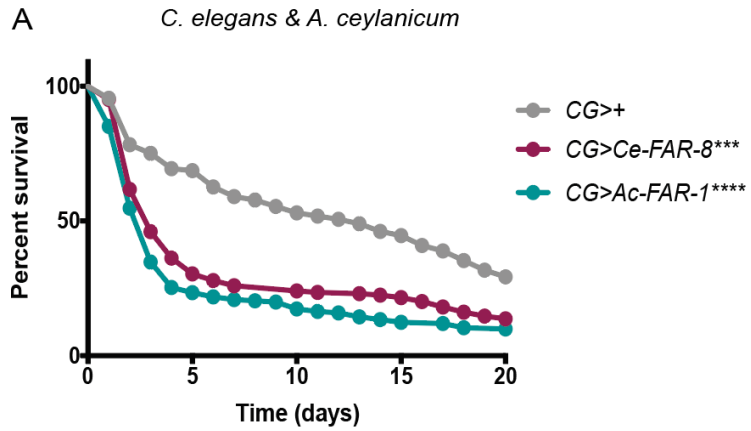

Supplemental Figure S2.7: FAR proteins from other species of nematodes show similar negative effects on the outcome of a S. pneumoniae infection. Flies expressing FAR-8 from the free-living nematode *Caenorhabditis elegans* or a FAR from the mammalian hookworm *Ancylostoma ceylanicum* (maker-ANCCEYDFT_Contig87-pred_gff_fgenesh-gene-3.1) with the CG driver had a significant decrease in survival after injected with 7,000 cells of *S.p.* Statistics shown as Log-rank test. All raw data available in supplemental materials.

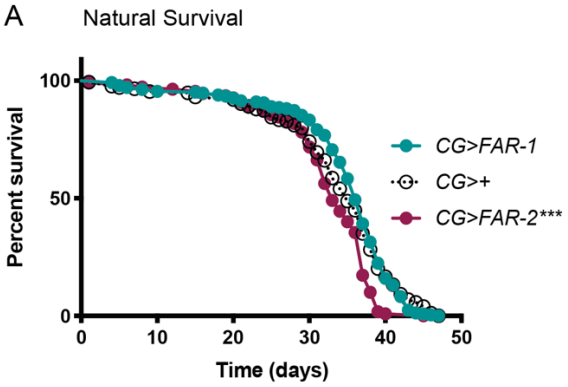

Supplemental Figure S2.8: Lifespan of FAR transgenic flies expressed with the fat-body and hemocytes specific driver CG. Lifespan is not altered within the timeframe where immunity studies took place (day 0 to 20). Statistics shown as Log-rank test. All raw data available in supplemental materials.

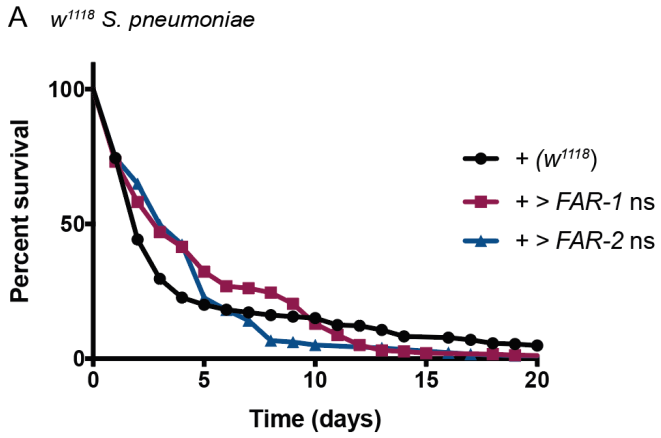

Supplemental Figure S2.9: Genetic control of 86Fa transgenic strains. As a control to validate the specific effects on immunity after promoting the FAR transgenics, FAR-1 & -2 expressing flies were crossed with w^{1118} flies. There was no significant difference observed between all genotypes validating the specific effects of FAR. All raw data available in supplemental materials.

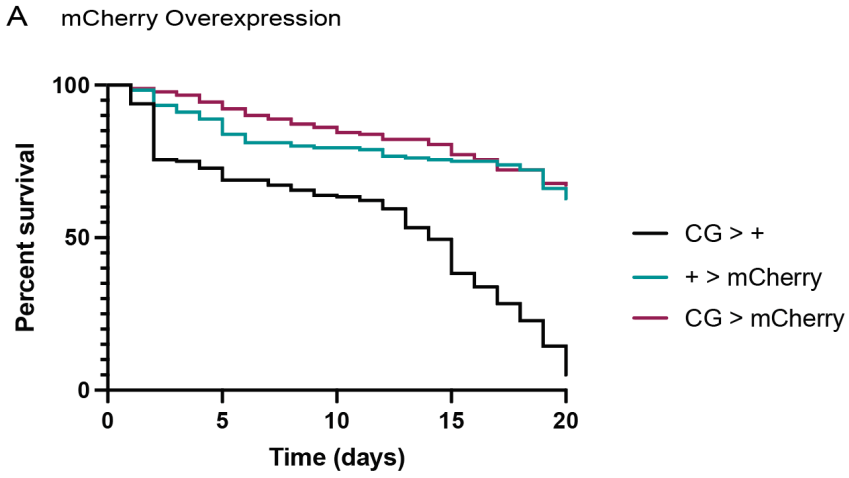

Supplemental Figure S2.10: mCherry control. When mCherry is overexpressed by the CG-Gal4 driver, there is no significant reduction in survival as compared to control crosses. All lines represent at least 180 flies.

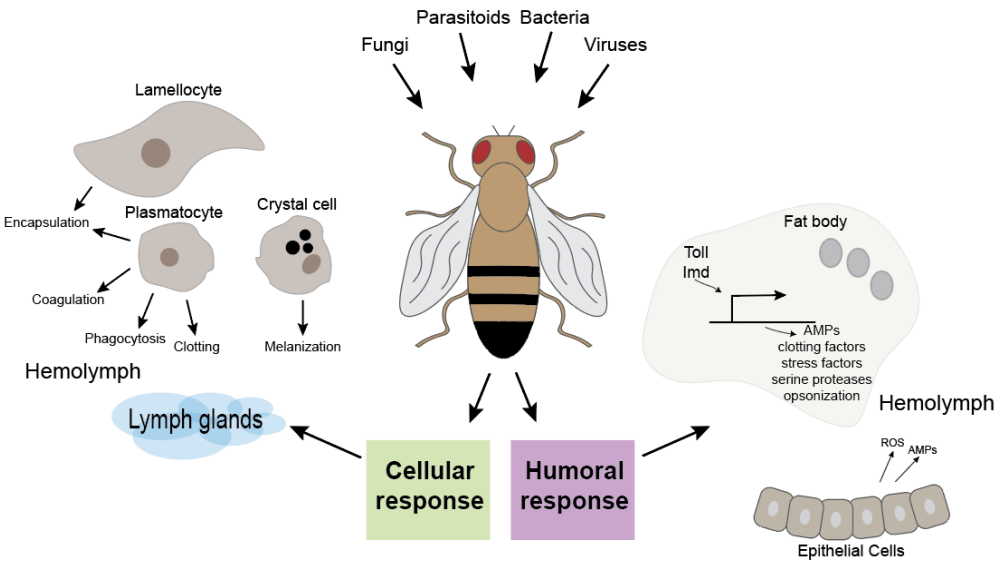

Supplemental Figure S2.11: Simplified overview of Drosophila immunity. Detection of pathogens elicits an array of interconnected innate immune responses specifically divided into the humoral, or systemic, and the cellular response. Humoral immunity leads to the production of antimicrobial peptides (AMPs) downstream of either the Toll or Imd pathways. Cellular immunity is carried out by different types of hemocytes that surround and kill invading microbes. Adapted from (Lemaitre, 2007 #90;Vanha-Aho, 2016 #94).

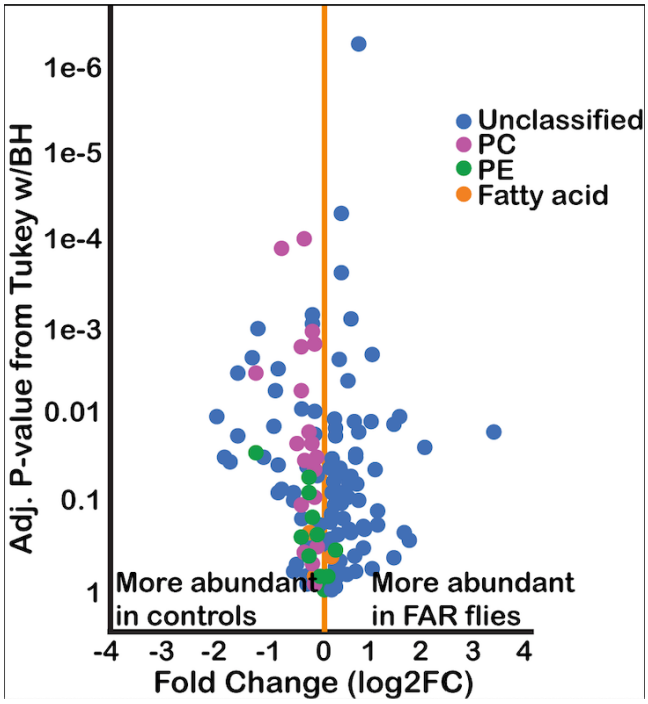

Supplemental Figure S2.12: Volcano plot comparing relative abundance of metabolites in CG>FAR-1 expressing and CG>+ control flies. Phosphatidylcholines (PC), phosphatidylethanolamines (PE) and multiple fatty acids were found to be more abundant in control flies, meaning they are depleted in FAR expressing flies as well as potential binding partners, or upstream compounds of FARs binding partners. All raw data available in supplemental materials. LC-MS analysis depicted in this figure was performed at the UC Riverside Metabolomics Core Facility.

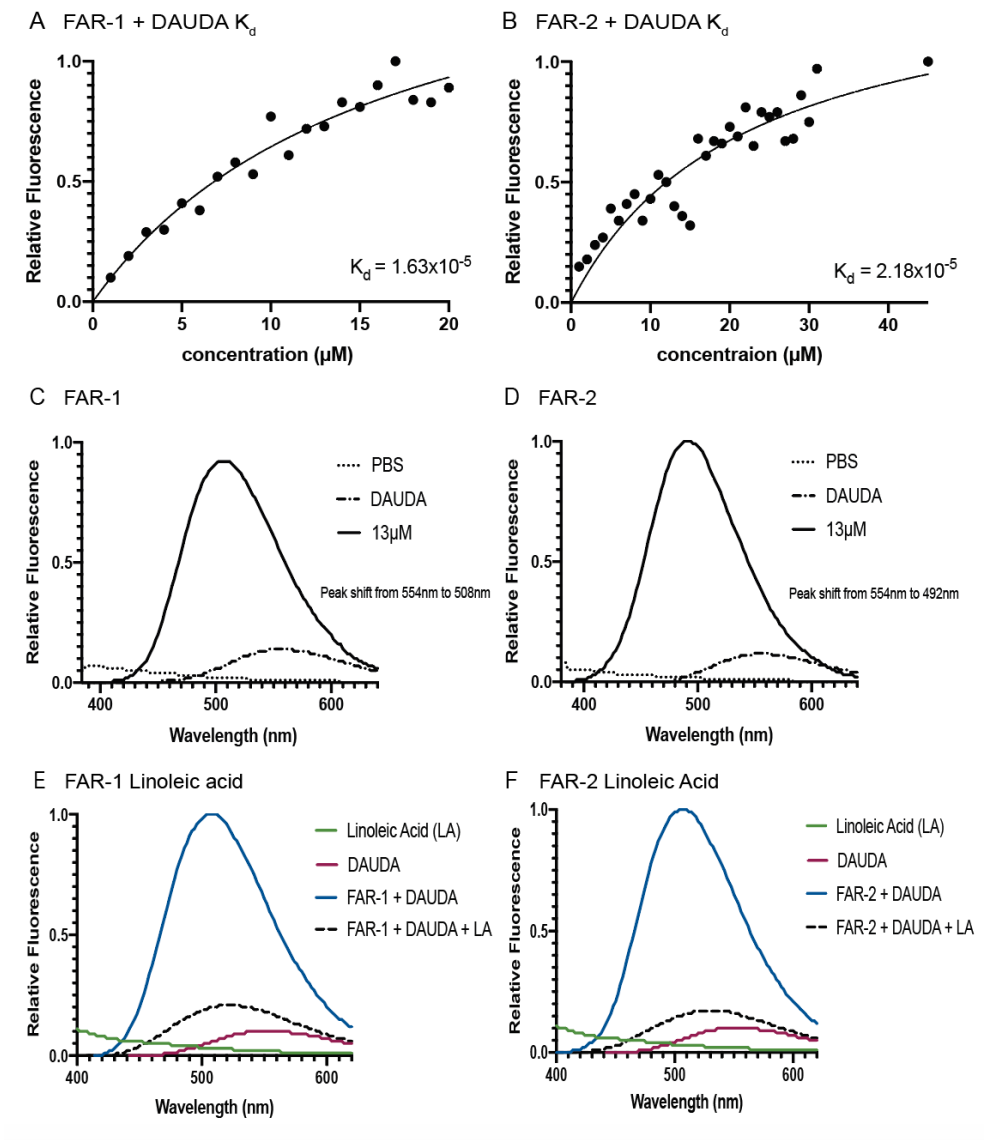

Supplemental Figure S2.13: In vitro binding properties of S. carpocapsae FARs to fatty acids. A&B) Plots of increasing concentration of FAR binding to 1μM 11-(Dansylamino) undecanoic acid (DAUDA) in PBS reveal a K_d in the 10 μM range. K_d was estimated by using the best-fit in Graphpad Prism. C&D) When DAUDA is bound to FAR (13 μM) *in vitro*, a ~50nm blue shift is observed in the peak. E&F) Full curve of *in vitro* competition assays shows a decrease in fluorescence when linoleic acid (10 μM) binds to and therefore displaces DAUDA (1 μM) from the fatty-acid binding pocket of FAR. All raw data available in supplemental materials.

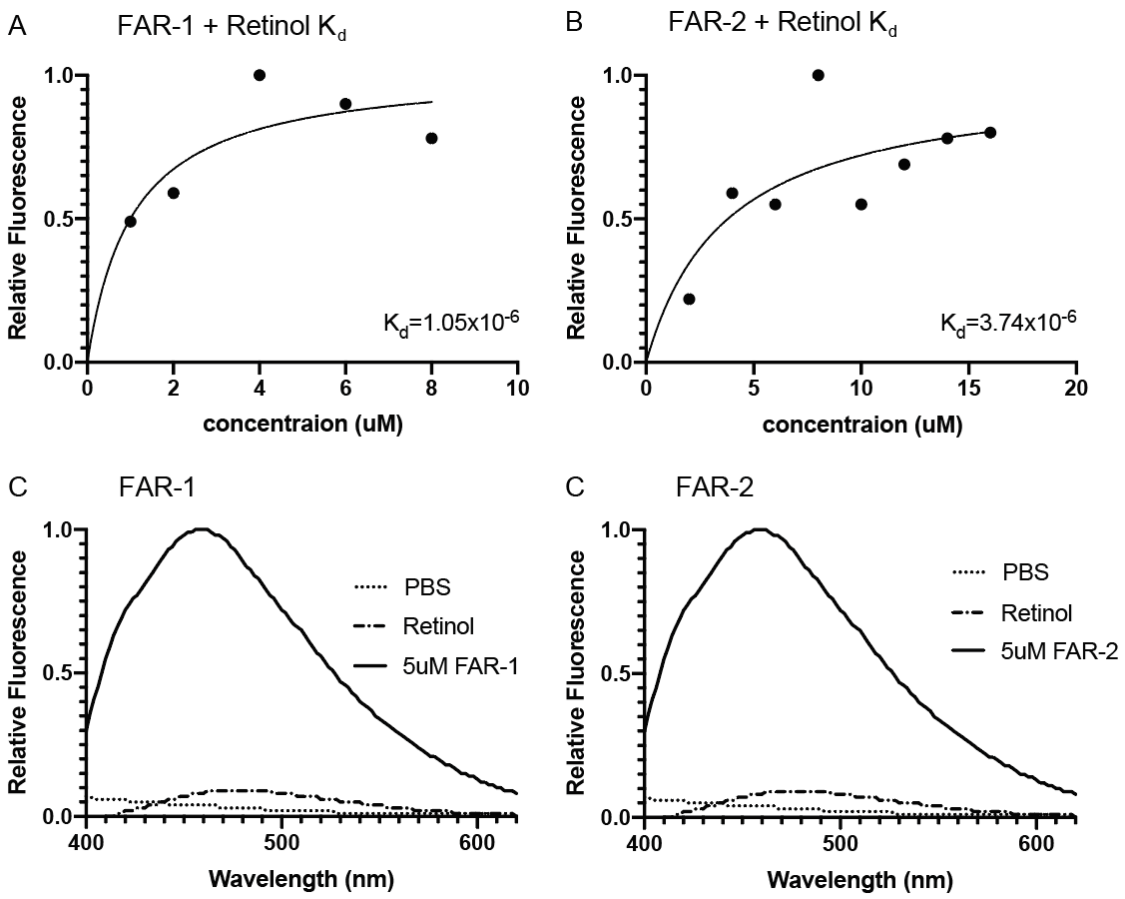

Supplemental Figure S2.14: In vitro binding properties of S. carpocapsae FARs to retinol. A&B) Plots of increasing concentration of Sc-FAR binding to 40µM retinol in PBS reveal a K_d in the 1 µM range. K_d was estimated by using the best-fit in Graphpad Prism. C&D) When retinol is bound to FAR (5 µM) *in vitro*, the peak fluorescence is greatly increased. All raw data available in supplemental materials.

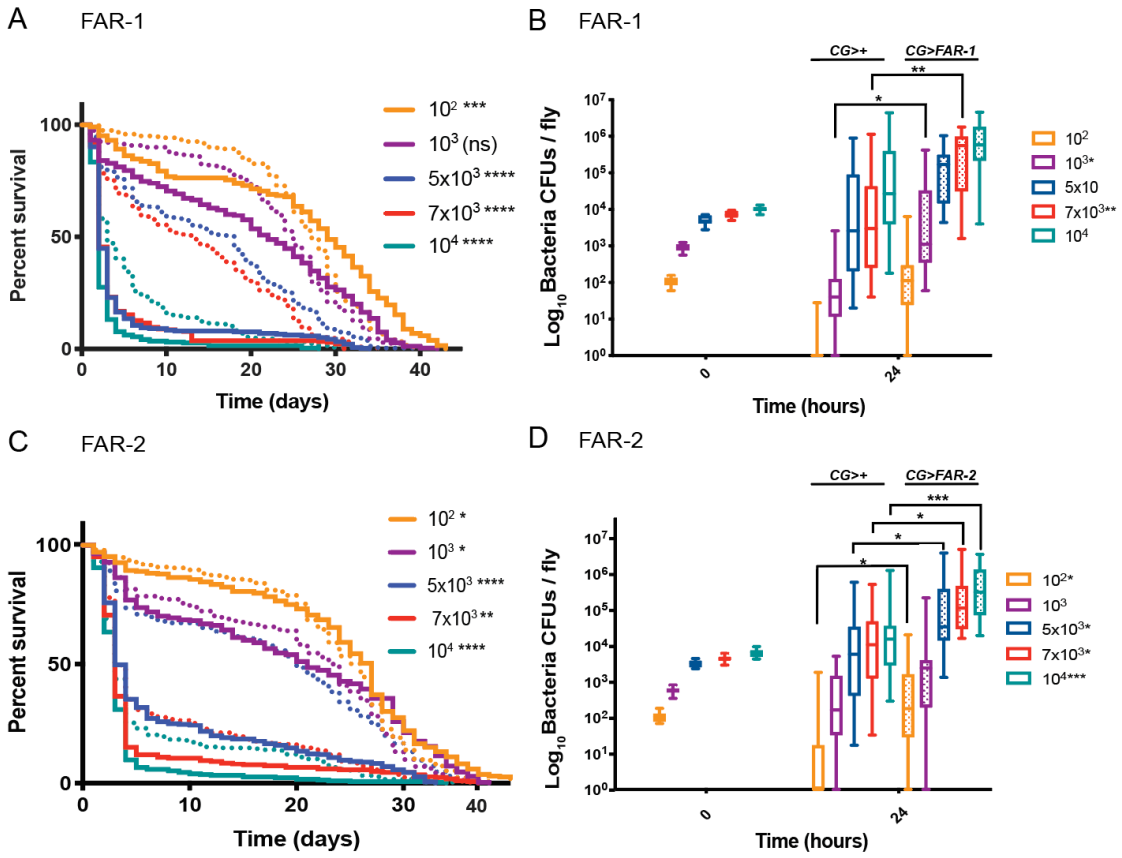

Supplemental Figure S2.15: FARs' role in increased mortality and microbe load is not limited to the LD30 dose. FAR-1 and -2 were expressed with the CG driver and injected with 100 to 100,000 CFUs of *S.p.* A&C) Survival was measured daily showing that FARs significantly increase mortality rate in most doses. B&D) In the presence of FAR, various doses of *S.p.* also cause an increase in microbe growth 24 hours p.i. Dotted lines show *CG>+* and solid lines show *CG>FAR-1* or *-2.* Statistics shown as Log-rank tests for survival curves and unpaired t-tests for microbe growth. All raw data available in supplemental materials.

References

1. Hotez, P.J., et al., *The global burden of disease study 2010: interpretation and implications for the neglected tropical diseases.* PLoS Negl Trop Dis, 2014. **8**(7): p. e2865.

2. Pullan, R.L., et al., *Global numbers of infection and disease burden of soil transmitted helminth infections in 2010.* Parasites & Vectors, 2014.

3. WHO. *Soil-transmitted helminth infections*. 2020 [cited 2020 08/31].

4. Shepherd, C., et al., *Identifying the immunomodulatory components of helminths.* Parasite Immunol, 2015. **37**(6): p. 293-303.

5. Cooper, D. and I. Eleftherianos, *Parasitic Nematode Immunomodulatory Strategies: Recent Advances and Perspectives.* Pathogens, 2016. **5**(3).

6. Kennedy, M.W., et al., *The unusual lipid-binding proteins of nematodes: NPAs nemFABPs and FARs.* Molecular Biology, Biochemistry and Immunology, 2013. **2**: p. 397-412.

7. Sani, B.P., et al., *Novel retinoid-binding proteins from filarial parasites* . Biochem J, 1985. **232**: p. 577-583.

8. Kennedy, M.W., et al., *The ABA-1 Allergen of the Parasitic Nematode Ascaris suum: Fatty Acid and Retinoid Binding Function and Structural Characterization.* Biochemistry, 1995. **34**: p. 6700-6710.

9. Kennedy, M.W., et al., *The Ov20 Protein of the Parasitic Nematode Onchocerca volvulus.* The Journal of Biological Chemistry, 1997. **272**(47): p. 29442-29448.

10. Jordanova, R., et al., *Fatty acid- and retinoid-binding proteins have distinct binding pockets for the two types of cargo.* J Biol Chem, 2009. **284**(51): p. 35818-26.

11. Kennedy, M.W., et al., *The gp15/400 polyprotein antigen of Brugia malayi binds fatty acids and retinoids.* Mol Biochem Parasitol, 1995. **71**: p. 41-50.

12. Garofalo, A., et al., *The FAR proteins of filarial nematodes: secretion, glycosylation and lipid binding characteristics.* Mol Biochem Parasitol, 2002. **122**: p. 161-170.

13. Zhan, B., et al., *Ligand binding properties of two Brugia malayi fatty acid and retinol (FAR) binding proteins and their vaccine efficacies against challenge infection in gerbils.* PLoS Negl Trop Dis, 2018. **12**(10): p. e0006772.

14. Iberkleid, I., et al., *Fatty acid-and retinol-binding protein, Mj-FAR-1 induces tomato host susceptibility to root-knot nematodes.* PLoS One, 2013. **8**(5): p. e64586.

15. Ramanathan, R., et al., *Microarray-based analysis of differential gene expression between infective and noninfective larvae of Strongyloides stercoralis.* PLoS Negl Trop Dis, 2011. **5**(5): p. e1039.

16. Bradley, J.E., et al., *River blindness: a role for parasite retinoid-binding proteins in the generation of pathology?* Trends in Parasitology, 2001. **17**: p. 471-475.

17. Ward, J.D., *Rendering the Intractable More Tractable: Tools from Caenorhabditis elegans Ripe for Import into Parasitic Nematodes.* Genetics, 2015. **201**(4): p. 1279-94.

18. Hallem, E.A., et al., *Nematodes, bacteria, and flies: a tripartite model for nematode parasitism.* Curr Biol, 2007. **17**(10): p. 898-904.

19. Lok, J.B., *Strongyloides stercoralis: a model for translational research on parasitic nematode biology.* WormBook, 2007: p. 1-18.

20. Dillman, A.R., et al., *Comparative genomics of Steinernema reveals deeply conserved gene regulatory networks.* Genome Biol, 2015. **16**: p. 200.

21. Ciche, T., *The biology and genome of Heterorhabditis bacteriophora.* WormBook, 2007: p. 1-9.

22. Troha, K. and N. Buchon, *Methods for the study of innate immunity in Drosophila melanogaster.* Wiley Interdiscip Rev Dev Biol, 2019. **8**(5): p. e344.

23. Hoffmann, J.A., et al., *Phylogenetic Perspectives in Innate Immunity.* Science, 1999: p. 1313-1318.

24. Lemaitre, B. and J. Hoffmann, *The host defense of Drosophila melanogaster.* Annu Rev Immunol, 2007. **25**: p. 697-743.

25. Hoffmann, J.A., et al., *Phylogenetic Perspectives in Innate Immunity.* Science, 1999. **284**: p. 1313-1318.

26. Castillo, J.C., S.E. Reynolds, and I. Eleftherianos, *Insect immune responses to nematode parasites.* Trends Parasitol, 2011. **27**(12): p. 537-47.

27. Lu, D., et al., *Activated entomopathogenic nematode infective juveniles release lethal venom proteins.* PLoS Pathog, 2017. **13**(4): p. e1006302.

28. Kim, I.H., et al., *The insect pathogenic bacterium Xenorhabdus innexi has attenuated virulence in multiple insect model hosts yet encodes a potent mosquitocidal toxin.* BMC Genomics, 2017. **18**(1): p. 927.

29. Ayres, J.S. and D.S. Schneider, *A signaling protease required for melanization in Drosophila affects resistance and tolerance of infections.* PLoS Biol, 2008. **6**(12): p. 2764-73.

30. Hanson, M.A., et al., *Synergy and remarkable specificity of antimicrobial peptides in vivo using a systematic knockout approach.* Elife, 2019. **8**.

31. Bath, J.L., et al., *Identification of a Secreted Fatty Acid and Retinol-Binding Protein (Hp-FAR-1) from Heligmosomoides polygyrus.* Journal of Nematology, 2009. **41**: p. 228-233.

32. Fairfax, K.C., et al., *Characterisation of a fatty acid and retinol binding protein orthologue from the hookworm Ancylostoma ceylanicum.* Int J Parasitol, 2009. **39**(14): p. 1561-71.

33. Fairfax, K.C., L.M. Harrison, and M. Cappello, *Molecular cloning and characterization of a nematode polyprotein antigen/allergen from the human and animal hookworm Ancylostoma ceylanicum.* Mol Biochem Parasitol, 2014. **198**(1): p. 37-44.

34. Rey-Burusco, M.F., et al., *(1)H, (1)(3)C and (1)(5)N chemical shift assignments of Na-FAR-1, a helix-rich fatty acid and retinol binding protein of the parasitic nematode Necator americanus.* Biomol NMR Assign, 2014. **8**(1): p. 19-21.

35. Rey-Burusco, M.F., et al., *Diversity in the structures and ligand-binding sites of nematode fatty acid and retinol-binding proteins revealed by Na-FAR-1 from Necator americanus.* Biochem J, 2015. **471**(3): p. 403-14.

36. Yuan, D., et al., *Genus-level evolutionary relationships of FAR proteins reflect the diversity of lifestyles of free-living and parasitic nematodes.* BMC Biol, 2021. **19**(1): p. 178.

37. Stanley, D. and Y. Kim, *Prostaglandins and Other Eicosanoids in Insects: Biosynthesis and Biological Actions.* Front Physiol, 2018. **9**: p. 1927.

38. Chandra Roy, M., D. Lee, and Y. Kim, *Host Immunosuppression Induced by Steinernema feltiae, an Entomopathogenic Nematode, through Inhibition of Eicosanoid Biosynthesis.* Insects, 2019. **11**(1).

39. Shen, L.R., et al., *Drosophila lacks C20 and C22 PUFAs.* J Lipid Res, 2010. **51**(10): p. 2985-92.

40. Stanley, D., J. Miller, and H. Tunaz, *Eicosanoid actions in insect immunity.* J Innate Immun, 2009. **1**(4): p. 282-90.

41. Shrestha, S., et al., *Genes encoding phospholipases A2 mediate insect nodulation reactions to bacterial challenge.* J Insect Physiol, 2010. **56**(3): p. 324-32.

42. Serhan, C.N., N. Chiang, and T.E. Van Dyke, *Resolving inflammation: dual anti-inflammatory and pro-resolution lipid mediators.* Nat Rev Immunol, 2008. **8**(5): p. 349-61.

43. Wall, R., et al., *Fatty acids from fish: the anti-inflammatory potential of long-chain omega-3 fatty acids.* Nutr Rev, 2010. **68**(5): p. 280-9.

44. Hwang, J., et al., *An entomopathogenic bacterium, Xenorhabdus nematophila, suppresses expression of antimicrobial peptides controlled by Toll and Imd pathways by blocking eicosanoid biosynthesis.* Arch Insect Biochem Physiol, 2013. **83**(3): p. 151-69.

45. Aymeric, J.L., A. Givaudan, and B. Duvic, *Imd pathway is involved in the interaction of Drosophila melanogaster with the entomopathogenic bacteria, Xenorhabdus nematophila and Photorhabdus luminescens.* Mol Immunol, 2010. **47**(14): p. 2342-8.

46. Stanley, D., *Prostaglandins and other eicosanoids in insects: biological significance.* Annu Rev Entomol, 2006. **51**: p. 25-44.

47. Vatanparast, M., et al., *EpOMEs act as immune suppressors in a lepidopteran insect, Spodoptera exigua.* Sci Rep, 2020. **10**(1): p. 20183.

48. Thompson, F.J., et al., *An expressed sequence tag analysis of the life-cycle of the parasitic nematode Strongyloides ratti.* Mol Biochem Parasitol, 2005. **142**(1): p. 32-46.

49. Vangaveti, V., B.T. Baune, and R.L. Kennedy, *Hydroxyoctadecadienoic acids: novel regulators of macrophage differentiation and atherogenesis.* Ther Adv Endocrinol Metab, 2010. **1**(2): p. 51-60.

50. Benson, D.A., et al., *GenBank.* Nucleic Acids Res, 2013. **41**(Database issue): p. D36-42.

51. Binggeli, O., et al., *Prophenoloxidase activation is required for survival to microbial infections in Drosophila.* PLoS Pathog, 2014. **10**(5): p. e1004067.

52. Cooper, D., et al., *The prophenoloxidase system in Drosophila participates in the anti-nematode immune response.* Mol Immunol, 2019. **109**: p. 88-98.

53. Rothman, J.A., et al., *Cadmium and Selenate Exposure Affects the Honey Bee Microbiome and Metabolome, and Bee-Associated Bacteria Show Potential for Bioaccumulation.* Appl Environ Microbiol, 2019. **85**(21).

54. Broeckling, C.D., et al., *RAMClust: a novel feature clustering method enables spectral-matching-based annotation for metabolomics data.* Anal Chem, 2014. **86**(14): p. 6812-7.

55. Schymanski, E.L., et al., *Identifying small molecules via high resolution mass spectrometry: communicating confidence.* Environ Sci Technol, 2014. **48**(4): p. 2097-8.

56. Sumner, L.W., et al., *Proposed minimum reporting standards for chemical analysis Chemical Analysis Working Group (CAWG) Metabolomics Standards Initiative (MSI).* Metabolomics, 2007. **3**(3): p. 211-221.

57. Kind, T., et al., *LipidBlast in silico tandem mass spectrometry database for lipid identification.* Nat Methods, 2013. **10**(8): p. 755-8.

58. Kwon, Y., et al., *Systemic organ wasting induced by localized expression of the secreted insulin/IGF antagonist ImpL2.* Dev Cell, 2015. **33**(1): p. 36-46.

59. Vanha-Aho, L.M., S. Valanne, and M. Ramet, *Cytokines in Drosophila immunity.* Immunol Lett, 2016. **170**: p. 42-51.

Chapter 3

Parasitic nematode secreted phospholipase A_2 suppresses toll activation and phagocytosis in the model host *Drosophila melanogaster*

Sophia C. Parks[§], Ogadinma K. Okakpu[§], Stephanie Martinez-Beltran, Isaiah Claudio, Susan Nguyen, Harpal Dhillon, and Adler R. Dillman[1*]

Department of Nematology, University of California, Riverside, California, 92521, USA.

[§]Equal contribution

*Corresponding: adlerd@ucr.edu

Abstract

A key mechanism for the success of parasitic nematode infection is the ability to evade or suppress host immunity. This immunomodulatory ability is likely due to the release of hundreds of excretory/secretory proteins (ESPs) upon infection. While ESPs have been shown to display immunosuppressive effects on a host, there are still gaps in understanding about the molecular interactions between individual proteins released and host immunity that has required further study. Our lab has recently identified a secreted phospholipase A_2 ($sPLA_2$) released from the entomopathogenic nematode (EPN) *Steinernema carpocapsae* we have named Sc-$sPLA_2$. Our studies showed that Sc-$sPLA_2$ increased mortality of *Drosophila melanogaster* to infection with *Streptococcus pneumoniae* and promoted increase of bacterial growth. Furthermore, our data showed that Sc-$sPLA_2$ was able to downregulate the toll pathway associated AMP *Drosomycin* and suppress phagocytosis in the hemolymph. Sc-$sPLA_2$ was also found to be lethal to *D.*

melanogaster with the severity being both dose and time dependent. Collectively, our data highlighted that Sc-sPLA$_2$ possessed both toxic and immunosuppressive capabilities.

Introduction

Nematode parasitism has been a biological health issue for living organisms causing significant morbidity and mortality to humans, illness to livestock, and a reduction of global crop yields [1-3]. Parasitic nematodes have ravaged human populations, with over 1.5 billion people being infected by soil-transmitted helminths alone [2]. This issue is further compounded by recurrent reinfection and emerging drug resistance. Parasitic nematodes are thus very effective parasites, capable of evading and compromising the immune response of various hosts including insects and vertebrates [4-6]. Despite the vast clinical knowledge on parasitic nematode infections, very little is understood about the underlying mechanisms that drive helminth ability to modulate host immunity. By elucidating the molecular mechanisms of parasitic nematode immunomodulation, more effective anti-helminth therapeutics can be produced, as well as potentially therapeutics for treating human immune pathologies such as auto immune diseases.

Ability of parasitic nematodes to evade and alter host immunity has been linked to their release of excretory/secretory proteins (ESPs). ESPs consist of a variety of proteins that have effects ranging from metabolic breakdown of host tissue to immunomodulatory capabilities. Immunomodulatory proteins are able to promote the survival of parasitic nematodes during infection by strategically altering the activation of the host immunity

[7]. Characterization of individual proteins has remained challenging due to the technical obstacles such as cost and time, that affect the plausibility of vertebrate model systems for testing hypotheses of potential effector proteins. The insect parasitic model system, however, allows for large populations to be tested with proteins isolated from insect parasitic nematodes such as entomopathogenic nematodes (EPNs) leading to molecular insight that may be translatable to vertebrate parasitic nematode infections [8-11]. Translatable insight of molecular mechanisms from EPN ESPs are due to the high homology they have with vertebrate parasitic nematodes such as *Strongyloides stercoralis* [12-14]. EPN *Steinernema carpocapsae* effector proteins were assessed using the model host *Drosophila melanogaster* due to its highly conserved innate immune system, with key immune signaling pathways and transcription factors resembling those in mammals [15]. *D. melanogaster* boasts two main immune responses: humoral and cellular [16,17]. The humoral immune response activates genes needed for synthesizing and secreting antimicrobial peptides (AMPs) from the fat body into the hemolymph [18-20]. Cellular immune responses are regulated by hemocyte function [21]. Hemocytes regulate several cellular response mechanisms like cell aggregate formation, phagocytosis, melanization, and encapsulation to help fight off infections [22,23]. Melanization occurs after the production of phenol-oxidase (PO) via up-regulation of prophenol oxidase (proPO) [24,25]. PO serves as a catalyst for melanization by mediating the oxidation of mono- and diphenols to quinones, which is followed by subsequent polymerization to form melanin generating reactive oxygen species (ROS) [26]. Activation of the immune response is generally regulated by two NF-kB signaling

pathways: Toll and Imd which are similar to human toll-like receptors (TLR) and tumor necrosis factor (TNF) signaling respectively [27]. Activation of the pathways are pathogen specific and depend on cellular properties such as cell wall composition. Systemic production of specific AMPs via the humoral response is dependent on whether the Toll or Imd pathway is activated [28-30]. As a result of the insect's innate immunity, an EPN must evade, suppress, or modulate the insect immune response by releasing effector proteins during infection in order to survive and complete their life cycle.

One family of effector proteins identified in the EPN *S. carpocapsae* was the secretory phospholipase A_2 proteins ($sPLA_2$). The $sPLA_2$ proteins are low mass (13-19 kDa), Ca2+ dependent secretory enzymes that consist of 12 groups [31]. sPLA2s cleave cellular, non-cellular and exogenous phospholipids to generate the eicosanoid precursor arachidonic acid (AA), saturated, monounsaturated, and polyunsaturated fatty acids (PUFAs) [32,33]. PUFAs generated include ω-3 eicosapentaenoic acid (EPA) and docosahexaenoic acid (DHA), both of which are precursors of anti-inflammatory lipid mediators [32]. Free AA produced from sPLA2s are oxygenated by cyclooxygenase (COX) to yield prostaglandins (PGs), and by lipoxygenases (LOX) to yield leukotrienes (LTs) respectively. Cytochrome P450 monooxygenase also changes a double bond in AA to epoxide leading to the production of epoxyeicosatrienoic acids (EETs) [34]. Most terrestrial insects however lack AA derived PUFAs, as their sPLA2s cleave linoleic acid which is then converted to AA by desaturases and long chain fatty acid elongase [35,36]. The newly formed AAs then undergo further conversion to PGs. Recently it has been discovered in insects that

AA is not converted to PGs by COX. It is instead converted to PGH_2, a five membered ring structure that is characteristic of PGs, via an insect peroxidase called peroxinectin (Pxt) [37,38]. PGH_2 is then converted into cell specific PGs via cell specific enzymes, such as PGE_2 synthase converting PGH_2 into PGE_2 [39]. PGs have been observed to play crucial roles in immune responses in insects by mediating the activation of hemocyte-spreading behavior involved in phagocytosis, nodulation, and encapsulation [34,40].

This study attempts to characterize the immunomodulatory effects of Sc-$sPLA_2$ on *D. melanogaster* against various bacterial infections. Survival and bacterial proliferation were assessed after a one-time dose of Sc-$sPLA_2$. Potential toxicity of the protein was also assessed by giving *D.* melanogaster one time dose of Sc-$sPLA_2$ alone. To understand the mechanisms contributing to immunosuppression, readouts of downstream immune responses were assessed that included AMP production, PO activity, and phagocytosis. Metabolomic analysis was conducted on the hemolymph of flies treated with a one-time dose of Sc-$sPLA_2$ to screen for potential change in lipid metabolite and fatty acid composition. A cell lysis assay was also conducted to see if any toxicity was linked to lysis of host cell membranes.

Results

Steinernema carpocapsae sPLA$_2$ protein has a toxic and immunomodulatory effect

We utilized *D. melanogaster* as a model host to screen for immunomodulation phenotypes against *Streptococcus pneumoniae* (*S.p.*) as it has been established as an

effective model system for measuring immunity [41]. To determine if subsequent phenotypes were a direct response to the enzymatic activity of the Sc-sPLA$_2$ protein, an enzymatic assay was conducted to quantify the biological activity of recombinantly expressed Sc-sPLA$_2$ and the mutant Sc-sPLA$_2$ (HH82-83QQ). 10 µgs of each protein was added to a 100 µl reaction with 1.67 µM of Red/Green BODIPY labeled PC substrate, and fluorescence emission intensity was measured at 515 nm and 575 nm and reported as a radiometric value (Figure 3.1). The mutant sPLA$_2$ displayed significantly less activity than the wild type, and overall had nominal activity while the wild type displayed a sizeable measurement for activity.

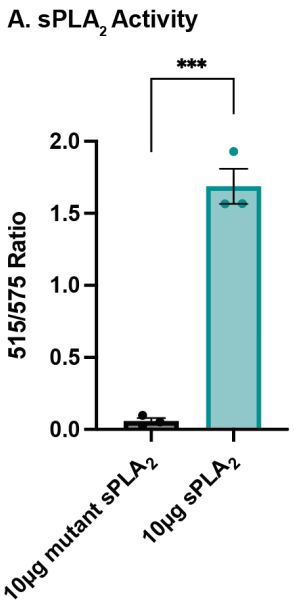

Figure 3.1: In vitro activity data of Sc-sPLA2 and mutant Sc-sPLA2 (HH82-83QQ) at 10 µgs each. Fluorescent emission intensity was measured at 515 and 575 nm and recorded as a ratiometric value. Negative control was substrate with no enzyme and was subtracted as background from both absorbance values before calculating the ratio. Substrate used was a Red/Green Bodipy labeled PC. Experiment was done in triplicate. All statistics shown as unpaired t-test, error bars depict mean with SEM.

Prior to assessing potential immunomodulatory phenotypes, toxicity of Sc-sPLA$_2$ was measured for a one-time dose injection in 5–7-day old male flies at multiple doses (Figure 3.2). Increasing percentage of toxicity was observed with an increase in dose. 5 ngs of the Sc-sPLA$_2$ protein saw very minimal toxicity by day 5, while 40 ngs had a near 65% survival rate. Denatured protein displayed no levels of toxicity throughout the 20-day period post injection, while all doses of Sc-sPLA$_2$ protein had an increase in toxicity post day 15. Upon evaluation of toxicity, each dose of Sc-sPLA$_2$ were then coinjected in the flies with 2000 cells *S.p.* where we observed a significant reduction in survival of the flies to bacterial infection after a one-time dose over the course of 20 days (Figure 3.3A). Sc-sPLA$_2$ significantly reduced the survival rate at each dose with the highest dose of 40 ngs displaying a survival rate of only 20% after day 1. Microbe growth was also observed 24 hours post coinjection. We observed an increase in microbial load after a one-time dose of Sc-sPLA$_2$ at all dose levels, with a trend of increasing bacterial cell growth correlating with higher protein dose (Figure 3.3B). The mutant Sc-sPLA$_2$ (HH82-83QQ) enzyme had no change to the survival of the flies during coinjection, confirming that the enzymatic activity of recombinantly expressed Sc-sPLA$_2$ was responsible for the immunomodulatory phenotypes observed.

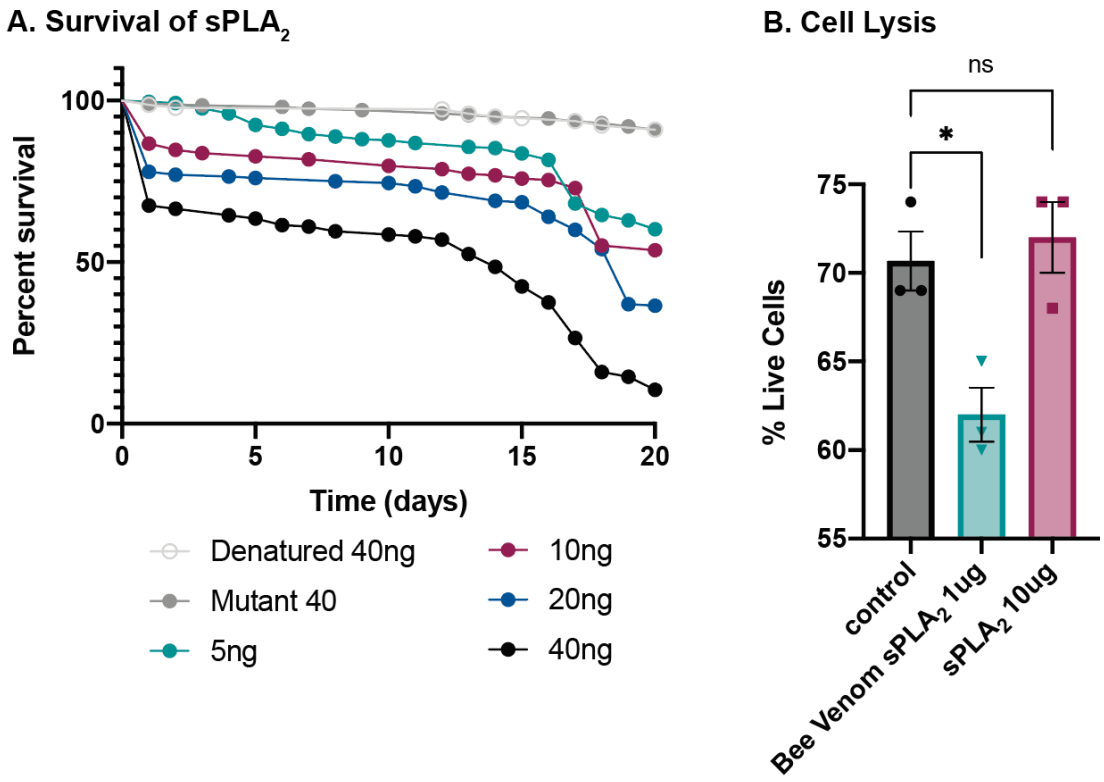

Figure 3.2: Survival rate of sPLA2 - only injected flies shows a dose-dependent toxic effect not caused by cell lysis. A) To measure the toxicity of the *S. carpocapsae* $sPLA_2$, 5-7 day old male flies were injected with various concentrations of protein and their survival was monitored for 20 days. Denatured protein shows no toxicity, and the intact protein shows a dose-dependent toxic effect with 40ng showing the most significant toxicity. B) Quantification of cell lysis was measured by % of live cells after staining with a Bio-Rad TC20 automated cell counter. Sc-$sPLA_2$ showed no significant changes to the % of live cells, while bee venom $sPLA_2$ had a significant reduction which indicated an increase in cell lysis. Reactions were done in triplicate. All statistics shown as unpaired t-test, error bars depict mean with SEM. Survival curves n≥180. All raw data available in supplemental materials.

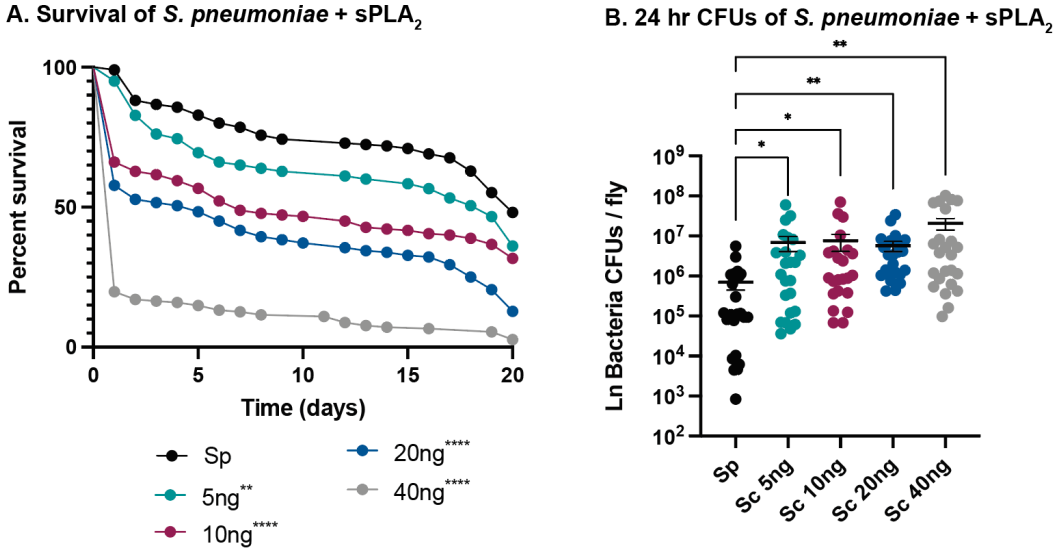

Figure 3.3: sPLA2 elicits a dose-dependent immunomodulatory effect on survival and 24-hour CFUs in *Streptococcus pneumoniae* and $sPLA_2$ coinjections. A&B) 5–7-day old male flies were coinjected with 2,000 cells of *S.p.* and various nanogram doses of $sPLA_2$. A) Their survival was monitored for 20 days, showing a significant reduction in the outcome of survival in all doses compared to the *S.p.* only injected flies. B) CFUs were measured 24 hours after injection and show a significant increase in microbe load in all protein groups compared to the control group. All controls for survival curves (black) are *S.p.*-injected only, without the addition of protein. Log-rank test p-value significance indicated by asterisks on Kaplan Meier graphs. CFU graphs show p-value significance of an unpaired t-test (error bars show mean+SEM). Survival curves n≥180, CFU graph n≥24. All raw data available in supplemental materials.

S. carpocapsae sPLA$_2$ suppresses specific downstream immune responses

D. melanogaster has a sophisticated and evolutionarily conserved immune system that can elicit an immune response via two types: humoral and cellular [16,17]. To establish the molecular mechanism that Sc-$sPLA_2$ utilizes to elicit immunomodulatory effects, we evaluated several readouts of immunity which included PO activity and AMP production. PO activity serves as a catalyst for melanization; thus 5–7-day old male flies were coinjected with Sc-$sPLA_2$ and 10,000 cells of *L. monocytogenes*, a bacteria that elicits a

robust disseminated melanization phenotype, to measure any changes to PO activity [26,42]. PO activity was quantified by measuring its absorbance at 492 nm 6 hours post injection. Treatment with Sc-sPLA$_2$ showed there were no significant changes to PO activity after a one-time dose of 40 ngs (Figure 3.4A). To further evaluate any specific downstream immune responses, AMP production was measured 24 hours post injection with a one-time dose of 40 ngs Sc-sPLA$_2$ and 2000 cells of *S.p.* The protein treatment had no significant effect on *Defensin* (Imd) but did elicit a significant reduction in *Drosomycin* (Toll) production suggesting a targeted effect on the Toll pathway by the protein (Figure 3.4B) [29,30].

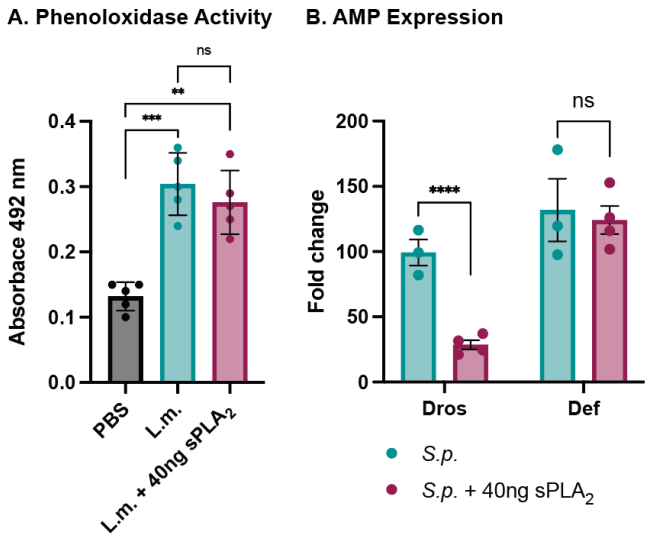

Figure 3.4: Specific downstream immune responses are affected by sPLA2 protein. A) Phenoloxidase activity was measured 6 hours after injection with either PBS control, 10,000 cells *Listeria monocytogenes,* a known melanizer, or *L.m.* plus protein. An increase in PO activity was observed in the bacteria injected group but was not altered by the presence of protein. Experiments were completed 6 times with 30 flies in each treatment group. B) Antimicrobial peptide production was measured by quantitative PCR 24 hours after injection with *S.p.* or *S.p.* plus protein. Two different AMPs were measured, *Drosomycin* (Toll) was decreased after protein injection and *Defensin* (Imd) was not affected by the protein. Experiments were repeated at least 3 times with 15 flies per treatment group. All statistics shown as unpaired t-test, error bars depict mean with SEM.

S. carpocapsae sPLA$_2$ reduces phagocytosis

Phagocytosis is an important downstream immune effector that is regulated by the cellular response in insects [22,23]. Phagocytic activity in *D. melanogaster* was visualized and quantified via injection of commercially available conjugates of *E. coli* and particles that fluoresce as a red color after exposure to the lysosome's low pH environment. These conjugates were also coinjected with the Sc-sPLA$_2$ to assess any changes in phagocytic activity. Results showed that a one-time dose of 40 ngs of protein was able to significantly decrease phagocytic activity 1 hour post injection (Figure 3.5). This result implies that Sc-sPLA$_2$ is having a targeted effect on the cellular response of *D. melanogaster* immunity.

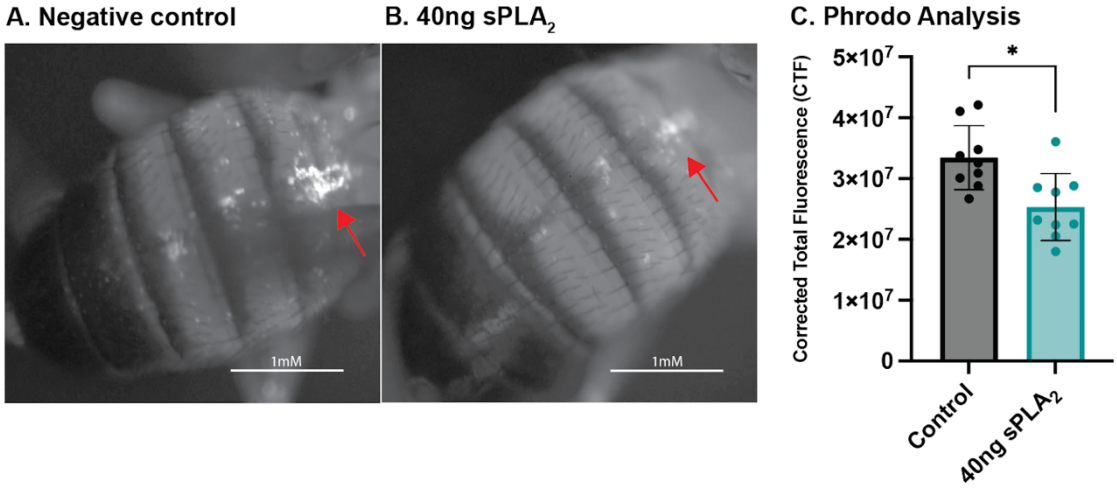

Figure 3.5: Phagocytosis is reduced by the addition of sPLA2 protein. Phagocytic activity was measured with the pHrodo assay showing fluorescence once phagocytosed. A) pHrodo only injected flies show higher amounts of fluorescence. B) Fluorescence is decreased in flies injected with pHrodo and 40ng of sPLA$_2$ protein. Representative images are depicted. C) We found the sPLA$_2$ protein to significantly reduce phagocytosis one hour post injection. Experiments were replicated 3 times with 3 flies per treatment group. All statistics shown as unpaired t-test, error bars depict mean with SEM.

S. carpocapsae sPLA$_2$ depletes 9,(10)-EpOME in fly hemolymph 12 hours post injection

To elucidate the underlying molecular mechanisms of Sc-sPLA$_2$ immunomodulatory effects, Mass spectrometry was utilized to analyze the hemolymph of 200 flies injected with the protein, and 200 flies coinjected with *S.p*. We used a targeted approach to identify any known lipid metabolites that were altered after treatment with the protein. sPLA$_2$ activity is the precursor to the production of immune response lipids and thus we anticipated this experiment would highlight any novel lipid metabolites whose composition would be affected [31]. Out of the lipid library used for analysis we saw significant quantities of 17 different lipid metabolites, and a significant reduction in only 9, (10)-EpOME 12 hours post injection (Figure 3.7). This reduction was observed in the Sc-sPLA$_2$ only treatment. 9, (10)-EpOME has been reported to be a low-level stimulator of neutrophilic burst, a process that occurs during phagocytosis resulting in increased anti-microbial ROS production [43,44]. EpOME synthesis is also enhanced in activated neutrophils which suggests they may be a target of Sc-sPLA$_2$ [45].

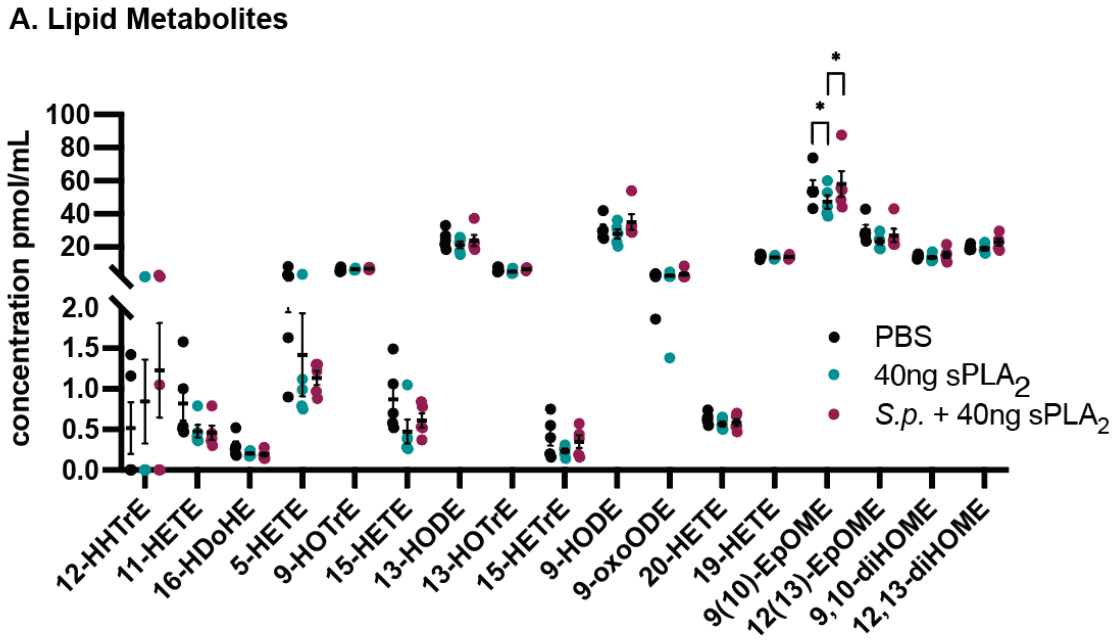

Figure 3.6: Injection of recombinant sPLA2 reduces 9,(10)-EpOME in fly hemolymph 12 hours post injection. Flies were injected with PBS, 40ng of $sPLA_2$ or 40ng $sPLA_2$ with 7,000 cells *S.p.* and pooled hemolymph was analyzed for downstream lipid metabolites 12 hours post injection. 9(10)-EpOME showed a significant reduction in the 40ng protein only group. Experiments were repeated 5 times with 200 flies per treatment group. Out of 131 metabolites, 17 were detected in fly hemolymph samples. Error bars show mean + SEM with statistics shown as unpaired t-test.

Discussion

It has been well established that $sPLA_2$ activity plays an important role in immune response by cleaving PUFAs such as AA from glycerophospholipids resulting in production of downstream immunomodulatory eicosanoids [32,33]. While this process is well defined in mammals, the presence of lipid signaling in insect immunity has not been validated and has even been disputed due to their lack of C20 and C22 PUFAs necessary for eicosanoid production [46]. It has been recently reported however that insects are able to generate eicosanoids and their precursor AA by converting cleaved LA into AA for

eicosanoid production [35,47]. With a potential mechanism in place for lipid signaling mediated immunity in insects, we evaluated the role Sc-sPLA$_2$ in host immunomodulation to bacterial infections in *D. melanogaster*.

We hypothesized that Sc-sPLA$_2$ would display immunosuppressive effects on a host due to being secreted by *S. carpocapsae* IJs during infection. sPLA$_2$ enzymes are notable for eliciting immunostimulatory responses via downstream production of proinflammatory eicosanoids from AA [32]. They also however are able to cleave PUFAs such as EPA and DHA which are converted to downstream anti-inflammatory mediators, indicating that sPLA$_2$ enzymes can also have immunosuppressive capabilities [32]. In addition to immunomodulatory capabilities, PLA$_2$ enzymes have been reported to display toxic effects in hosts. This is facilitated by necrotic cell lysis via enzymatic cleavage of the phospholipid cell membrane by PLA$_2$s, resulting in loss of cell membrane integrity and release of cellular components [48,49]. Sc-sPLA$_2$ was able to display a dose dependent toxic effect in *D. melanogaster*. At a low dose of Sc-sPLA$_2$ (5 ngs) the flies had around a 95% survival rate by day 5 in comparison to the high dose (40 ngs) that had 65% survival rate by day 5. After day 5 toxicity had a slow increase for all doses up until day 15 where another notable increase in toxicity occurred resulting in lower rates of survival. This highlighted that the enzyme's toxic effects on the host were both time and dose dependent. To assess if toxicity was in relation to cell lysis, we incubated *D. melanogaster* S2 cells with 10 µgs of Sc-sPLA$_2$ for 24 hours. We found no significant change in the amount of cell lysis in comparison to the negative control, indicating that

the toxic effects are by highly likely to be by another mechanism. In addition to toxicity, we evaluated the ability of Sc-sPLA$_2$ to suppress the immunity of *D. melanogaster* against *S. pneumoniae* infections. We found that a one-time dose of either 5, 10, 20 or 40 ng caused a significant reduction in survival of the flies over a period of 20 days. In addition to reduced survival, we observed an increase in 24-hour microbial growth of *S. pneumoniae* after coinjection with each dose in the fly. This confirmed that the sPLA$_2$ was affecting the flies' resistance to infection and elicited an immunosuppressive phenotype. The sPLA$_2$ displaying an immunosuppressive phenotype at a 5-ng dose has importance when it comes to biological relevance, as 20 IJs of *S. carpocapsae* secrete 10 ng of ESPs in 24 hours [50]. Due to the high protein composition (472) of *S. carpocapsae* it will generally be secreted in low quantities at first in a natural infection. With enough IJs however, and working in concert with other immunomodulatory proteins, it is likely that Sc-sPLA$_2$ aids in overcoming the host immune response in a natural infection.

We evaluated the effects of Sc-sPLA$_2$ had on downstream immunity in the fly. Fly immunity starts with pathogen specific recognition by the toll and imd pathway, which then leads to either a cellular immune response by hemocytes, or a humoral immune response via production of toll or Imd specific AMPs [21,28]. Melanization is independent of the toll and Imd pathway and is dependent on the PO cascade [24,25]. Our findings showed that Sc-sPLA$_2$ had no effect on PO activity but caused a reduction in the expression of the AMP *Drosomycin*, and phagocytosis [29]. These findings suggest that the PLA$_2$ suppresses toll pathway recognition and cellular immune response. In

addition to evaluating readouts of immunity, hemolymph of Sc-sPLA$_2$ injected flies and coinjected flies with *S. pneumoniae* was analyzed with Mass spectrometry to screen for any changes to the lipid metabolite composition. Findings showed that Sc-sPLA$_2$ treated only flies had a reduction in 9,(10)-EpOME. This lipid metabolite is synthesized by activated neutrophils in mammals and is a known low-level stimulator of respiratory burst, a process that occurs during phagocytosis [43-45]. Overall, this suggests that the molecular effects underlying the sPLA$_2$ suppression of the cellular immune response is via the reduction of phagocytosis by the fly hemocytes.

In summary this study showed that Sc-sPLA$_2$ experimentally dampened the immunity of *D. melanogaster* by suppression of phagocytosis and the toll pathway. In addition to immunomodulation, the pLA$_2$ also displayed dose dependent toxicity to the host that was not elicited by cell lysis. We hypothesize that the lipids being cleaved by the pLA$_2$ enzyme are from hemocytes which disrupts their ability to recognize and phagocytize cells, while producing a toxic molecular product to the host. Further elucidating the specificity of the molecular mechanisms affected by Sc-sPLA$_2$ can further validate the presence of lipid signaling in *D. melanogaster* immunity, which would improve the tools available for biomedical research addressing inflammatory diseases.

Methods

Plasmid construction

A 414 -bp DNA fragment of Sc-sPLA$_2$ gene L596_023809 was amplified by PCR using primers 5’ –

ACCATCATCACCACAGCCAGGGCAAACTTATCAAGAAGAATGTCG – 3’ (forward primer) and 5’ – TTAAGCATTATGCGGCCGCATTACGCGTGGAAATCGAGC – 3’ (reverse primer) in which a *Bam*HI site at the 5′ end and a *Hind*III site at the 3′ end were introduced for cloning it into a pETDuet-1 vector. The mutant Sc-sPLA$_2$(HH82-83QQ) had two histidine amino acid sequences at positions 82 and 83, mutated to glutamine. The mutant was synthesized, optimized and inserted into a pETDuet-1 vector utilizing a *Bam*HI site at the 5′ end and a *Hind*III site at the 3′ position. The mutant construct was generated by Bio Basic Inc.

Recombinant protein expression and purification

Sc-sPLA$_2$ and mutant Sc-sPLA$_2$ (HH82-83QQ) were recombinantly expressed using *E. coli* BL21 DE3 cells in LB media for 24 hours after induction with IPTG. Sc-sPLA$_2$ was purified from inclusion bodies with Thermo Scientific™ HisPur™ Ni-NTA Resin via gravity filtration. The protein was refolded with a 24-hour dialysis against a 20 mM Tris, 1.0 M Urea, 300 mM NaCl, and 5 % glycerol pH 8.0 buffer. After refolding the protein was dialyzed once more for 24 hours and stored in a 20 mM Tris, 300 mM NaCl, and 5 % glycerol pH 8.0 buffer. Mutant Sc-sPLA$_2$ (HH82-83QQ) was first purified with Thermo Scientific™ HisPur™ Ni-NTA Resin via gravity filtration. The protein was dialyzed against a 20 mM Tris pH 8.0 buffer for 24 hours. Further purification was conducted with FPLC using a Mono Q™ anion exchange column, after which the protein was isolated using size exclusion and stored in a 20 mM Tris, 300 mM NaCl, and 5 % glycerol pH 8.0

buffer. Both Sc-sPLA$_2$ and mutant Sc-sPLA$_2$ (HH82-83QQ) presence were confirmed using SDS-PAGE. Concentrations were measured using Invitrogen™ Qubit™ Protein and Protein Broad Range (BR) Assay Kits, and the proteins were flash frozen with liquid nitrogen and stored at −80 °C.

Protein Activity Assay

Biological activity of Sc-sPLA$_2$ and mutant Sc-sPLA$_2$ (HH82-83QQ) was assessed utilizing the EnzChek™ Phospholipase A2 Assay Kit. Each reaction contained 10 µgs of protein and 50 µl 1.67 µM Red/Green BODIPY labeled phosphatidylcholine (PC) substrate for a total of 100 µl. Reaction time was 30 minutes at room temperature. Negative control was designated as buffer only plus the substrate. Emission intensity was measured at 515 and 575 nm with excitation at 460 nm, and the activity was recorded as a ratiometric value (515/575 nm). Negative control values at 515 and 575 nm were subtracted from the protein reactions before calculation of the activity ration. Reactions were triplicated as technical replicates.

Fly stock/ maintenance

All fly strains were grown on D2 glucose medium from Archon Scientific (Durham, North Carolina) and kept at 25°C with 50% humidity on a 12h light 12h dark cycle.

Bacterial stock maintenance

Methods were adapted from Parks et. al 2021. *Streptococcus pneumoniae* was grown by shaking in glass vials with 5 mL tryptic soy (TS) broth (Difco TS broth, catalase, streptomycin) at 37°C with 5% CO_2 overnight. The overgrown culture was diluted in catalase (100 µL) and TS to yield a final volume of 20 mL in a flask and incubated shaking until the OD_{600} ~ 0.4 (about 1 hour). The culture was then diluted again to a final volume of 50 mL, with 150 µL catalase, and incubated until the OD_{600} ~ 0.2 - 0.4 (above 0.5 is no longer in log phase). 5% glycerol was added to the final culture and stored then in 1mL aliquots at -80°C. To use the aliquots, one tube was thawed, spun down at 14,000 rpm for 5 minutes, the supernatant was removed, and the pellet was resuspended in the desired amount of PBS (50 - 60 µL yields ~ 100,000 CFUs) and serially diluted to yield the appropriate CFU doses. For quantification of CFUs, *S.p.* was plated on TSA agar plates supplemented with 50 mL/L sheep's blood. *Listeria monocytogenes* (serotype 4b, 19115, (ATCC, VA)) was also grown in batches in brain heart infusion (BHI) medium at 37°C in aerobic condition. Cultures were grown overnight in a flask inoculated with a fresh colony and re-diluted under log phase (below OD_{600} ~ 0.2) and grown up to the desired OD_{600} (~0.4). The entire volume was transferred to a 50mL centrifuge tube for vortexing. Before freezing, a 5% glycerol solution was added to the culture and 1mL aliquots were stored at -80°C. To use the aliquots, one tube was thawed, spun down at 14,000 rpm for 5 minutes, the supernatant was removed, and the pellet was resuspended in the desired amount of PBS (90 - 100 µL yields ~ 100,000 CFUs) and serially diluted to

yield the appropriate CFU doses. For quantification of CFUs, *L.m.* was plated on BHI plates.

Fly injections, survival and CFUs

Methods were adapted from Parks et. al 2021. For injections and immune assays, 5-7-day-old male flies were anesthetized with CO_2 and injected with various CFU doses yielding a total volume of 50 nL precisely using a MINJ-FLY high-speed pneumatic injector (Tritech Research, CA) and individually pulled calibrated glass needles. Flies were injected into the abdomen close to where the thorax meets and slightly ventral from the dorsal-ventral cuticle axis, easily visible below the haltere. Survival studies were carried out for all of the pathogens we tested. After injection of the CFU dose or phosphate buffered saline (PBS) control, flies were placed in vials in groups of 30 with a total of 60 flies per experimental or control group. Flies injected with the human pathogens (*S.p.* and *L.m.)* were kept at 28°C with 50% humidity. The number of dead flies was counted daily, and Kaplan-Meier survival curves were generated with GraphPad Prism software with statistics shown as log-rank analysis (Mantel-Cox). Survival experiments were at least triplicated. CFUs were determined by homogenizing a single infected, or buffer-injected fly in 200 µL of PBS, serially diluted and plated on the appropriate agar plates and incubated overnight. Colonies were counted the next day. At least five flies per condition were homogenized for CFU quantification each time an injection experiment was done to measure time 0 CFUs which are representative of all fly strains. All treatment groups were injected at the same time for each experimental

replicate. Using GraphPad Prism software, results are shown as scatter plots with statistical significance analyzed using an unpaired t-test.

Phenoloxidase Activity

Methods adapted from Parks et. al 2021. Flies were injected with 10,000 CFUs of *L. monocytogenes* to elicit an immune induced melanization cascade. Phenoloxidase activity was measured as previously described [51,52]. To collect hemolymph, 20-30 flies 6 hours post injection (p.i.) were pricked through the thorax and placed in a pierced 0.5 µL Eppendorf tube and covered with glass beads, then placed inside a 1.5 µL Eppendorf tube containing 30 µL of PBS. Samples were centrifuged at 10,000 rpm for 20 minutes at 4°C. Using a clear 96-well plate, each well contained 160 µL L-Dopa (3 mg/mL) dissolved in phosphate buffer (37.5% 1 M potassium phosphate, 62.5% 1 M sodium phosphate, pH 6.5), 35 µL of hemolymph sample and 5 µL $CaCl_2$ (20 mM). PO activity was measured by kinetic reads at 29°C at 492 nm every minute for 120 min with 5 seconds of shaking between reads. The OD of a blank control was subtracted from all biological values. Experiments were replicated five times with three technical replicates per experiment. Data were plotted as mean+SEM by taking the peak OD value (timepoint ~ 60 min). Statistics shown as an unpaired t-tests done in GraphPad Prism.

Antimicrobial peptide gene expression – qPCR

Methods adapted from Parks et. al 2021. Total RNA was extracted from 15 *S. pneumonia* or *S.p.* plus recombinant protein injected flies 24 hours post-injection using Trizol reagent

(Molecular Research Center, Inc; Cincinnati, Ohio) according to the manufacturer instructions. Integrity of RNA was confirmed by observing bands on an agarose gel and concentration was determined by nanodrop. Reverse transcription of RNA using ProtoScript II First Strand cDNA synthesis kit (New England BioLabs, NE, E6560L) following the manufacturer protocol, in a MultiGene OptiMax Thermal Cycler (Labnet international, NJ). The qRT-PCR was done with a CFX Connect Bio-Rad system with Perfecta SYBR green supermix (QuantaBio, MA) and gene specific primers for *Defensin, Drosomycin*, and *Tubulin* (Integrated DNA Technologies, IA). Experiments were carried out with three technical replicates and repeated four times with plots shown as bar graphs with individual points representing each replicate. Statistics shown as One-way ANOVA done in GraphPad Prism.

Cell culture and lysis assay by sPLA2s

For the cell lysis assay, S2 cells were cultured in a 24-well plate with 0.5 ml medium until cells reached ~75% confluency. After reaching desired confluency, Sc-sPLA$_2$ and bee venom sPLA$_2$ (from EnzChek™ Phospholipase A2 Assay Kit) were filtered with a 0.45 µm filter before being added to the cell medium. 10 µgs of Sc-sPLA$_2$ and 1 µg of bee venom sPLA$_2$ were added, and the cell medium was diluted with filtered 20 mM Tris, 300 mM NaCl, and pH 8.0 buffer to a final volume of 0.6 ml (600 µl). Cells were incubated at 28 °C for 24 hours. After incubation, supernatant was removed and cells were resuspended with a new volume of 600 µl filtered 20 mM Tris, 300 mM NaCl, and pH 8.0 buffer. 10 µl of cells were then added to 10 µl of trypan blue and placed on a

dual-chamber slide where percent of live cells were quantified by a Bio-Rad TC20 cell counter.

Phrodo Phagocytosis

Injections were carried out as previously described for *S. pneumoniae* except with a 4 mg/ml suspension of pHrodo Red *E. coli* BioParticles Conjugate for phagocytosis as a substitute for the bacterial solution. This solution was diluted 1:4 in PBS containing either 5, 10, or 40 ngs of Sc-sPLA$_2$ immediately prior to injection. A negative control of no protein was injected for analysis along with the 3 different protein doses. 3 flies were injected for each treatment group with a total of 3 biological replicates each. Injected lies were incubated at 28 °C with 50% for 1 hour. After incubation, the dorsal side of the abdomen of the flies was imaged with an X-Cite® 120Q fluorescence lamp, and a ZEISS Axiocom 506 Color microscope camera attached to a ZEISS SteREO Discovery.V12 microscope at 10x magnification. ImageJ software was used to measure area-normalized corrected total fluorescence of isolated red channels.

Hemolymph only metabolomics – UCSD

A mix of 26 deuterated internal standards was added to 10uL of hemolymph. Eicosanoids were extracted by solid phase extraction (SPE) using Phenomenex Strata-X polymeric reversed phase columns. Samples were brought to dryness and taken up in buffer A (water/acetonitrile/acetic acid 60/40/0.02, v/v/v). Samples were analyzed using a Waters Acquity UPLC interfaced with an AB

Sciex 6500 QTrap instrument. Chromatographic separation was achieved by a step gradient starting with100% buffer A to 100% buffer B (acetonitrile/isopropanol 50/50, v/v) over 5 min. Standard curves were obtained in parallel using identical conditions. Data analysis was performed with Analyst and Mulitquant software packages. We monitored 159 MRMs.

Reference:

Wang Y, Armando AM, Quehenberger O, Yan C, Dennis EA. Comprehensive ultra-performance liquid chromatographic separation and mass spectrometric analysis of eicosanoid metabolites in human samples. J Chromatogr A. 2014 Sep 12;1359:60-9. doi: 10.1016/j.chroma.2014.07.006. Epub 2014 Jul 12. PMID: 25074422; PMCID: PMC4592635.

Statistics

All statistics were done with GraphPad Prism 9.1.0 for Mac. Statistical significance indicated with asterisks indicating the following p-value cut offs: 0.05-0.033*, 0.033-0.002**, 0.002-0.0002*** and <0.0001****.

Supplemental

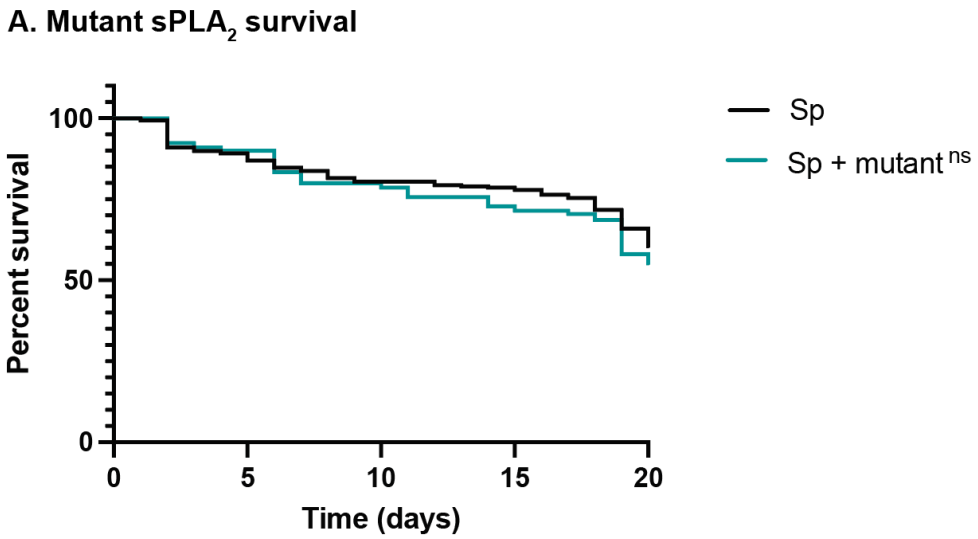

Supplemental figure S3.1: Inactive mutant sPLA2 does not show an immunomodulatory effect. Flies were injected with 2,000 cells S.p. or 2,000 cells S.p. plus mutant $sPLA_2$ and survival was monitored for 20 days. There is no significant difference between the two treatment groups. Each treatment group represents at least 180 flies on the Kaplan Meier graph with significance shown as log-rank Mantel-Cox) test.

References

1. Hotez, P.J., et al., *The global burden of disease study 2010: interpretation and implications for the neglected tropical diseases.* PLoS Negl Trop Dis, 2014. **8**(7): p. e2865.

2. Pullan, R.L., et al., *Global numbers of infection and disease burden of soil transmitted helminth infections in 2010.* Parasit Vectors, 2014. **7**: p. 37.

3. L'Ollivier, C. and R. Piarroux, *Diagnosis of human nematode infections.* Expert Rev Anti Infect Ther, 2013. **11**(12): p. 1363-76.

4. Hao, Y.J., et al., *Transcripts analysis of the entomopathogenic nematode Steinernema carpocapsae induced in vitro with insect haemolymph.* Mol Biochem Parasitol, 2010. **169**(2): p. 79-86.

5. Davis, E.L., et al., *Nematode Parasitism Genes.* Annu Rev Phytopathol, 2000. **38**: p. 365-396.

6. Garg, G. and S. Ranganathan, *Helminth secretome database (HSD): a collection of helminth excretory/secretory proteins predicted from expressed sequence tags (ESTs).* BMC Genomics, 2012. **13 Suppl 7**: p. S8.

7. Cooper, D. and I. Eleftherianos, *Parasitic Nematode Immunomodulatory Strategies: Recent Advances and Perspectives.* Pathogens, 2016. **5**(3).

8. Castelletto, M.L., et al., *Diverse host-seeking behaviors of skin-penetrating nematodes.* PLoS Pathog, 2014. **10**(8): p. e1004305.

9. Dillman, A.R., et al., *Olfaction shapes host-parasite interactions in parasitic nematodes.* Proc Natl Acad Sci U S A, 2012. **109**(35): p. E2324-33.

10. Hallem, E.A., et al., *A sensory code for host seeking in parasitic nematodes.* Curr Biol, 2011. **21**(5): p. 377-83.

11. Hallem, E.A., et al., *Nematodes, bacteria, and flies: a tripartite model for nematode parasitism.* Curr Biol, 2007. **17**(10): p. 898-904.

12. Ciche, T., *The biology and genome of Heterorhabditis bacteriophora.* WormBook, 2007: p. 1-9.

13. Dillman, A.R., et al., *Comparative genomics of Steinernema reveals deeply conserved gene regulatory networks.* Genome Biol, 2015. **16**: p. 200.

14. Lok, J.B., *Strongyloides stercoralis: a model for translational research on parasitic nematode biology.* WormBook, 2007: p. 1-18.

15. Vanha-Aho, L.M., S. Valanne, and M. Rämet, *Cytokines in Drosophila immunity.* Immunol Lett, 2016. **170**: p. 42-51.

16. Lemaitre, B. and J. Hoffmann, *The host defense of Drosophila melanogaster.* Annu Rev Immunol, 2007. **25**: p. 697-743.

17. Jiang, H., A. Vilcinskas, and M.R. Kanost, *Immunity in lepidopteran insects.* Adv Exp Med Biol, 2010. **708**: p. 181-204.

18. Imler, J.L. and P. Bulet, *Antimicrobial peptides in Drosophila: structures, activities and gene regulation.* Chem Immunol Allergy, 2005. **86**: p. 1-21.

19. Casanova-Torres, Á. and H. Goodrich-Blair, *Immune Signaling and Antimicrobial Peptide Expression in Lepidoptera.* Insects, 2013. **4**(3): p. 320-38.

20. Rolff, J. and P. Schmid-Hempel, *Perspectives on the evolutionary ecology of arthropod antimicrobial peptides.* Philos Trans R Soc Lond B Biol Sci, 2016. **371**(1695).

21. Ribeiro, C. and M. Brehélin, *Insect haemocytes: what type of cell is that?* J Insect Physiol, 2006. **52**(5): p. 417-29.

22. Marmaras, V.J. and M. Lampropoulou, *Regulators and signalling in insect haemocyte immunity.* Cell Signal, 2009. **21**(2): p. 186-95.

23. Honti, V., et al., *The cell-mediated immunity of Drosophila melanogaster: hemocyte lineages, immune compartments, microanatomy and regulation.* Dev Comp Immunol, 2014. **42**(1): p. 47-56.

24. Eleftherianos, I. and C. Revenis, *Role and importance of phenoloxidase in insect hemostasis.* J Innate Immun, 2011. **3**(1): p. 28-33.

25. Lu, A., et al., *Insect prophenoloxidase: the view beyond immunity.* Front Physiol, 2014. **5**: p. 252.

26. Cooper, D., et al., *The prophenoloxidase system in Drosophila participates in the anti-nematode immune response.* Mol Immunol, 2019. **109**: p. 88-98.

27. Hoffmann, J.A., et al., *Phylogenetic perspectives in innate immunity.* Science, 1999. **284**(5418): p. 1313-8.

28. De Gregorio, E., et al., *The Toll and Imd pathways are the major regulators of the immune response in Drosophila.* EMBO J, 2002. **21**(11): p. 2568-79.

29. Valanne, S., J.H. Wang, and M. Rämet, *The Drosophila Toll signaling pathway.* J Immunol, 2011. **186**(2): p. 649-56.

30. Myllymäki, H., S. Valanne, and M. Rämet, *The Drosophila imd signaling pathway.* J Immunol, 2014. **192**(8): p. 3455-62.

31. Murakami, M., et al., *Secreted phospholipase A2 revisited.* J Biochem, 2011. **150**(3): p. 233-55.

32. Murakami, M. and I. Kudo, *Phospholipase A2.* J Biochem, 2002. **131**(3): p. 285-92.
33. Burke, J.E. and E.A. Dennis, *Phospholipase A2 structure/function, mechanism, and signaling.* J Lipid Res, 2009. **50 Suppl**: p. S237-42.

34. Kim, Y., et al., *Eicosanoid-mediated immunity in insects.* Dev Comp Immunol, 2018. **83**: p. 130-143.

35. Chandra Roy, M., D. Lee, and Y. Kim, *Host Immunosuppression Induced by.* Insects, 2019. **11**(1).

36. Hasan, M.A., et al., *Variation in pathogenicity of different strains of Xenorhabdus nematophila; Differential immunosuppressive activities and secondary metabolite production.* J Invertebr Pathol, 2019. **166**: p. 107221.

37. Stanley, D. and Y. Kim, *Prostaglandins and Other Eicosanoids in Insects: Biosynthesis and Biological Actions.* Front Physiol, 2018. **9**: p. 1927.

38. Park, J. and Y. Kim, *Prostaglandin mediates down-regulation of phenoloxidase activation of Spodoptera exigua via plasmatocyte-spreading peptide-binding protein.* Arch Insect Biochem Physiol, 2014. **85**(4): p. 234-47.

39. Ahmed, S., D. Stanley, and Y. Kim, *An Insect Prostaglandin E.* Front Physiol, 2018. **9**: p. 1231.

40. Stanley, D., *Prostaglandins and other eicosanoids in insects: biological significance.* Annu Rev Entomol, 2006. **51**: p. 25-44.

41. Parks, S.C., et al., *Parasitic nematode fatty acid- and retinol-binding proteins compromise host immunity by interfering with host lipid signaling pathways.* PLoS Pathog, 2021. **17**(10): p. e1010027.

42. Ayres, J.S. and D.S. Schneider, *A signaling protease required for melanization in Drosophila affects resistance and tolerance of infections.* PLoS Biol, 2008. **6**(12): p. 2764-73.

43. Dahlgren, C. and A. Karlsson, *Respiratory burst in human neutrophils.* J Immunol Methods, 1999. **232**(1-2): p. 3-14.

44. Thompson, D.A. and B.D. Hammock, *Dihydroxyoctadecamonoenoate esters inhibit the neutrophil respiratory burst.* J Biosci, 2007. **32**(2): p. 279-91.

45. Ishizaki, T., T. Ozawa, and N.F. Voelkel, *Leukotoxins and the lung.* Pulm Pharmacol Ther, 1999. **12**(3): p. 145-55.

46. Shen, L.R., et al., *Drosophila lacks C20 and C22 PUFAs.* J Lipid Res, 2010. **51**(10): p. 2985-92.

47. Hasan, M.A., S. Ahmed, and Y. Kim, *Biosynthetic pathway of arachidonic acid in Spodoptera exigua in response to bacterial challenge.* Insect Biochem Mol Biol, 2019. **111**: p. 103179.

48. Ownby, C.L., et al., *Melittin and phospholipase A2 from bee (Apis mellifera) venom cause necrosis of murine skeletal muscle in vivo.* Toxicon, 1997. **35**(1): p. 67-80.

49. Hurley, B.P. and B.A. McCormick, *Multiple roles of phospholipase A2 during lung infection and inflammation.* Infect Immun, 2008. **76**(6): p. 2259-72.

50. Lu, D., et al., *Activated entomopathogenic nematode infective juveniles release lethal venom proteins.* PLoS Pathog, 2017. **13**(4): p. e1006302.

Chapter 4

Immunostimulatory Lipids in Drosophila Bacterial Infection

Sophia C. Parks[1], Susan Nguyen[1], Daiki Fujinaga[2], Naoki Yamanaka[2], and Adler R. Dillman[1*] [1]Department of Nematology, University of California, Riverside, California, 92521, USA.

[2]Department of Entomology, University of California, Riverside, California, 92521, USA.

*Corresponding: adlerd@ucr.edu

Abstract

Eicosanoids are C20 polyunsaturated fatty acids (PUFAs) that carry out essential roles in mammalian and insect systems including development, reproduction, and immunity. Insects have been shown to have low levels of C20s in circulation and it has been hypothesized that eicosanoids are synthesized from C18 precursors such as linoleic acid. Here we show that Drosophila exhibits higher levels of C18s that are depleted in the hemolymph post bacterial infection. Interestingly, these depleted lipids are able to rescue the outcome of infection as well as certain prostaglandins. This work identifies lipids that are essential for immunity and displays that Drosophila may also utilize pro- and anti-immune lipid signaling to mitigate bacterial infections. Our understanding of immune signaling in the fly and its analogies to the mammalian system will allow for an even more detailed use as a model organism in immune studies.

Introduction

Polyunsaturated fatty acids (PUFAs) are essential to most organisms and are involved in carrying out key roles in development, regulation of key bodily functions, and immunity. In mammalian systems, PUFAs typically act as substrates for three major lipid biosynthesis pathways to form eicosanoids after being hydrolyzed from the membrane by phospholipase A_2 as arachidonic acid. They can be converted to prostaglandins (PGs) by cyclooxygenases (COXs), leukotrienes and hydroxyeicosatrienoic acids among many others by lipoxygenases (LOXs), and epoxyeicosatrienoic acid (EET) by cytochrome P450 (CYP) [1-3]. Although less thoroughly researched than in mammalian systems, oxylipins have also been demonstrated to play important biological roles in insects [4]. One of the earlier studies about prostaglandins in insects demonstrates that PGs are involved in egg-laying behavior of the cricket species *Teleogryllus commodus* [4,5]. The transfer of a PG-synthesizing complex from the male's spermatophore to the female's storage organ during mating, and the presence of PGE2 in mated females in addition to PGE_2's ability to induce egg release in females have both demonstrated that PGs play a crucial role in *T. commodus* reproduction [5]. In silkmoth *Bombyx mori,* inhibition of PG synthesis by aspirin and indomethacin is shown to interfere with follicle development to late choriogenesis, and LOX and COX products in *Rhodnius plexus'* ovaries have been shown, by use of pharmaceutical inhibitors, to upregulate and downregulate the uptake of Rhodnius heme binding protein, respectively [6,7,8]. In ticks, PGE_2 reportedly influences the fluid secretion rates and composition. Inhibition of PLA_2 and COX in salivary glands of *Amblyomma americanum* results in decreased fluid secretion, and stimulation of these

salivary glands with PGE_2 leads to increased levels of Ca2+ and inositol 1,4,5-trisphosphate release alongside exocytosis of bioactive proteins [4,6]. In humans, eicosanoids' role in immune responses as lipid mediators are well-known, but research also supports that eicosanoids are involved in cellular and humoral immune responses in insects. Initially, the role of eicosanoids in insect immunity was first discovered when pharmacological inhibition of PLA_2 in *Manduca sexta* decreased the organism's ability to clear bacteria from the hemolymph, a phenotype that was rescued with the addition of arachidonic acid [7]. Because the timeframe of experiments on *M. sexta* was sufficiently short, it was suggested that eicosanoids likely influence cellular immunity, which is more instantaneous compared to humoral immunity [7]. Other markers of cellular immune responses in insects were subsequently investigated. Nodulation in *M. sexta* larvae in response to bacterial challenge is observed to decrease in a dose-dependent manner when treated with PLA_2 inhibitor dexamethasone, and this effect is reversed when infected insects are treated with eicosanoid-precursor PUFAs [8]. Similarly, dexamethasone injection in *Drosophila melanogaster* larvae results in reduced melanotic encapsulation when infected with *Leptophilina boulardi*, and increase of phagocytosis due to PGE_2 stimulation is observed in waxmoth *Galleria mellonella*, beet armyworm *Spodoptera exigua*, and *Rhodnius prolixus* [9,10]. The role of eicosanoids in *D. melanogaster* immune signaling is of special interest since fruit flies are often utilized as a model organism for disease. Host defense in fruit flies include physical barriers and innate immunity, which can further be divided into cellular and humoral immunity. Cellular immunity involves phagocytosis and encapsulation by hemocytes in hemolymph, while

humoral immunity results in production of antimicrobial peptides (AMPs) from the fat body [11,12]. Two signaling pathways regulate AMP production: the Toll pathway, and the immune deficiency (imd) pathway, both sharing similarities to mammalian's Toll-like receptor/interleukin 1 receptor signaling cascade and TNF-R pathway, respectively [11]. A functional link between PLA_2-generated fatty acids and lipopolysaccharide(LPS)-activated imd pathway has been established. Culturing transgenic larvae in PLA_2 inhibitors dexamethasone and *p*-bromophenacyl bromide results in the suppression of LPS-activated imd pathway, and this suppression effect is reversed upon addition of arachidonic acid [13]. Although the *D. melanogaster* genome possesses PLA_2 sequences in its genome, the lack of mammalian COX gene homologs initially raised questions as to how fruit flies could have synthesized eicosanoids *in vitro*, until a COX-like peroxidase called peroxinectin (Pxt) was discovered and provided a novel mechanism for PG synthesis in fruit flies and insects [14,15]. Despite various research into lipids in insect immunity, the role of eicosanoids and other lipids in *D. melanogaster* immunity has not been sufficiently characterized. This study provides evidence to support that lipids and eicosanoids are essential in *D. melanogaster's* immune responses.

Results

Analysis of fly hemolymph reveals lipids that are significantly reduced after bacterial infection

To determine how lipids are involved in immune signaling in the model organism *Drosophila melanogaster*, we utilized *Streptococcus pneumoniae* (*S.p.*) as an immune

challenge, which was previously established, to identify changes in lipid metabolites post infection (Parks, 2021). Since lipids are cleaved from the membrane via a phospholipase A_2, and lipid metabolites are clearly detected in fly hemolymph samples, we began with searching for lipids altered by an infection in circulation [16]. After isolating the hemolymph of 5–7-day old male flies of 2,000 total PBS injected or *S.p.* injected flies, 13 out of 86 lipid metabolites were detected. All of the lipids detected in this study were C18 lipids, although C20s have been previously detected in fly hemolymph [16]. Out of the 13 lipids detected, 6 were significantly decreased 12 hours post injection, some of which are upstream lipid precursors such as oleic and linoleic acid, others, such as ODEs, are oxidized metabolites found further downstream the lipid pathway (Figure 4.1). We saw similar effects at 6 hours post infection with downstream oxidized derivatives of linoleic acid showing depletion (Supplemental figure S4.1) revealing that even in a short period post infection, lipid metabolites are being altered.

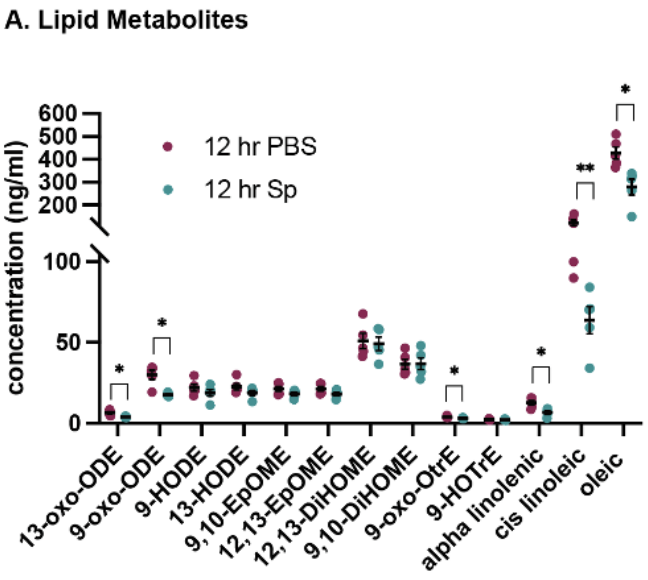

Figure 4.1: An *S. pneumoniae* induced immune challenge significantly reduces lipid metabolites in fly hemolymph 12 hours post infection. Flies were injected with 7,000 cells of *S.p.* and hemolymph was collected for mass spectrometry analysis 12 hours post injection. 13-oxo-ODE, 9-oxo-ODE, 9-oxo-OtrE, a-linolenic acid, cis linoleic acid, and oleic acid were significantly reduced in infected flies. Experiments were repeated 5 times with 200 flies per treatment group per replicate yielding a total of 2,000 flies. Error bars depict mean + SEM with statistics shown as a Welch's t-test.

Lipids predicted to be involved in immune responses are able to rescue the outcome of infection

All of the lipids that had a significant reduction post infection, as well as arachidonic acid, the eicosanoid precursor, were coinjected with *S.p.* to observe whether these depleted lipids are able to alter the course of infection. Interestingly, the dose response survival curves show specific beneficial effects. Some upstream lipids such as alpha-linolenic acid and oleic acid provide a positive effect to the fly as low as the 50 and 100µM doses (Figure 4.2A and 4.2D) while linoleic acid requires a higher dose of at least 250µM to elicit the same response (Figure 4.2B). Arachidonic acid was previously

detected in the fly's hemolymph and due to its key involvement as an eicosanoid and prostaglandin precursor it was included in our rescue study (Parks 2021). Interestingly, even a 50μM dose offers significant protection from death caused by bacterial infection (Figure 4.2C). It is striking that arachidonic, linoleic, alpha-linolenic and oleic acids were able to completely rescue the flies from bacterial infection at higher doses of 500μM and 1mM, bringing the 15-day survival rate from one percent in bacteria only injected flies to over 90 percent in coinjected flies (Figure 4.2 A, B, C, D). Not all lipids are able to elicit this protective effect; the geometric isomer of linoleic acid, linoelaidic acid, shows no protective effect even at the highest dose of 1mM (Supplemental Figure S4.2). This demonstrates that the protective lipids are specific and are likely involved in immune signaling in the fly. Oxidized derivatives of linoleic acid, oxo-ODEs and oxo-OtREs, were also tested for their potential beneficial effects. We found these lipids to be beneficial at lower doses of 50 and 100μM and toxic at the higher dose of 250μM (Figure 4.2E and F, Supplemental Figure S4.3).

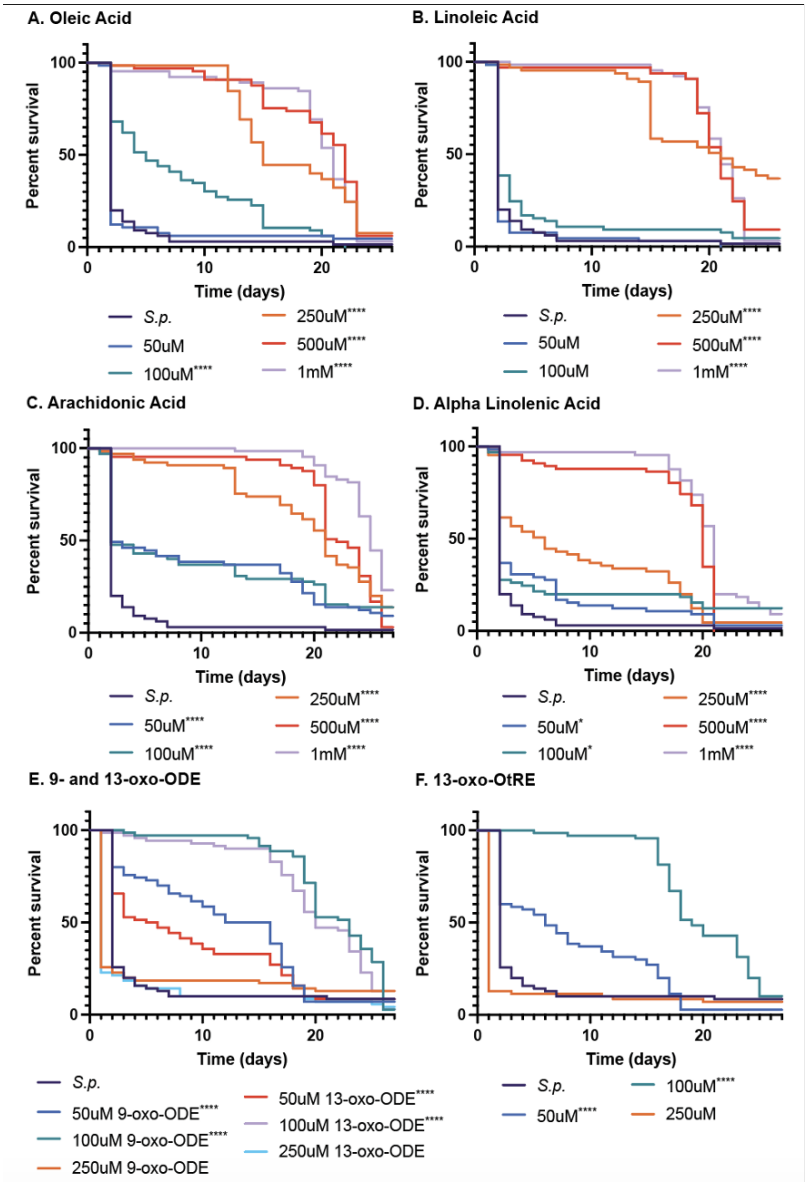

Figure 4.2: Upstream lipids and downstream oxylipins rescue bacterial infections in a dose dependent manner. Flies were injected with 7,000 cells *S.p.* along with various doses of lipid. A) Oleic acid shows a significant beneficial effect on the outcome of infection starting at 100mM. B) Linoleic acid displays beneficial effects at 250mM. C&D) Arachidonic acid and alpha linolenic acid are both effective starting at the lowest dose of 50mM. E&F) Downstream oxylipins oxo-ODE and OtRE all have a positive effect on the fly's ability to survive a bacterial infection at the 50 and 100mM doses and a detrimental effect at the higher dose of 250mM. All controls are *S.p.*-only injected shown in dark blue. Experiments were replicated at least 3 times with a total of at least 180 flies per treatment group. Statistics shown as Log-rank test as asterisks next to the experimental group labeling under the graph.

Prostaglandins known to be important for mammalian immune responses are also able to rescue the outcome of infection

Even though no prostaglandins were detected in our hemolymph samples, it has been proposed that *D. melanogaster* does have a putative eicosanoid biosynthesis pathway that leads to prostaglandins [17]. We tested common, stable prostaglandins at multiple doses to determine their effects on the outcome of infection and found them all to be beneficial at the highest dose of 250µM (Figure 4.3). Prostaglandin E_2 (PGE_2) is the most effective prostaglandin tested, as it significantly improves the outcome of infection at even the lowest dose of 50µM (Figure 4.3B). Interestingly, PGE_2 is hypothesized to be synthesized from linoleic acid in insects and is likely the most plausible prostaglandin to be circulating in fly hemolymph.

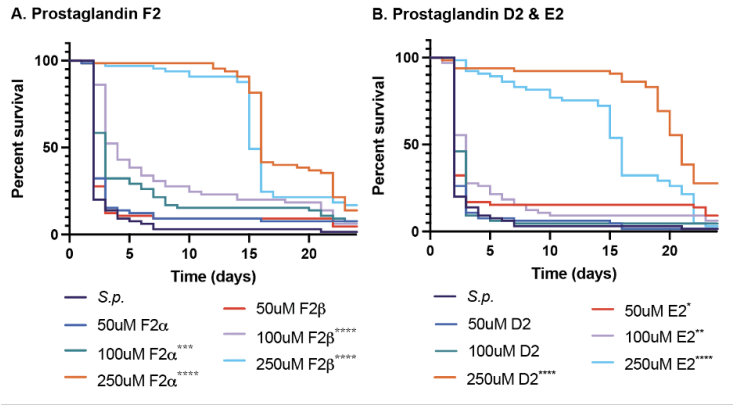

Figure 4.3: Downstream prostaglandins significantly improve the outcome of a bacterial infection. Flies were injected with 7,000 cells *S.p.* along with various doses of prostaglandins. A) Prostaglandins F2a and F2b provide significant improvement in the outcome of infection at the 100 and 250mM doses. B) Prostaglandin D2 is only beneficial at the highest dose of 250mM whereas E2 has a positive effect beginning with 50mM. Experiments were replicated at least 3 times with a total of at least 180 flies per treatment group. Statistics shown as Log-rank test as asterisks next to the experimental group labeling under the graph.

Discussion

The *Drosophila* innate immune response consists of two main pathways; the humoral immune response that leads to antimicrobial peptide production and the cellular immune response that mainly consists of hemocyte cells controlling the proliferation and survival of the pathogen in circulation [11]. The mechanisms that instigate the innate immune responses in *Drosophila* and mammalian systems are highly conserved [12]. Many experiments have shown that oxylipins are essential for insects to carry out an immune response and clear an infection, yet not much is known about their relation to the outcome of infection in the fly. Previous research has shown that bacterial infections increase synthesis of phospholipids in the fat body, the major organ for the humoral immune response in *Drosophila*, which can then be converted to downstream eicosanoids [18].

Eicosanoid metabolites are essential for immune signaling in many different animals including insects. Here we show that C18 lipids are depleted after infection, signifying that they are being utilized by the fly to fight the infection. In insects, it is likely that C18s such as linoleic acid are being cleaved by endogenous phospholipase A_2's (PLA_2) and converted to eicosanoids by different enzymes [19]. Once linoleic acid is cleaved from the membrane it is elongated via an elongase to a C20 and converted to arachidonic acid by a desaturase. From there, it can be converted to PGH2 by peroxinectin and to PGE_2 by PGE_2-synthase [19]. On the other hand, some linoleic acid may be oxygenated

by a desaturase and converted to C18 oxylipins such as the EpOMEs and DiHOMEs. Since insects generally have relatively low concentrations of C20s in circulation to minimize damage caused by oxidative stress, it is relevant that C18s are the dominant lipids found in the hemolymph samples [19]. We also show that the lipids that are depleted by an infection are able to rescue the infection even at low doses. This leads to the hypothesis that providing more of the necessary eicosanoid precursors in the fly allows them to create more pro-immune signaling molecules, leading to a beneficial effect on the outcome of infection. The lipids that are able to rescue the infection must be feeding into the eicosanoid pathway and being converted by specific enzymes since the geometric isomer of linoleic acid, linoelaidic acid, is unable to rescue in the same way.

Prostaglandins are synthesized from arachidonic acid by peroxinectin in *Drosophila* and are required for many functions including development, reproduction, and immunity [15]. The ability of prostaglandins to also rescue the infection at low doses supports the hypothesis that *Drosophila* and other insects are able to synthesize downstream eicosanoids from C18 derivatives. Prostaglandins F_2, D_2 and E_2 are all able to rescue the infection with E2 having the most beneficial effect. This is an interesting result since PGE2 has a proposed direct synthesis pathway in insects [20]. It is likely that the eicosanoid receptors are highly conserved and that the ligands able to activate the downstream immune pathways are diverse, but that only a few are endogenously found in the fly. Since the detection of lipids and eicosanoids in the hemolymph is relatively low, it is hard to determine the concentration of them present in the fly.

In mammals, the eicosanoid pathway from arachidonic acid diverges into prostaglandins, leukotrienes, and epoxyeicosatrienoic acids all communicating proinflammatory or antiinflammatory signals [17]. This work provides insight into a potential conserved system in the fly where lipid signaling may also yield pro- or anti-immune responses depending on the activated pathways. Overall, this study provides more evidence to support a functional eicosanoid biosynthesis pathway in the fruit fly and that eicosanoid lipid signaling is involved in innate immune functions. The ability of specific lipids and prostaglandins to completely rescue a bacterial infection gives new insight to the interconnected immune responses of *Drosophila* and mammalian systems.

Methods

Fly stock/ maintenance

All fly strains were grown on D2 glucose medium from Archon Scientific (Durham, North Carolina) and kept at 25°C with 50% humidity on a 12h light 12h dark cycle.

Bacterial stock maintenance

Methods adapted from Parks et. al 2021. *Streptococcus pneumoniae* was grown by shaking in glass vials with 5 mL tryptic soy (TS) broth (Difco TS broth, catalase, streptomycin) at 37°C with 5% CO_2 overnight. The overgrown culture was diluted in catalase (100 μL) and TS to yield a final volume of 20 mL in a flask and incubated shaking until the OD_{600} ~ 0.4 (about 1 hour). The culture was then diluted again to a final

volume of 50 mL, with 150 µL catalase, and incubated until the OD_{600} ~ 0.2 - 0.4 (above 0.5 is no longer in log phase). 5% glycerol was added to the final culture and stored then in 1mL aliquots at -80°C. To use the aliquots, one tube was thawed, spun down at 14,000 rpm for 5 minutes, the supernatant was removed, and the pellet was resuspended in the desired amount of PBS (50 - 60 µL yields ~ 100,000 CFUs) and serially diluted to yield the appropriate CFU doses. *S.p.* was plated on TSA agar plates supplemented with 50 mL/L sheep's blood when needed.

Fly bacterial and lipid injections, survival and CFUs

Methods adapted from Parks et. al 2021. For injections and metabolomics assays, 5-7-day-old male flies were anesthetized with CO_2 and injected with various CFU doses of *S. pneumoniae*, with or without the addition of various fatty acids, yielding a total volume of 50 nL precisely using a MINJ-FLY high-speed pneumatic injector (Tritech Research, CA) and individually pulled calibrated glass needles. The lipids linoleic acid, arachidonic acid, alpha-linolenic acid, oleic acid, 9-oxo-ODE, 13-oxo-ODE, 9-oxo-OtRE and all prostaglandins (Caymen Chemical, Ann Arbor, USA) were dissolved in ethanol were freshly diluted in PBS for coinjection. Flies were injected into the abdomen close to where the thorax meets and slightly ventral from the dorsal-ventral cuticle axis, easily visible below the haltere. Survival studies were carried out for all of the lipids tested. After injection of the CFU dose or phosphate buffered saline (PBS) control, flies were placed in vials in groups of 30 with a total of 60 flies per experimental or control group. Flies injected with the human pathogen *S.p.* were kept at 28°C with 50% humidity. The

number of dead flies was counted daily, and Kaplan-Meier survival curves were generated with GraphPad Prism software with statistics shown as log-rank analysis (Mantel-Cox). Survival experiments were at least triplicated. CFUs were determined by homogenizing a single infected, or buffer-injected fly in 200 µL of PBS, serially diluted and plated on blood agar plates and incubated overnight. Colonies were counted the next day. At least five flies per condition were homogenized for CFU quantification each time an injection experiment was done to measure time 0 CFUs which are representative of all treatment groups. All flies in various treatment groups were injected at the same time for each experimental replicate. Using GraphPad Prism software, results are shown as scatter plots with statistical significance analyzed using an unpaired t-test.

Lipidomic analysis – Lipotype (Germany)

Sample preparation for analysis of PUFA-derived lipid mediators and metabolites - 500 µL plasma were spiked with a mixture of antioxidants, and an internal standard consisting of:14,15-DHET-D11, 15-HETE-d8, 20-HETE-d6, 8,9-EET-d11, 9,10-DiHOME-d4, d4-12(13)-EpOME, d4-13-HODE, d4-PGB2, d4-PGE2-13,14-dihydro-15-keto, d4-PGF2a, LTB4-D4, PGE2-D4 with 1 ng each (Cayman Chemical, Ann Arbor, USA). Methanol and sodium hydroxide were added for protein precipitation and alkaline hydrolysis at 60 °C for 30 minutes. After centrifugation and pH adjustment, the obtained supernatant was added to Bond Elute Certify II columns (Agilent Technologies, Santa Clara, USA) for solid phase extraction. The eluate was evaporated on a heating block at 40 °C under a stream of nitrogen to obtain a solid residue. Residues were dissolved in

100 µL methanol/water. 3.2 LC/ESI-MS/MS. The residues were analyzed using an Agilent 1290 HPLC system with binary pump, multisampler and column thermostat with a Zorbax Eclipse plus C-18, 2.1 x 150 mm, 1.8 µm column using a gradient solvent system of aqueous acetic acid (0.05%) and acetonitrile/methanol 50:50 (v/v). The flow rate was set at 0.3 mL/min, the injection volume was 20 µL. The HPLC was coupled with an Agilent 6495 Triplequad mass spectrometer (Agilent Technologies, Santa Clara, USA) with electrospray ionisation source. Analysis was performed with Multiple Reaction Monitoring in negative mode, with at least two mass transitions for each compound. Data Quality - The dynamic range was determined prior to analysis. Based on these data, limits of quantification and coefficients of variation for the different lipid classes were determined. Limits of quantification are in the lower pg range, depending on the analyte. The average coefficient of variation for a complete set of analytes is <15%.

Statistics

All statistics were done with GraphPad Prism 9.1.0 for Mac. Statistical significance indicated with asterisks indicating the following p-value cut offs: 0.05-0.033*, 0.033-0.002**, 0.002-0.0002*** and <0.0001****.

Supplemental

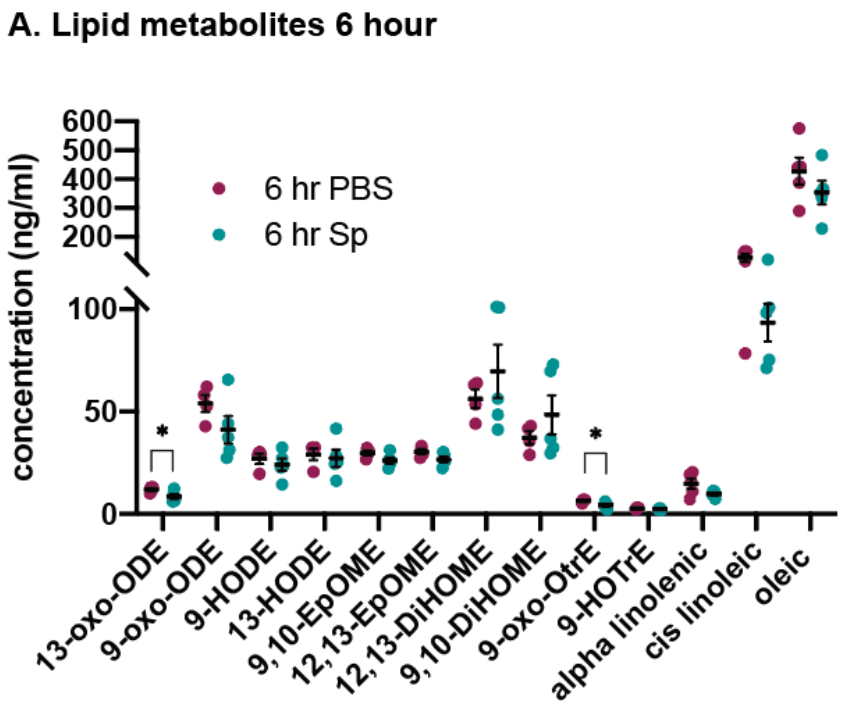

Supplemental Figure S4.1: Downstream oxylipins are depleted 6 hours post injection. Flies were injected with 7,000 cells of *S.p.* and hemolymph was collected for mass spectrometry analysis 6 hours post injection. 13-oxo-ODE and 9-oxo-OtrE were significantly reduced in infected flies. Experiments were repeated 5 times with 200 flies per treatment group per replicate yielding a total of 2,000 flies. Error bars depict mean + SEM with statistics shown as a Welch's t-test.

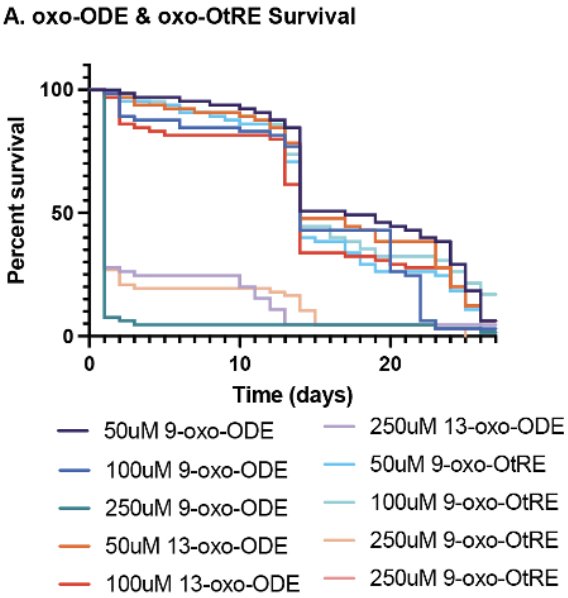

Supplemental Figure S4.2: The oxylipin derivatives oxo-ODE and -OtRE are toxic at high doses. To determine why rescue of the infection at the higher doses of these lipids were not possible we injected them individually. The 250mM doses of these lipids are toxic to the fly. Experiments were replicated at least 3 times with a total of at least 180 flies per treatment group.

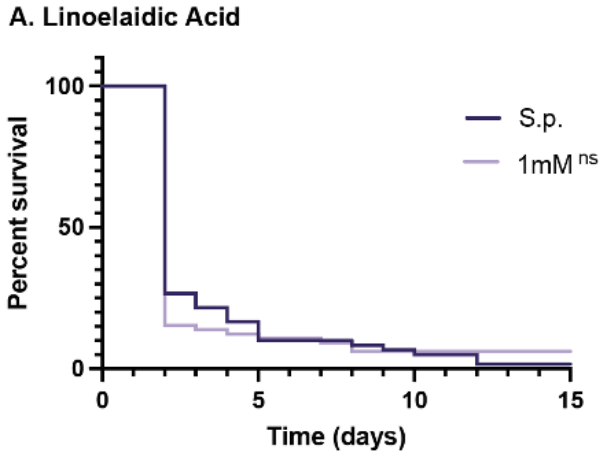

Supplemental Figure S4.3: The ability of lipids to significantly alter the course of infection is specific. The geometric isomer of linoleic acid linoelaidic acid is unable to rescue a bacterial infection. A) Flies were injected with *S.p.*-only or *S.p.* plus 1mM linoelaidic acid and no difference was seen.

References

1. Tan, L., et al., *Drosophila Fed ARA and EPA Yields Eicosanoids, 15S-Hydroxy-5Z,8Z, 11Z, 13E-Eicosatetraenoic Acid, and 15S-Hydroxy-5Z,8Z,11Z,13E,17Z-Eicosapentaenoic Acid.* Lipids, 2016. **51**(4): p. 435-49.

2. Park, J., D. Stanley, and Y. Kim, *Roles of peroxinectin in PGE2-mediated cellular immunity in Spodoptera exigua.* PLoS One, 2014. **9**(9): p. e105717.

3. Stanley, D., J. Miller, and H. Tunaz, *Eicosanoid actions in insect immunity.* J Innate Immun, 2009. **1**(4): p. 282-90.

4. Stanley, D., *Prostaglandins and other eicosanoids in insects: biological significance.* Annu Rev Entomol, 2006. **51**: p. 25-44.

5. W., L., et al., *Prostaglandins: Their role in egg-laying of the cricket Teleogryllus commodus.* Proc Natl Acad Sci U S A, 1981. **78**(12): p. 7835-7838.

6. Qian, Y., et al., *Prostaglandin E2 in the salivary glands of the female tick, Amblyomma americanum (L.): calcium mobilization and exocytosis.* Insect Biochem Mol Biol, 1998. **28**: p. 221-228.

7. Stanley-Samuelson, D.W., et al., *Insect immune response to bacterial infection is mediated by eicosanoids.* Proc Natl Acad Sci U S A, 1991. **88**: p. 1064-2068.

8. Miller, J.S., T. Nguyen, and D. Stanley-Samuelson, *Eicosanoids mediatei nsectn odulationr esponses to bacterial infections.* Proc Natl Acad Sci U S A, 1993. **91**(26): p. 12418-12422.

9. Carton, Y., et al., *Dexamethasone Inhibition of the Cellular Immune Response of Drosophila melanogaster Against a Parasitoid.* Journal of Parasitology, 2002. **88**(2): p. 405-407.

10. Shrestha, S., et al., *Genes encoding phospholipases A2 mediate insect nodulation reactions to bacterial challenge.* J Insect Physiol, 2010. **56**(3): p. 324-32.

11. Lemaitre, B. and J. Hoffmann, *The host defense of Drosophila melanogaster.* Annu Rev Immunol, 2007. **25**: p. 697-743.

12. Hoffmann, J.A., *The immune response of Drosophila.* Nature, 2003. **426**.

13. Yajime, M., et al., *A newly established in vitro culture using transgenic Drosophila reveals functional coupling between the phospholipase A2-generated fatty acid cascade and lipopolysaccharide-dependent activation of the immune deficiency (imd) pathway in insect immunity.* Biochem J, 2003. **371**: p. 205-210.

14. Kim, I.H., et al., *The insect pathogenic bacterium Xenorhabdus innexi has attenuated virulence in multiple insect model hosts yet encodes a potent mosquitocidal toxin.* BMC Genomics, 2017. **18**(1): p. 927.

15. Tootle, T.L. and A.C. Spradling, *Drosophila Pxt: a cyclooxygenase-like facilitator of follicle maturation.* Development, 2008. **135**(5): p. 839-47.

16. Parks, S.C., et al., *Parasitic nematode fatty acid- and retinolbinding proteins compromise host immunity by interfering with host lipid signaling pathways.* PloS Pathog, 2021.

17. Scarpati, M., et al., *A combined computational strategy of sequence and structural analysis predicts the existence of a functional eicosanoid pathway in Drosophila melanogaster.* PLoS One, 2019. **14**(2): p. e0211897.

18. Martinez, B.A., et al., *Innate immune signaling in Drosophila shifts anabolic lipid metabolism from triglyceride storage to phospholipid synthesis to support immune function.* PLoS Genet, 2020. **16**(11): p. e1009192.

19. Stanley, D. and Y. Kim, *Prostaglandins and Other Eicosanoids in Insects: Biosynthesis and Biological Actions.* Front Physiol, 2018. **9**: p. 1927.

20. Kim, Y., et al., *Eicosanoid-mediated immunity in insects.* Dev Comp Immunol, 2018. **83**: p. 130-143.

Chapter 5

Conclusions and Final Remarks

Parasitic nematodes utilize many different mechanisms to enhance their ability to successfully infect and survive host tissues. One of the key mechanisms behind this are the variety of ES proteins that do function as immune effectors. Understanding the mechanisms behind these effectors is vital to furthering our understanding of the variety of diseases that nematodes cause. One of the main difficulties in studying parasitic nematodes is the lack of an appropriate model system that is viable and safe. My work has utilized the model insect host *Drosophila melanogaster* and the entomopathogenic generalist nematode *Steinernema carpocapsae*.

In Chapters 1 and 2, I started with the characterization of the fatty acid- and retinol-binding (FAR) proteins. They had long been speculated to be immunomodulatory in the host and this work lays a foundation for the mechanism behind these effects. This work shows that FARs significantly affect the host's ability to resist a bacterial infection and lead to the suppression of key *Drosophila* immune mechanisms such as phenoloxidase activity and antimicrobial peptide production. I also show that FARs alter the in vivo availability of various fatty acids in fly hemolymph leading to the hypothesis that FARs are disrupting immune lipid signaling to elicit their effects.

After working on FAR proteins, the focus of my project switched to a different nematode effector, the secreted phospholipase A_2 protein in Chapter 3. This protein cleaves lipids

directly from the cell membrane lipid bilayer and can yield to downstream lipids and eicosanoids that have many known functions in insect and mammalian systems. Interestingly, this protein from *S. carpocapsae* also elicited an immunomodulator effect on Drosophila, this time more specifically to the toll signaling response and the cellular immune function of phagocytosis.

It is interesting that FARs, which sequester fatty acids from host tissue, and $sPLA_2$, which cleaves fatty acids from the membrane and leads to increased lipid synthesis, both show immunosuppressive effects. I hypothesize that this is likely due to the parasitic nematode secreted PLA_2 is cleaving lipids and leading to lipid interactions that are immunosuppressive and working in concert with the parasitic nematode FARs that are limiting the availability of pro-immune lipids. Although this hypothesis needs further testing, both proteins shown to have this immunosuppressive activity are involved in lipid sequestration and production and so my attention turned to the possibility of lipid and/or eicosanoid regulated immunity in the fly. In mammals, downstream eicosanoids such as prostaglandins are responsible for a pro- or anti- inflammatory response and play a key role in immune signaling. My work, in Chapter 4, shows that lipids and eicosanoids are able to rescue the outcome of infection in *Drosophila*, leading to a novel understanding of lipid immunity in this model host. I show that C18 PUFAs are depleted in the fly hemolymph and can completely rescue a bacterial infection. Prostaglandins, which are C20 eicosanoids, are able to do the same.

Although this work greatly enhances the knowledge in the field of both nematode effector proteins and *Drosophila* immunity, more can be done to further elucidate the mechanisms behind these phenomena. The FAR proteins contain two binding pockets, one for fatty acids and the other for retinols. I hypothesize that the fatty acid binding pocket is the only pocket necessary for its immunomodulatory effects. Mutant FARs can be utilized to confirm this hypothesis. Fly's also exhibit endogenous PLA_2 enzymes that likely aid in the induction of pro- or anti- immune mechanisms. Further identification of how the C18 and C20 lipids are beneficial to infection can be done to hone in on the fly's mechanism of pro- and anti- immune signaling. With this work, I have strived to further characterize immune effectors present in the ES of parasitic nematodes and to further identify the similarities of *Drosophila* immunity to the mammalian system. This work lays a foundation for the continued use of Drosophila as a model for mammalian diseases and elucidating host parasite interactions.